

Neutrino Detector

| Experiment | Year |
|------------------|-------|
| KGF | 1965 |
| EPR | 1965 |
| Homestake | |
| Gargamelle | 1973 |
| BEBC | 1980s |
| IIL/Granobole | 1981 |
| CDHS/WA1 | 1980s |
| CHARM/WA18 | 1980s |
| E531/FNAL | 1980s |
| Ronvo | 1985 |
| Krasnoyarsk | 1990 |
| LSND | 1990s |
| KARMEN | 1990s |
| Gorsgen | 1986 |
| Soudan II | 1983 |
| NUSEX | 1986 |
| MACRO | 1980s |
| BAKSAN | 1980s |
| Frejus | 1988 |
| Bugey | 1995 |
| Gallex | 1990 |
| SAGE | 1990 |
| BNL-E736/776 | 1990s |
| CHOOZ | 1998 |
| NOMAD | 2000 |
| CHORUS | 2000 |
| NuTeV | 2000 |
| Polo Verdo | 2000 |
| IMB | 19-- |
| Kamokande | 19-- |
| Super-Kamiokande | 1996 |
| TEXONO | 2002 |
| MINOS | 2005 |

| | |
|------------------------------|------|
| EGADS | 2009 |
| MINERvA | 2010 |
| T2K | 2010 |
| Daya Bay | 2011 |
| Double Chooz | 2011 |
| RENO | 2011 |
| MINOS+ | 2013 |
| NovA | 2014 |
| LarIAT | 2015 |
| MicroBooNE | 2015 |
| MAJORANA | |
| DEMONSTRATOR | 2015 |
| STEREO | 2016 |
| NA61/SHINE | 2016 |
| CUORE | 2017 |
| PROSPECT-I | 2018 |
| BeEST | 2019 |
| NINJA expt | 2019 |
| KARTIN | 2019 |
| JSNS2 | 2020 |
| SNO+ | 2020 |
| SND@LHC | 2021 |
| e4nu | 2022 |
| ICARUS at SBN | 2022 |
| IceCube Neutrino Observatory | 2005 |
| JLab E12-14-012 | 2017 |
| FASER | 2019 |
| NuDot | 2019 |
| LEGEND-200 | 2022 |
| NEXT-100 | 2022 |
| SBN | 2022 |
| nEXO | 2022 |
| NUCLEUS | 2023 |
| JUNO | 2023 |

| | |
|---------------------------------|------|
| SBND | 2023 |
| Ricochet | 2023 |
| Water Cherenkov Test Experiment | 2024 |
| IceCube Upgrade | 2026 |
| Hyper-Kamiokande | 2027 |
| DUNE | 2029 |
| LiquidO | 2013 |
| COHERENT | 2014 |
| CDEX-300 | 2020 |
| NUXE | 2020 |
| ANNIE | 2020 |
| EMPHATIC | 2022 |
| ECHO | 2022 |
| HOLMES | 2022 |
| Modern Modular Bubble Chamber | |
| LDRD | 2022 |
| FASERnu | 2022 |
| PROSPECT-II | 2023 |
| LEGEND-1000 | 2024 |
| PALEOCCENE | 2024 |
| IceCube-Gen2 | 2025 |
| SBC-CEvNS | 2025 |
| FLArE | 2026 |
| LDMX | 2026 |
| FASERnu2 | 2026 |
| AdvSND | 2026 |
| NEXT-HD | 2026 |
| IsoDAR | 2027 |
| Project 8 | 2028 |
| CDEX-1T | 2028 |
| NEXT with barium tagging | 2028 |

| | |
|----------|------|
| CUPID | 2029 |
| Trinity | 2030 |
| nuSTORM | 2030 |
| Theia | 2030 |
| CUSO | 2032 |
| GRAND | 2032 |
| CUPID-1T | 2035 |
| ESSnuSB | 2037 |
| SBN-BD | 2039 |
| PIP2-BD | 2039 |
| AMANDA | |
| ANTERUS | |
| BAIKAL | |
| DUMUND | |
| GVD | |
| HPW | |
| NEMO | |
| NESTOR | |
| KM3NET | |
| ICeCube | |
| P-ONE | |
| TRIDENT | |

- This is the list in my table, but certainly not a complete one (Nobel winning expt are missing)
- What to talk in four hours ?

Summary of preschool lectures

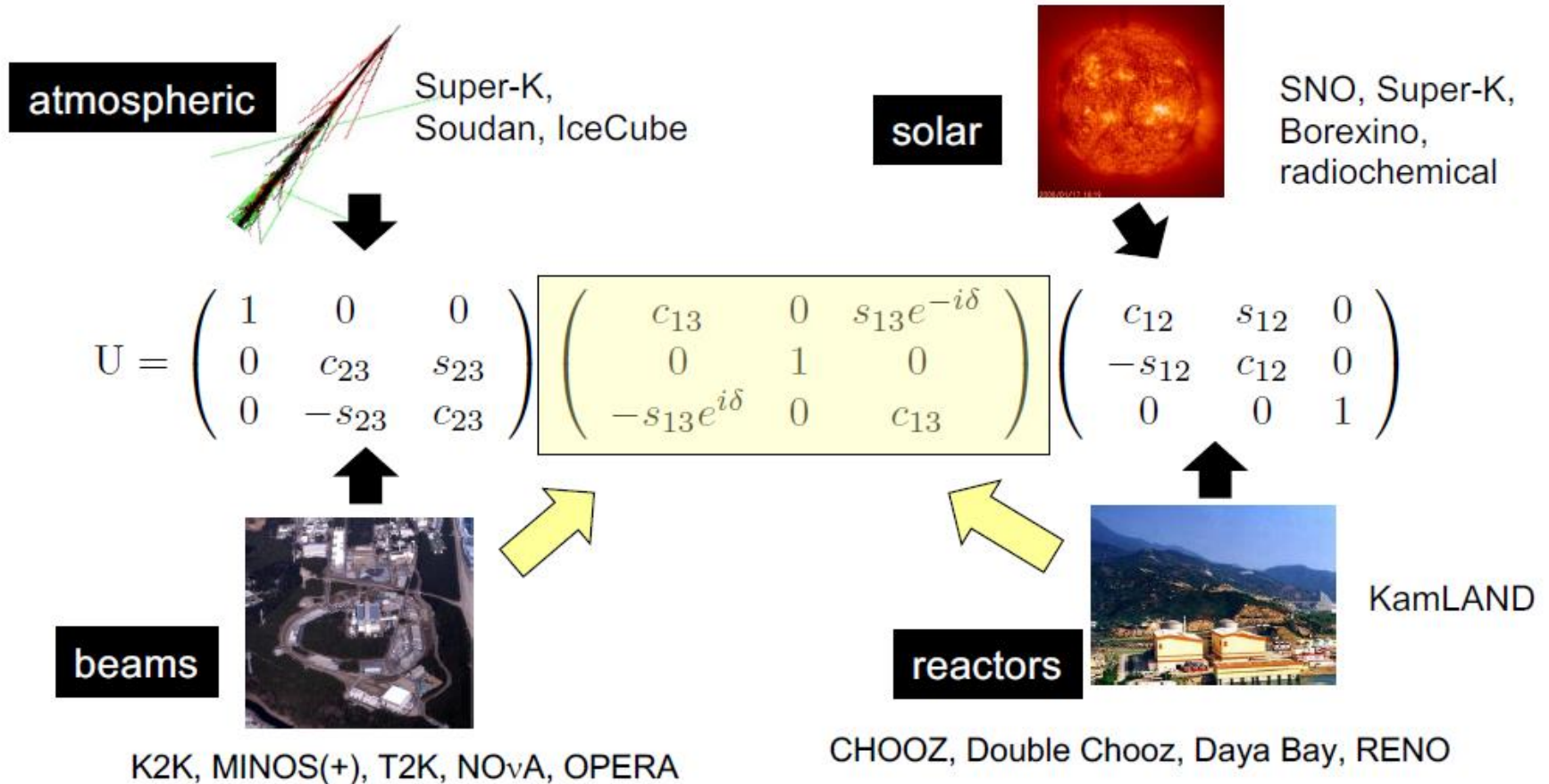
- HEP detectors are built to detect so-called “stable particles” ($c\tau \geq 1\text{m}$)
 - $p, \bar{p}, k^\pm, \pi^\pm, e^\pm, \gamma, n, \bar{n}, k_{Long}, \mu^\pm, \nu, \bar{\nu}$
- The best approach is to utilize the electromagnetic interactions between particle and the detector medium to design HEP experiments
 - Exception for neutrino (Weak) as well as neutral hadrons (Strong), but.....
- Signal is mainly from the ionization energy loss of charge particles ($-dE/dx$) as well as Cherenkov, Transition Radiation etc), not from the trajectory of neutral particle or from any interaction directly
- All signals in particle detectors are due to induction by moving charges.
 - Once the charges have arrived at the electrodes the signals are ‘over’.
- Energy resolution in
 - Calorimeter : $\frac{\sigma(E)}{E} \propto \frac{a}{\sqrt{E}}$
 - Tracking device : $\frac{\sigma(p)}{p} \propto b p$
- Experiments of rare events has to be done in underground
 - Not only to remove direct muon signal, but also the backgrounds from muon induced “cosmogenic isotopes”

Disclaimers

- **Most of the contents are not my own work, almost all plots, data and many text are taken from others' presentations, others' works in published paper, e.g. large content of Kamikande from talk of Yuichi Oyama (KEK/J-PARC) at Vietnam school on Neutrino, July 10-21, 2017**
- **Primary emphasis of these four lectures is to give few examples of**
 - **Development of detector elements to achieve well defined physics goals**
 - **Calibration of systems**
 - **But, I will not talk about other important ingredients of it, i.e., engineering (civil, mechanical, electrical, electronics, computer, chemical.....)**
- **Plan**
 1. **Introduction, sources, interactions, general neutrino detector concepts**
 - ❖ **What order should I follow ?**
 2. **Kamiokanda → HK**
 3. **JUNO + DUNE**
 4. **Other detectors**

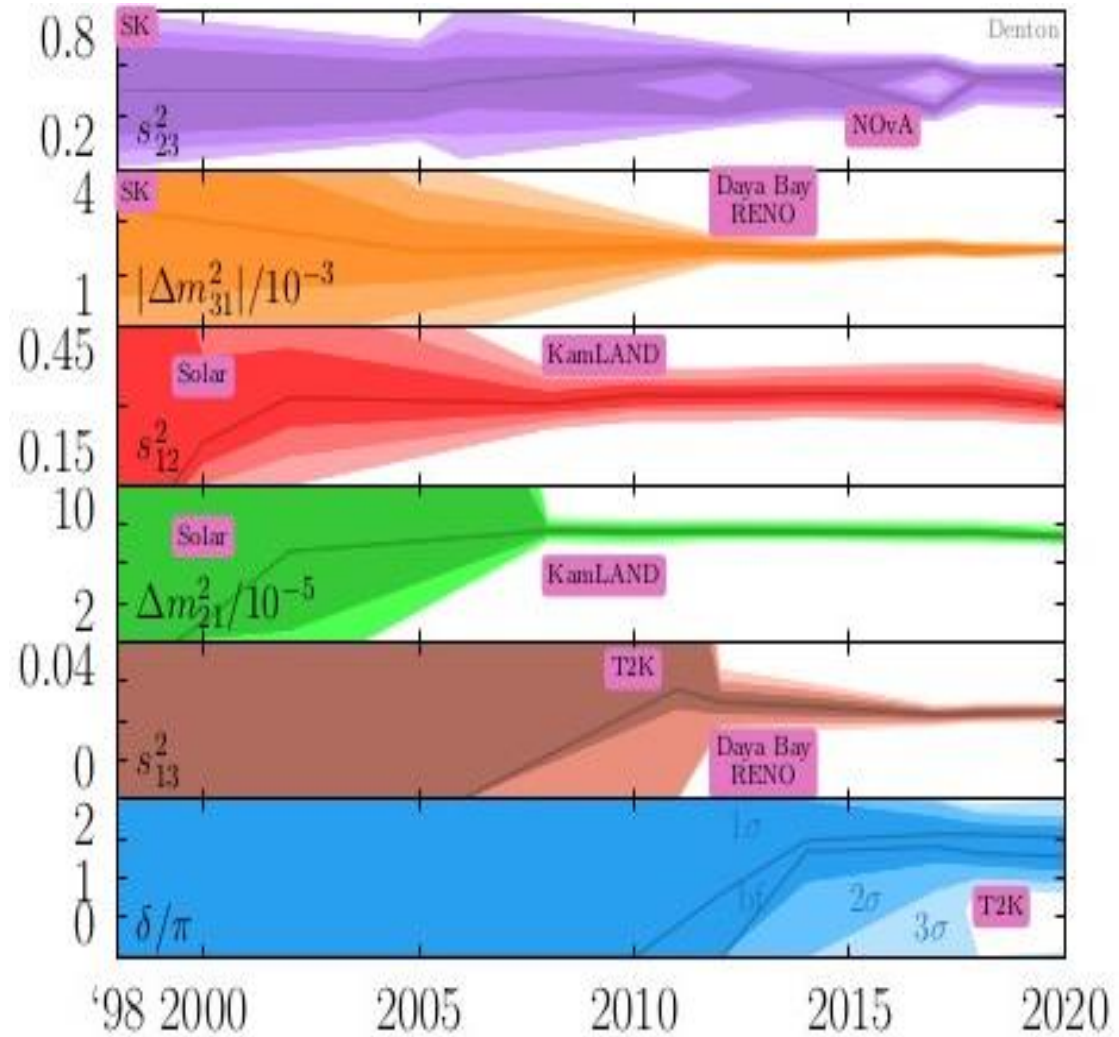
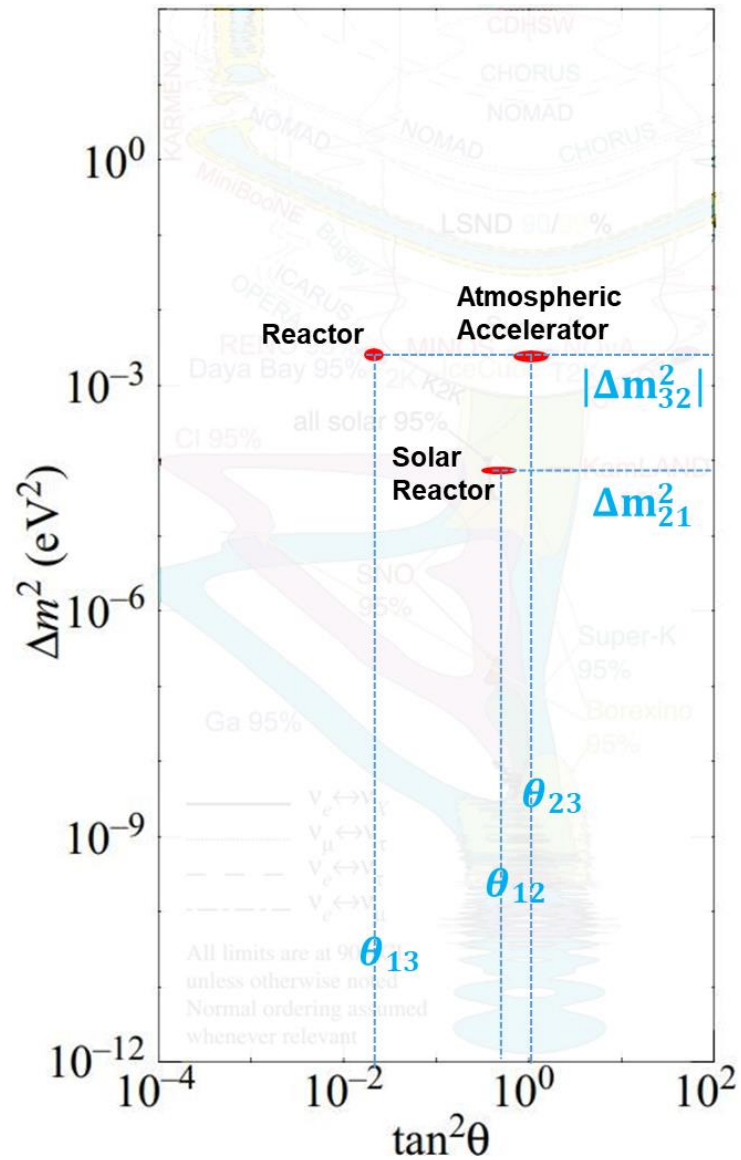
Neutrino mixing matrix and experiments

Neutrino oscillation experiments so far have told us about the mixing angles and Δm^2 values



- δ_{CP} : Measured from asymmetry of ν_{μ} and $\bar{\nu}_{\mu}$ oscillation
- α_{21} and α_{31} are majorana phase, do not appear in neutrino oscillation

Time evolution of our understandings



Sources of neutrinos

Atmospheric - cosmic ray interaction in upper atmosphere produce π^\pm and μ^\pm whose decay generates roughly two ν_μ for every ν_e , $E_\nu \sim \text{GeV}$, neutrino flux $\Phi(\nu_e) \sim 10^3 \text{ m}^{-2} \text{ sec}^{-1}$

Sun - $E_\nu \sim 0.1\text{-}15 \text{ MeV}$, $\Phi(\nu_e) \sim 6 \times 10^{14} \text{ m}^{-2} \text{ sec}^{-1}$

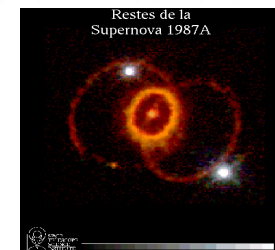
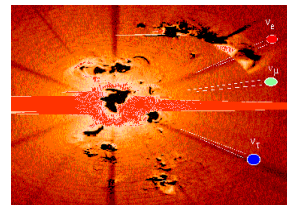
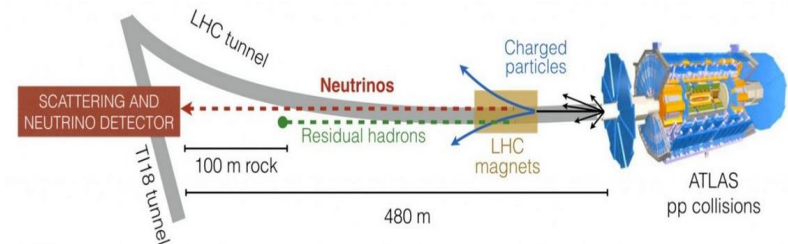
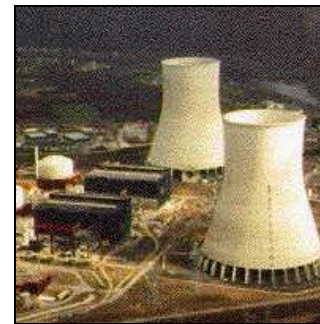
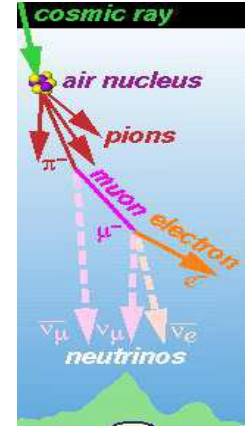
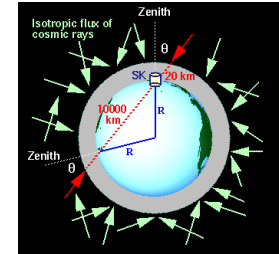
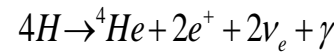
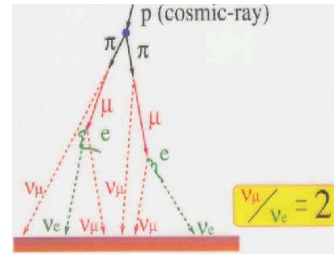
Man made sources such as nuclear power reactors - $E \sim 0.1\text{-}5 \text{ MeV}$, $\Phi(\nu_e) \sim 10^{13} \text{ m}^{-2} \text{ sec}^{-1}$ **GWth⁻¹ at 1 km and accelerators**, $E < 200 \text{ GeV}$, $\Phi(\nu_e) \sim 10^9 \text{ m}^{-2} \text{ sec}^{-1}$ at 1 km (+New LHC expt upto TeV)

Particle accelerator : upto $10^{15}/\text{s}$

Geo (earth's crust & interior) – from beta decays of ^{40}K , U, Th chains (contributing $\sim 40\%$ heat production in earth) $E \sim 0.1\text{-}2 \text{ MeV}$, $\Phi(\nu_e) \sim 6 \times 10^6 \text{ cm}^{-2} \text{ sec}^{-1}$

Supernova – exploding stars in cosmos - 99% energy released as neutrinos (N_ν over $\sim 10 \text{ sec} \sim 10^{60}$) : $E_b \sim 10^{53} \text{ ergs}$, $E_\nu \sim 10\text{-}30 \text{ MeV}$

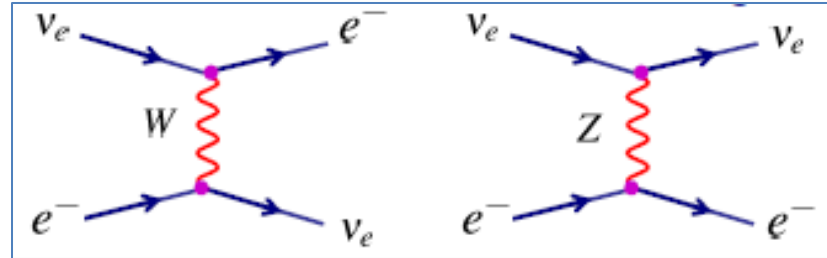
Big bang cosmic background - $E_\nu \sim 4 \times 10^{-4} \text{ eV}$ 330 cm^{-3} (like 2.7K microwave bkgd)



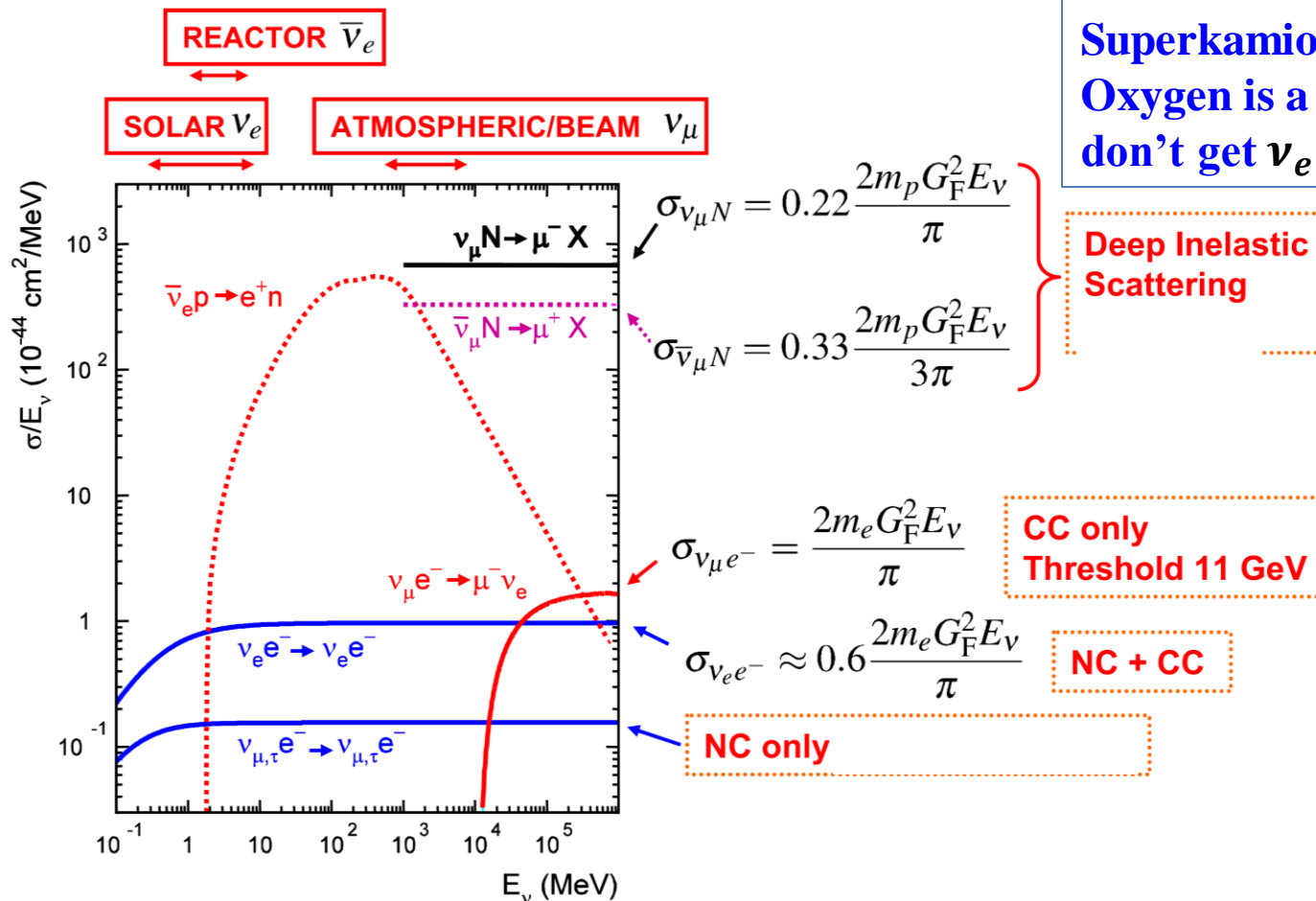
Neutrino CC interactions at experiments

- For electron neutrinos there is one more lowest order diagramme for the same final states of CC interaction

- Due to **negative interference** $|M_{CC} + M_{NC}|^2 < |M_{CC}|^2$, $\sigma_{\nu_e e} \approx 0.6 \sigma_{\nu_e e}^{CC}$

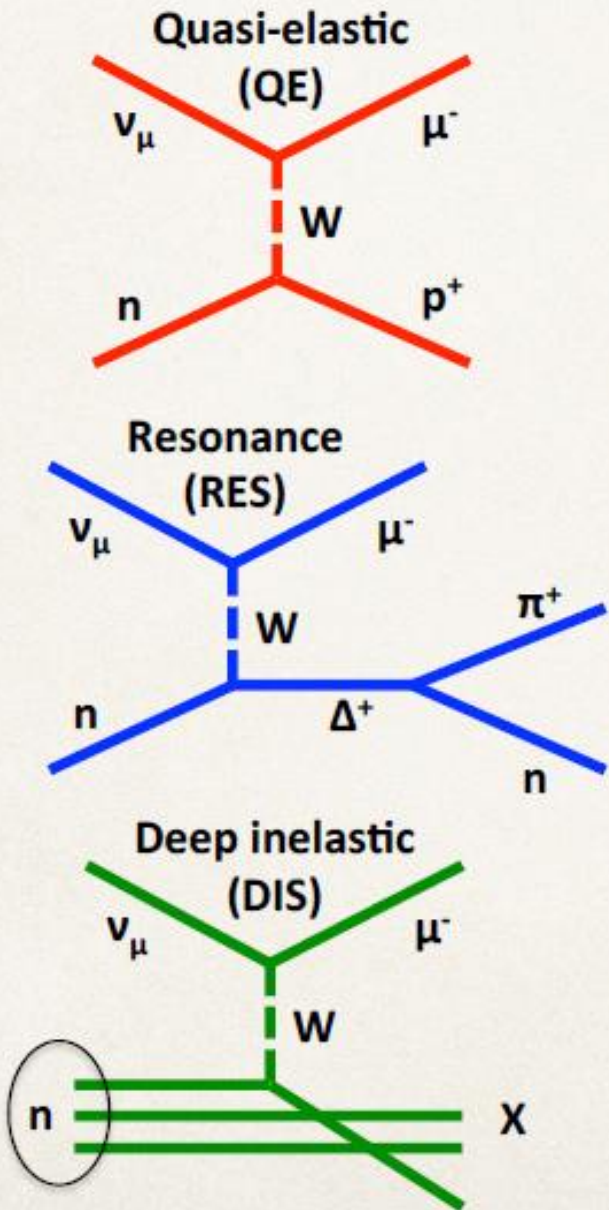
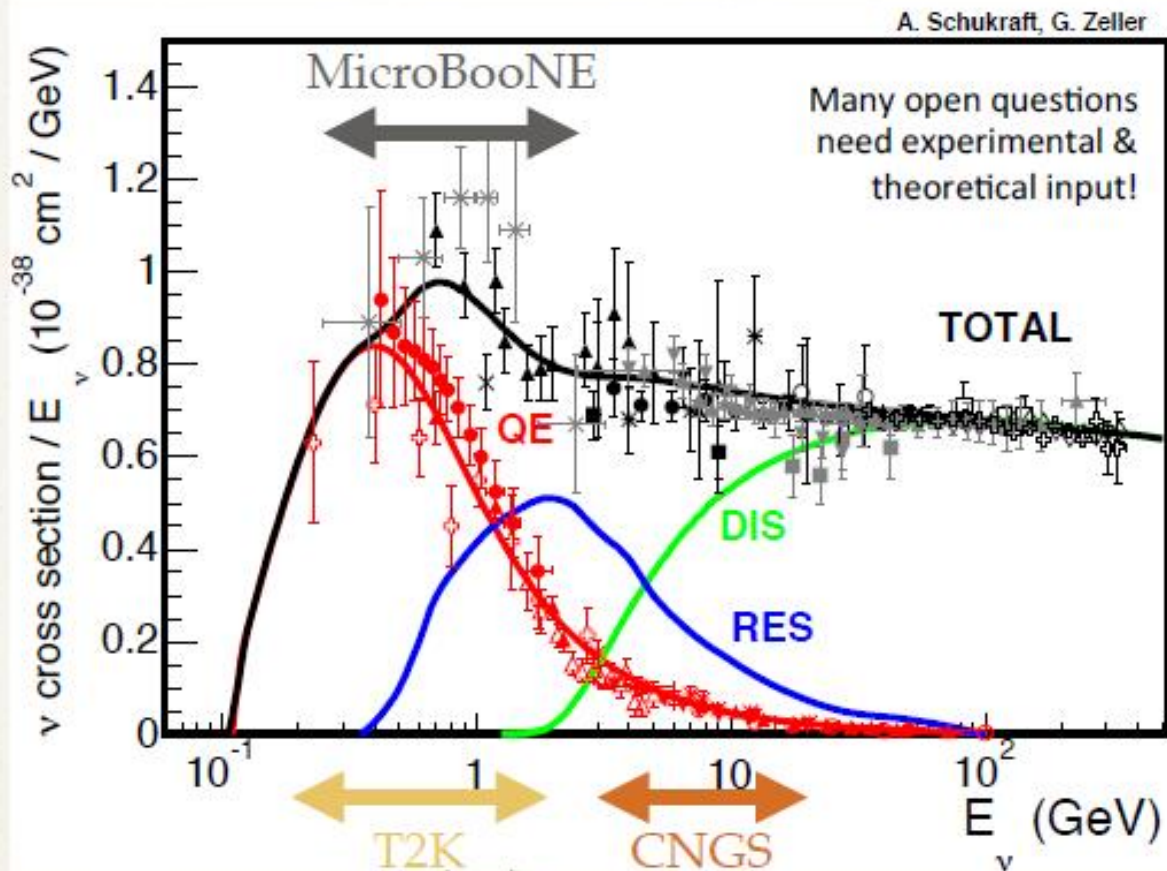


Water Cherenkov, e.g.,
 Superkamiokande : Because of
 Oxygen is a doubly magic nucleus,
 don't get $\nu_e + n \rightarrow e^- + p$



Neutrino interaction with nucleons

Lots of interesting (nuclear) physics over all energy ranges.

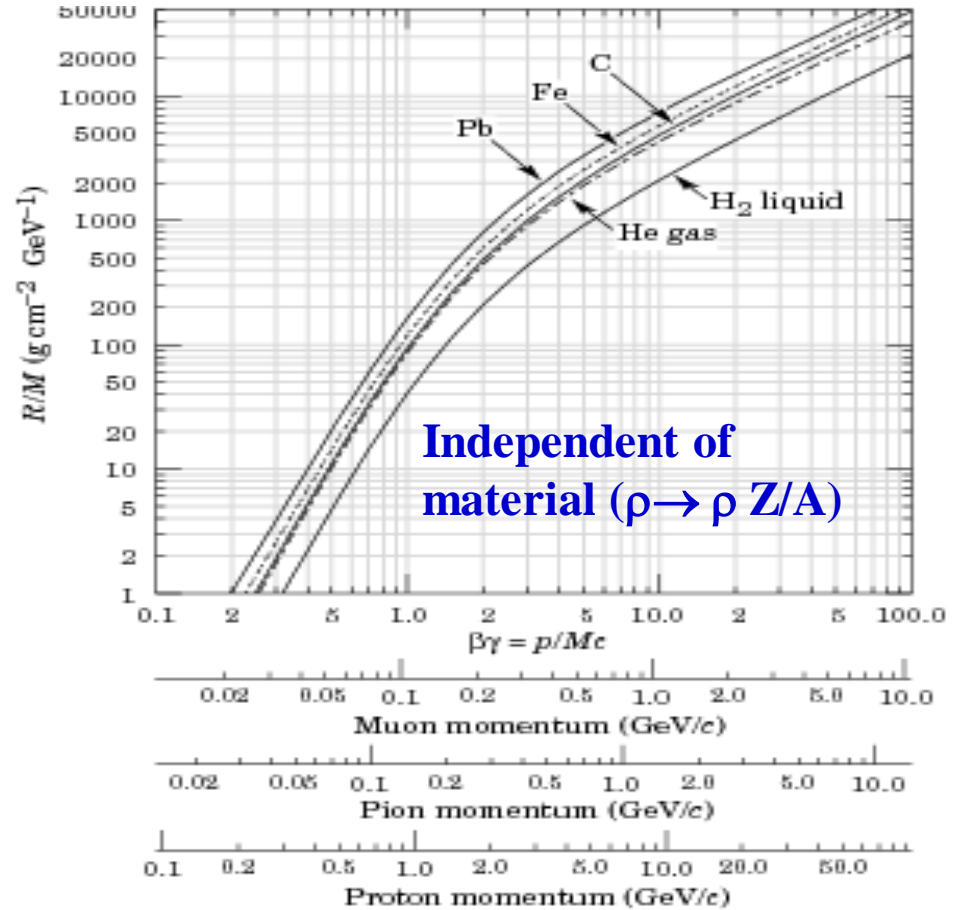
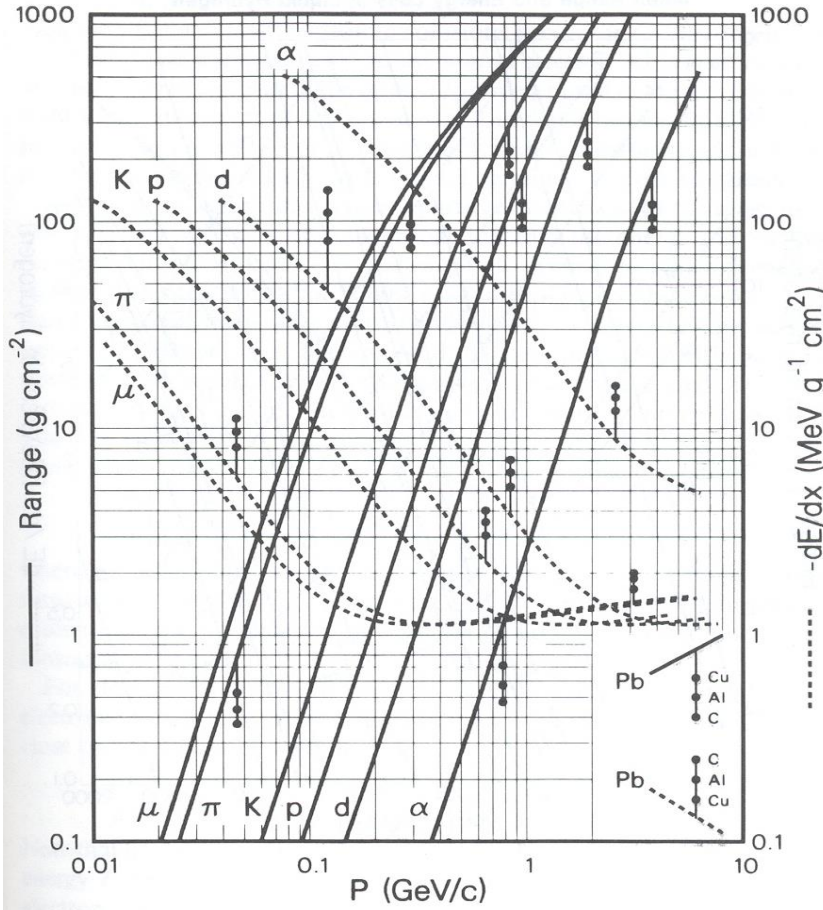


Reference: J. Formaggio, G. Zeller, Rev. Mod. Phys. 84, 1307 (2012)

Ionisation energy loss and range : Bethe Bloch formula

$$-\frac{1}{\rho} \frac{dE}{dx} = 4\pi \frac{e^4}{m_e c^2} \frac{Z_1^2}{\beta^2} N_A \frac{Z_2}{A} \left[\ln \left(\frac{2m_e c^2 \beta^2 \gamma^2}{I} \right) - 2\beta^2 - \delta(\beta\gamma) - \frac{C(I, \beta\gamma)}{2Z} \right]$$

Mean Range and Energy Loss in Lead, Copper, Aluminum, and Carbon



$$R(T) = \int_0^T - \left[\frac{dE}{dx} \right]^{-1} dE$$

Proton with $p=1$ GeV, Target : lead with $\rho=11.34\text{g/cm}^3$
 $R/M = 200 \text{ g cm}^{-2} \text{ GeV}^{-1} \Rightarrow R = 200/11.34/1 \text{ cm} \sim 20 \text{ cm}$

This is an useful concept for small range/energy

Measurement of ionization : *Ionisation chamber*

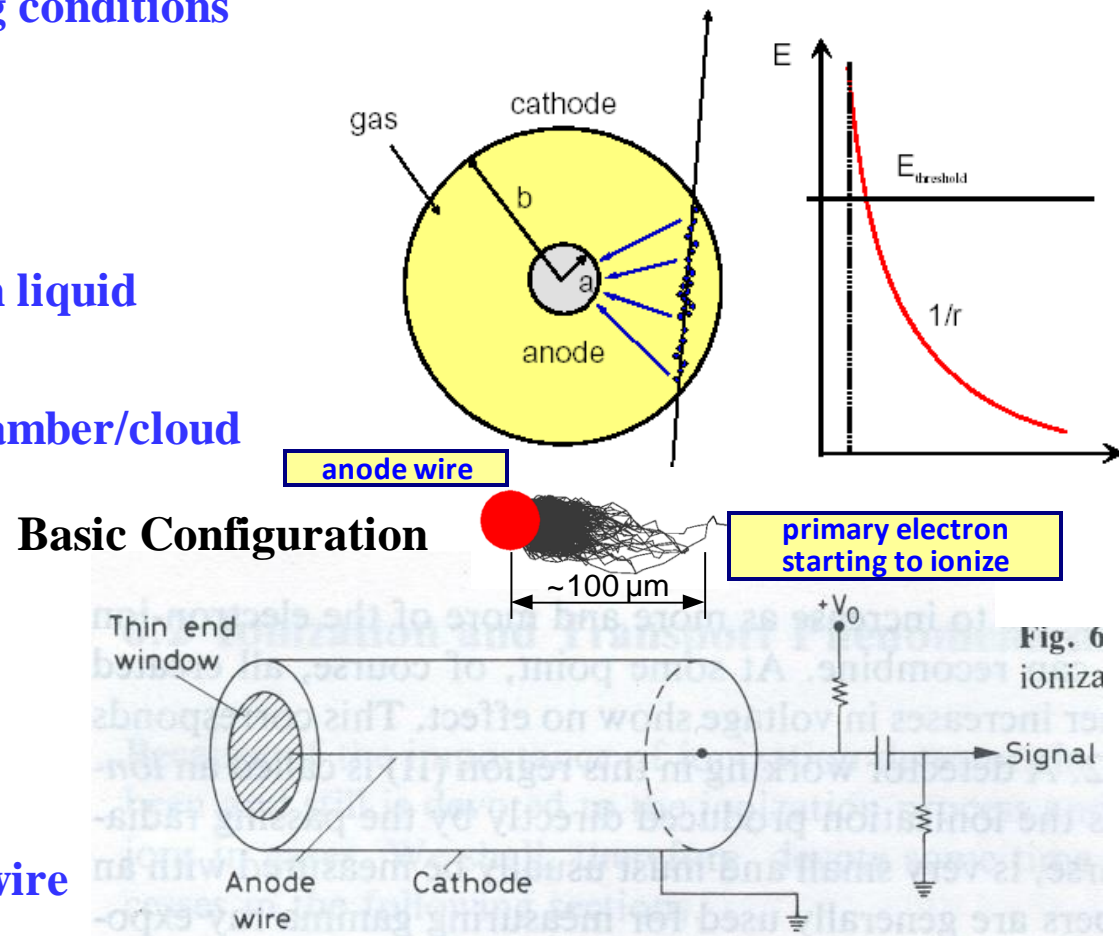
- First electrical devices developed for radiation detection
- Direct collection of ionisation, electrons and ions produced in a gas by passing radiation
- In general there are many types of ionisation chambers, but all are same devices working under different operating conditions

- Ionisation chamber
- Proportional counter
- Geiger Müller counter
- Measurement of ionisation in liquid
- Semiconductor detector
- Spark chamber/streamer chamber/cloud chamber/bubble chamber

$$E(r) = \frac{1}{r} \frac{V_0}{\ln(b/a)}$$

- **a = radius of the central wire**
- **b = inside radius of the cylinder**
- **r = radial distance from anode wire**

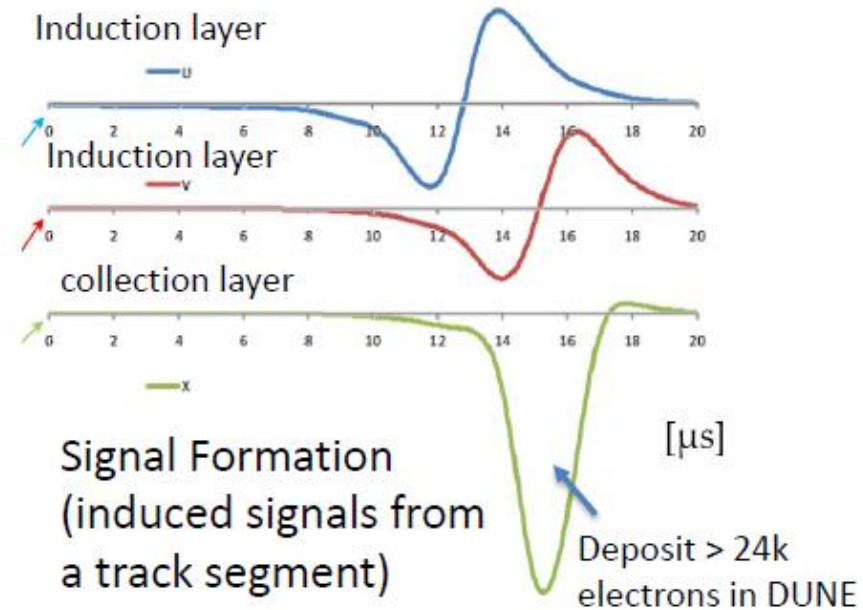
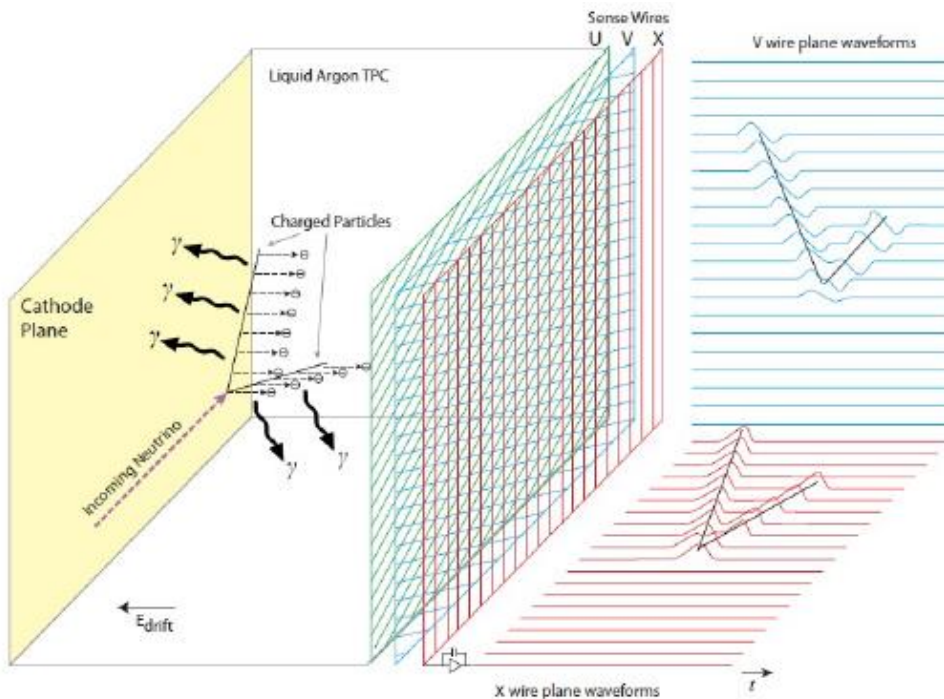
If radiation penetrate the cylinder, certain number of electron-ion pair will be created, number of free electron-ion pair \propto energy deposited



LArTPC (Liquid Argon Time Projection Chamber)

Charged particles passing through detector ionize the argon atoms, and the ionization electrons drift (**few m**) in the electric field to the anode wall on a timescale of **milliseconds**. The anode consists of layers of active wires forming a grid.

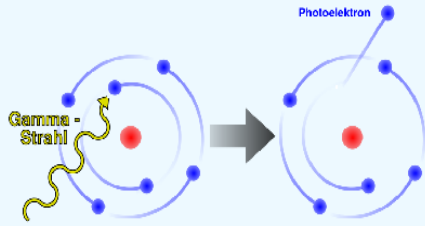
- MIP ionization $\sim 6000 e^-/\text{mm}$; Drift velocity $1.6\text{mm}/\mu\text{s}$ @ $500\text{V}/\text{cm}$
- Scintillation light yield $5000 \gamma/\text{mm}$ @ 128 nm (or $\sim 4000 \gamma/\text{MeV}$)



- Time information: when ionization electrons arrive (drift distance)
- Geometry information: which wires are fired (transverse position)
- Charge information: how many ionization electrons (energy deposition)

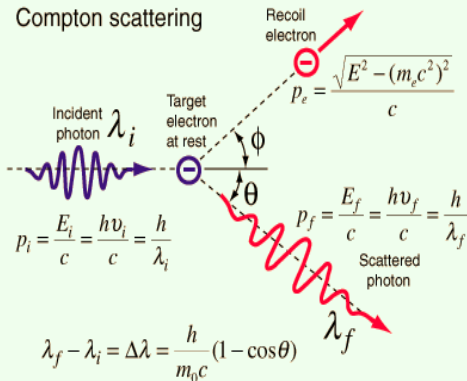
Interaction of photon

✓ 1-Photoelectric effect



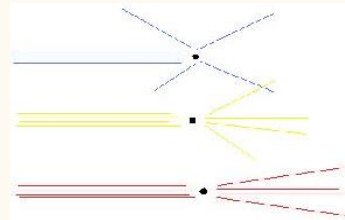
cross section scales with $Z^{4,5}$ and E^{-3}

✓ 2-Compton scattering



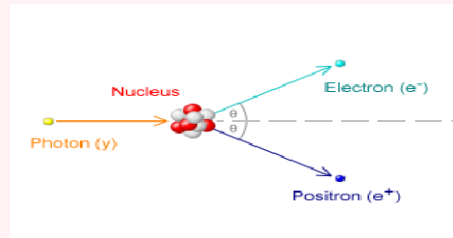
cross section scales with Z and $1/E$

✓ 4-Coherent (Rayleigh) scattering



elastic scattering of γ by the atomic electron, no energy loss just change of direction at low energy ... $\sigma \sim 1/\lambda^4$

✓ 3-Electron positron pair production cross section



raises with Z and energy and reaches an asymptotic value above 1 GeV

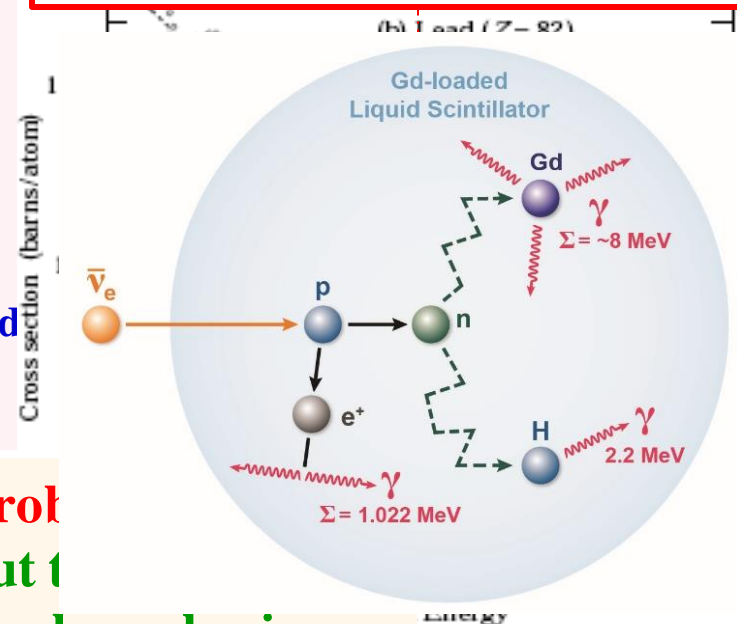
Inherent to pr light

- **Gamma** : Either Compton or p.e. → Electron → Ionisation energy loss → charge/visible photon
- **Produced gamma (MeV)** are very much different than the **visible photon (eV)**
- **Neutron** : Capture in nucleus → Binding energy → gamma & same chain

✓ 5-Photo nuclear reactions between 5-20 MeV, cross section does not exceed 1% of all other processes.

$\gamma n, \gamma p$ or induced nuclear fission

Prob but 1 Nuclear physics



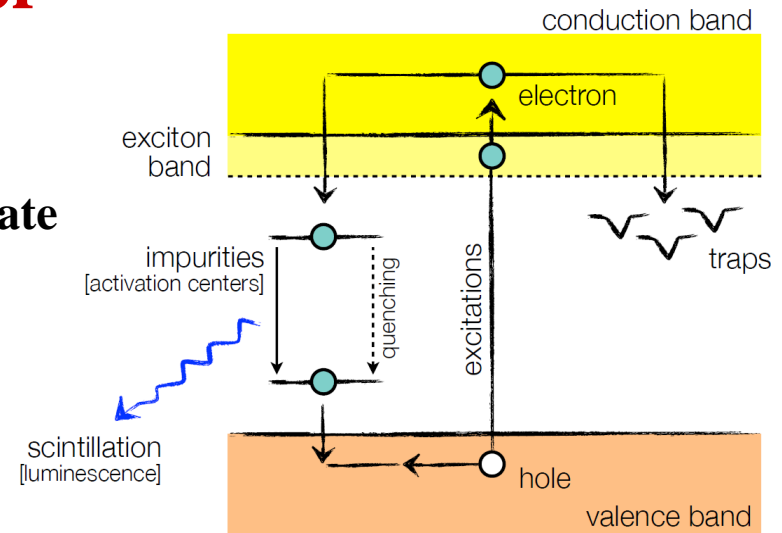
Scintillator

- **Principle**

- Ionizing particle produce free electron
- Elevate electron from ground state to excited state
- Excited state decays to emit light

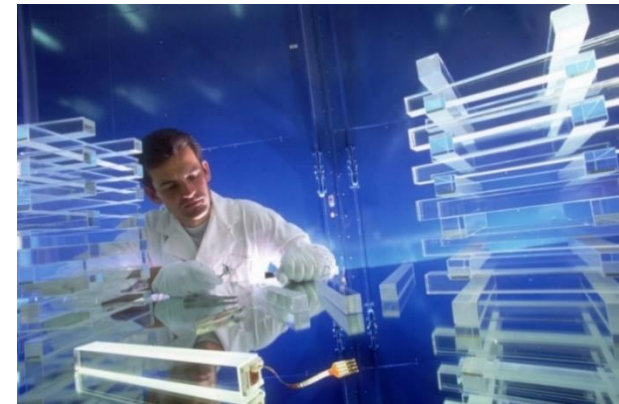
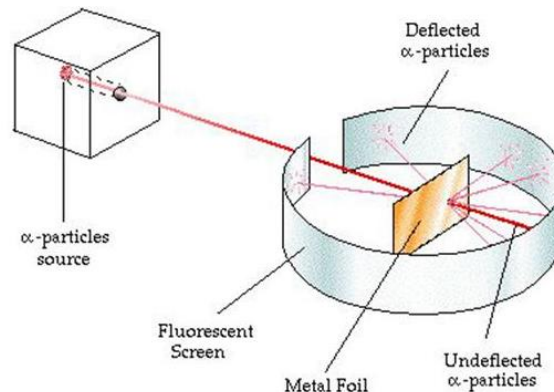
- **Requirements**

- Convert charged particle K.E. into detectable light with a high scintillation efficiency
- Scintillation output is linear to incident K.E.
- Transparent to the wavelength of its own emission
- Short decay time
- Refractive index is near 1.5, to permit efficient coupling to Phototransducer
- Good optical properties, manufacture in large scale



Energy bands in impurity activated crystal showing excitation, luminescence, quenching and trapping

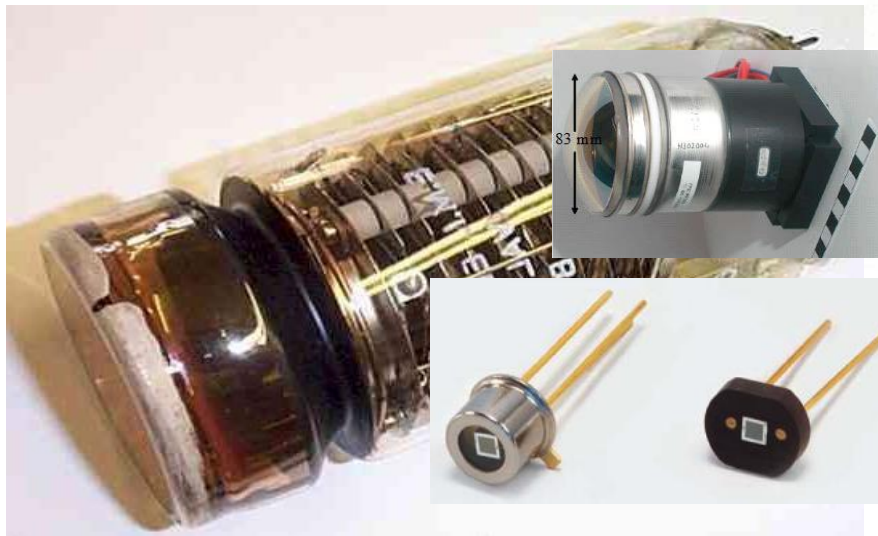
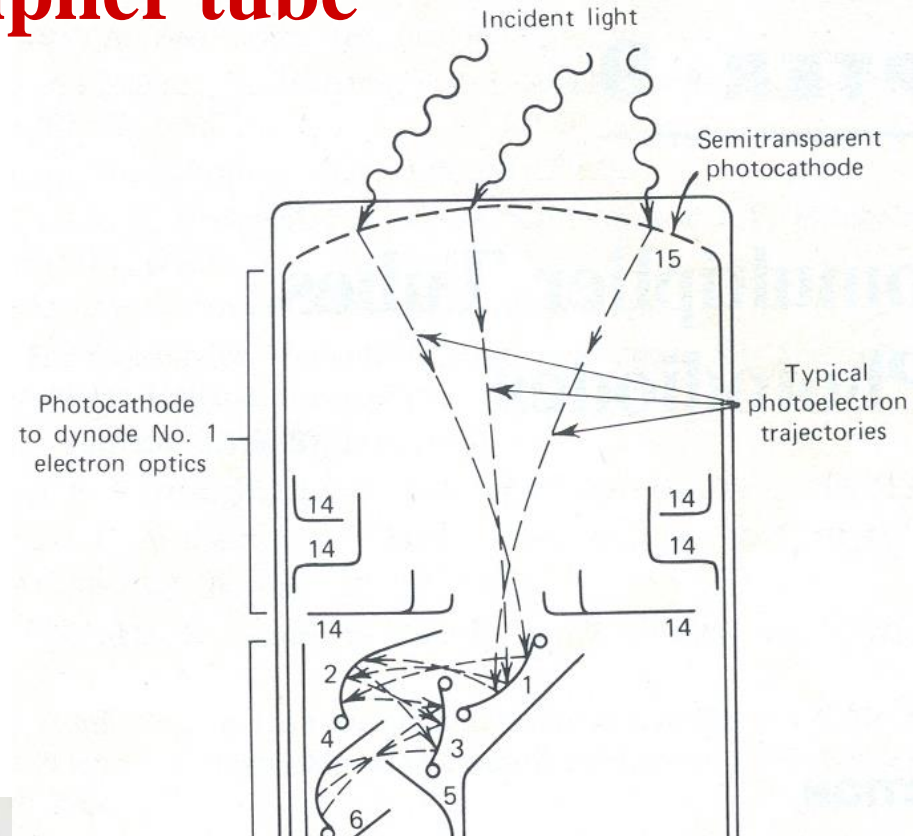
- **Inorganic**
- **Organic**
 - Liquid, plastic
- **Noble gases**



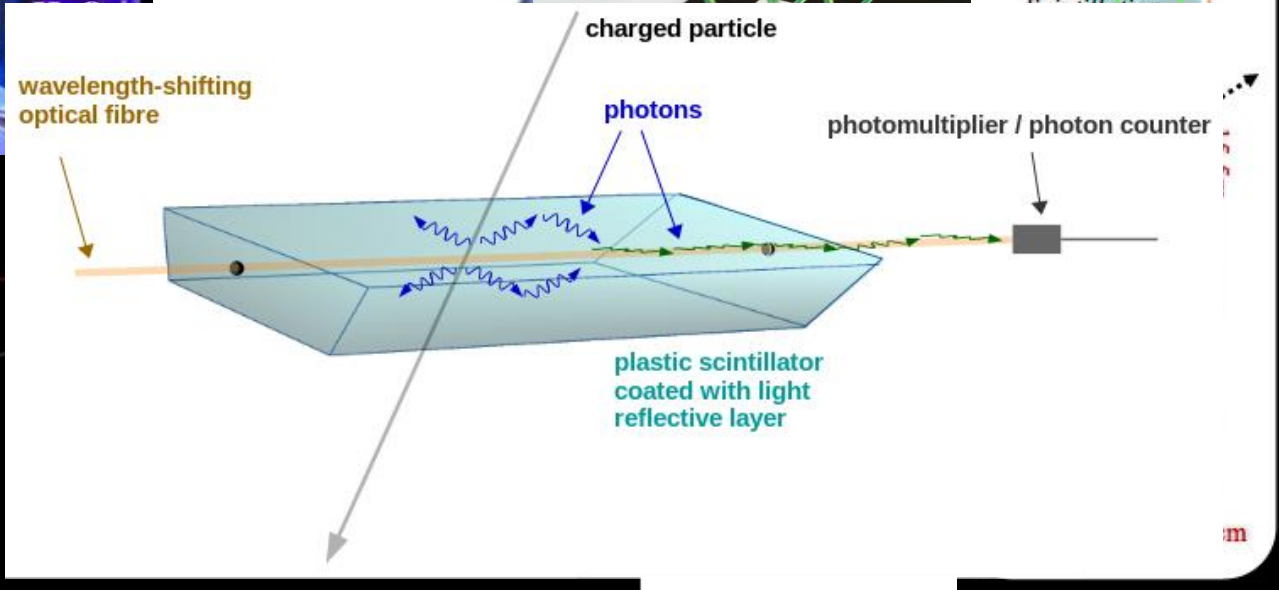
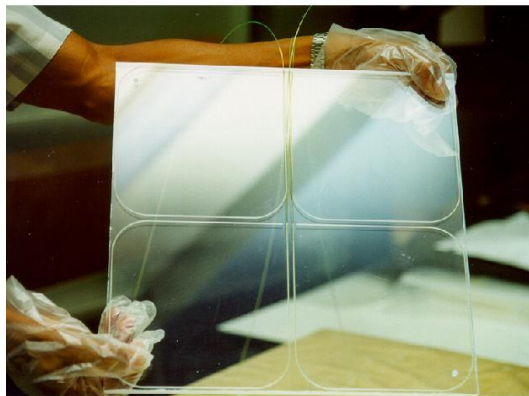
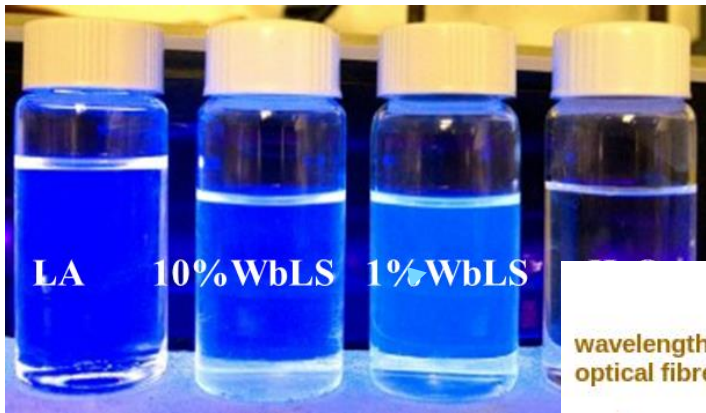
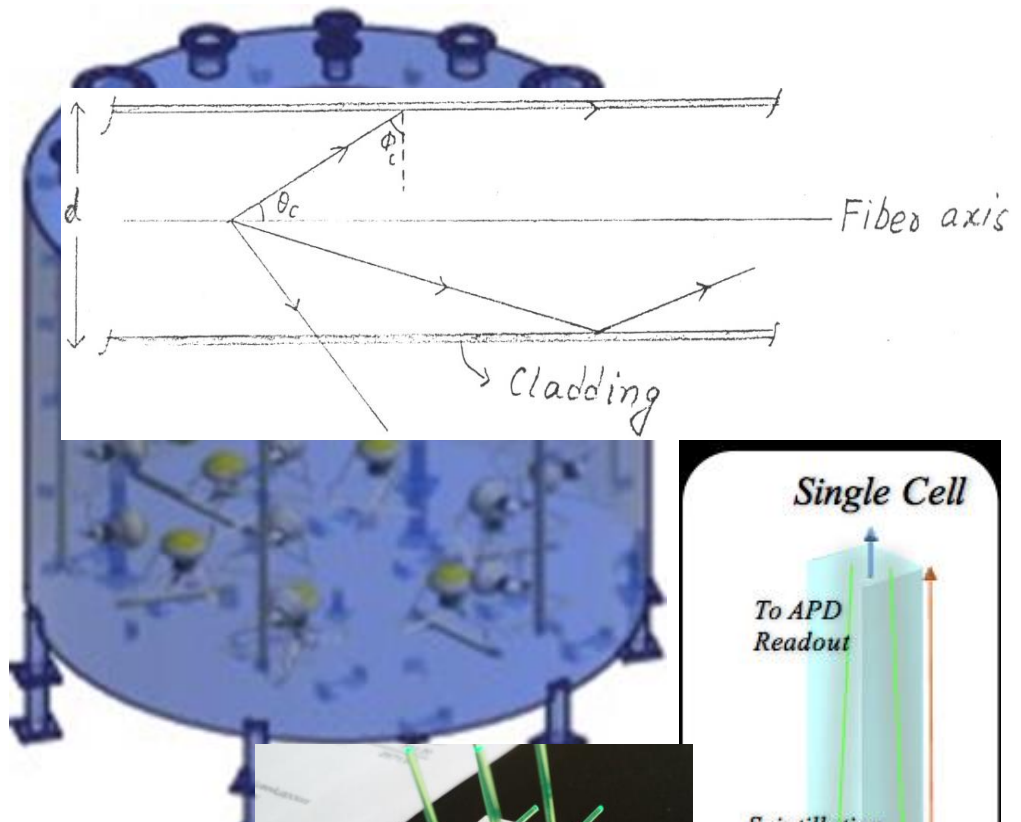
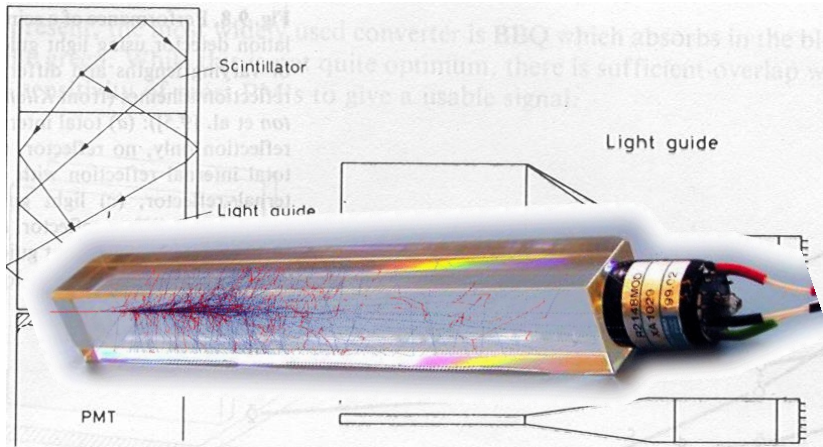
Photomultiplier tube

An electron tube device which convert light into measurable electric current

- A window to admit light
- A photo cathode that emits electrons in response to light
- An electron optical system which focuses the emitted electron
- A series of electrodes called dynode which multiply electrons by secondary emission
- An anode which collect secondary electrons



Scintillator detector



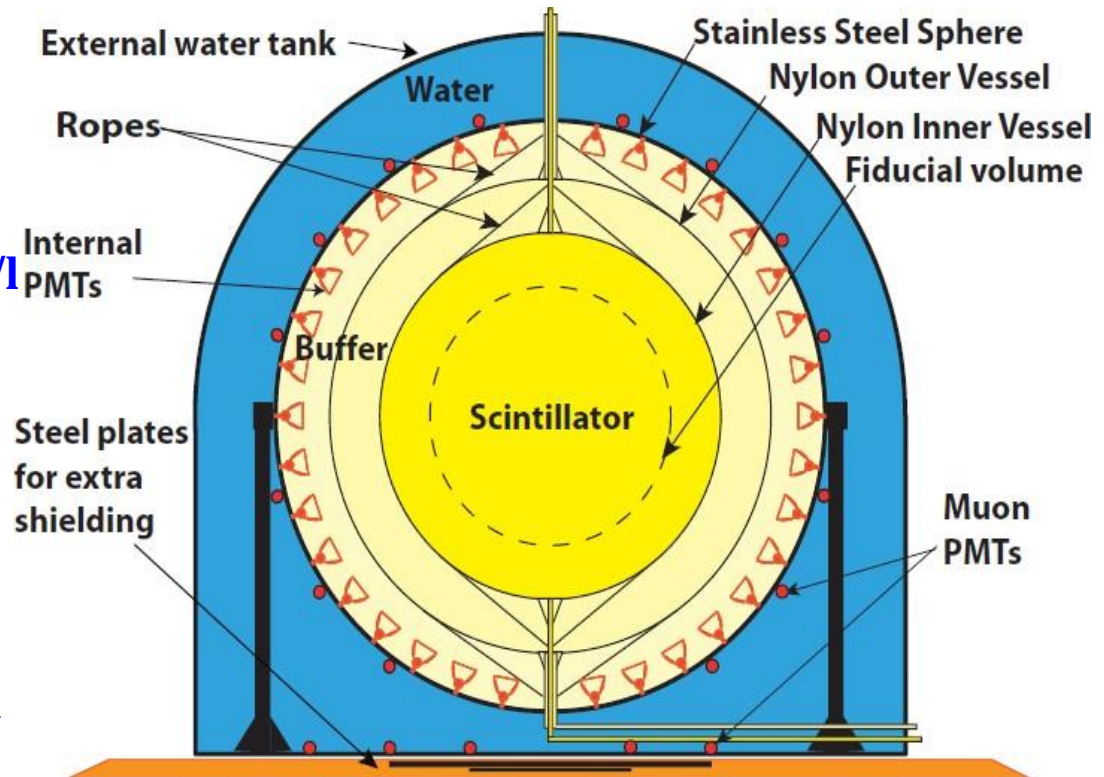
A Scintillator Detector in Neutrino experiment : Borexino

- Steel water tank (WT) of 9m base radius and 16.9m height filled with ~1kt ultrapure water
 - 208 8" PMT on floor and outer surface of a SS sphere, 6.85m radius
- The inner detector within SSS equipped with
 - 2212 8" PMT (from 1931 in Dec 2007 to 1183 in April 2019) : Photocathode coverage : 34%
 - Three ID layers with insertion of two 125 μ m thick nylon balloons. Inner vessel (IV) and outer vessel (OV) with radii 4.25 and 5.50m
 - The two layers between the SSS and the IV, separated by the OV, form the outer buffer (OB) and the inner buffer (IB).

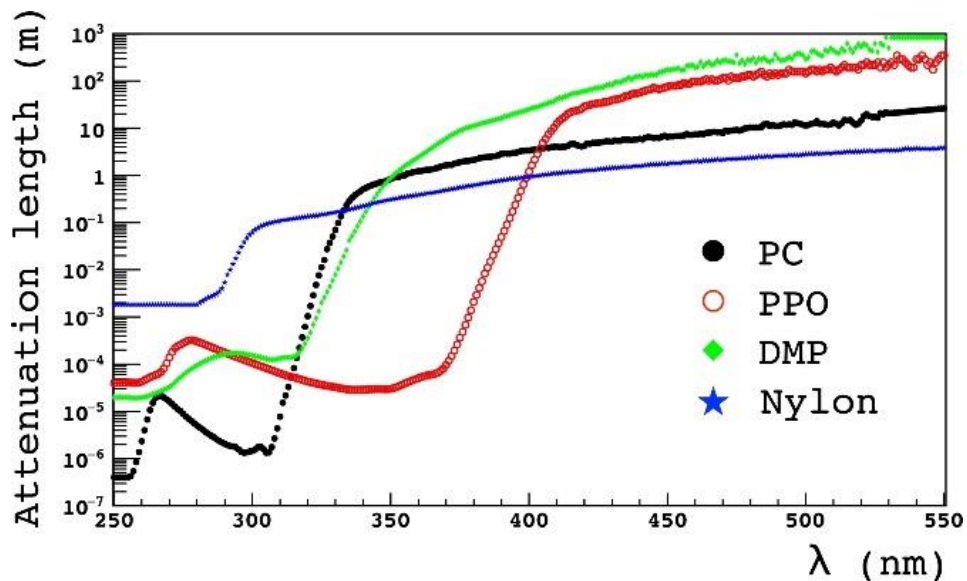
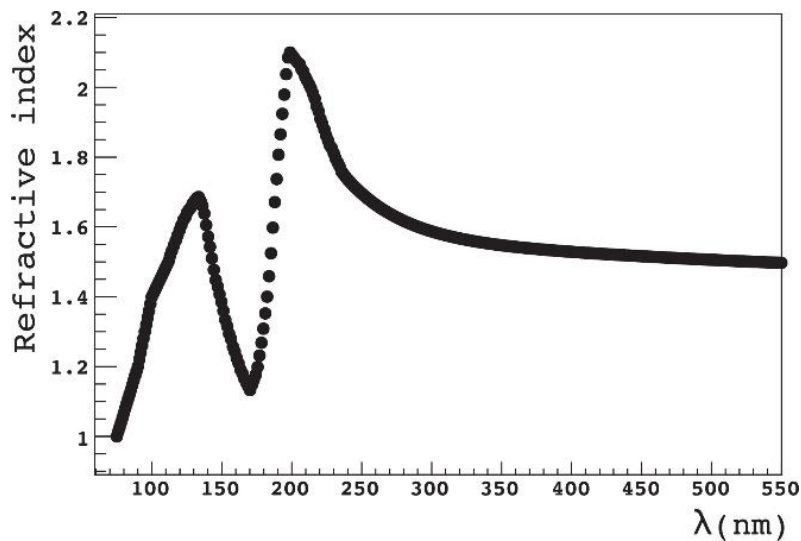
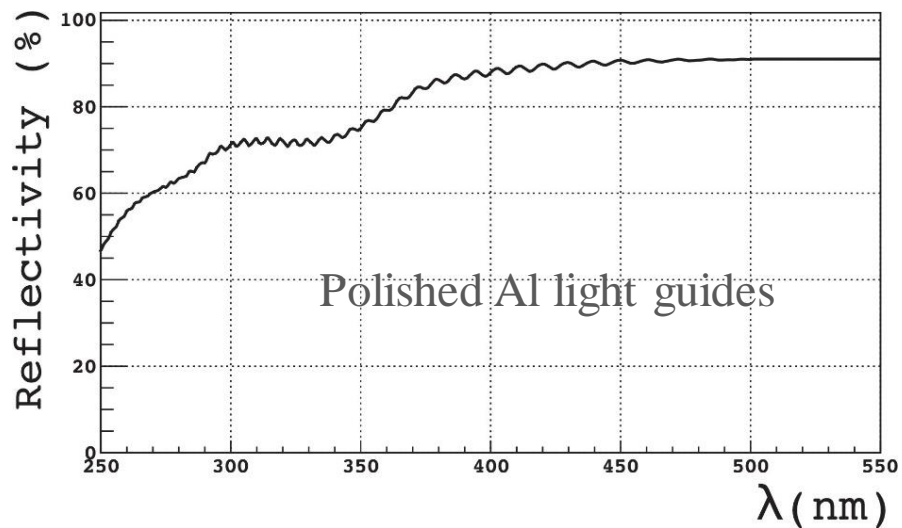
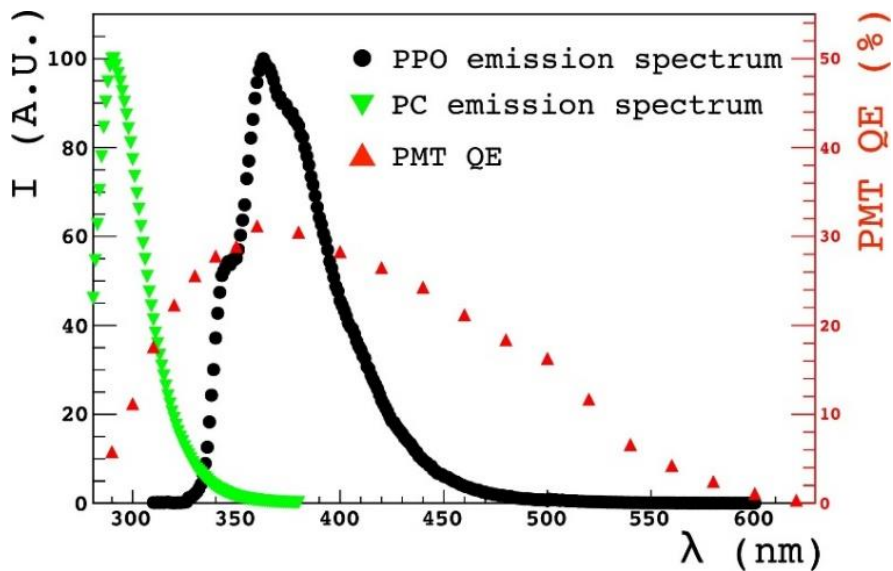
• Liquid scintillator

- Pseudocumene (PC, 1,24-trimethylbenzene, $C_6H_3(CH_3)_3$)
- Fluorescent dye PPO (2,5-diphenyloxazole, $C_{15}H_{11}NO$), 1.5g/l
- Density : $(0.878 \pm 0.004) \text{ g/cm}^3$
- Target mass : 278 ton
- Proton density : $(6.007 \pm 0.001) \times 10^{28} \text{ ton}^{-1}$

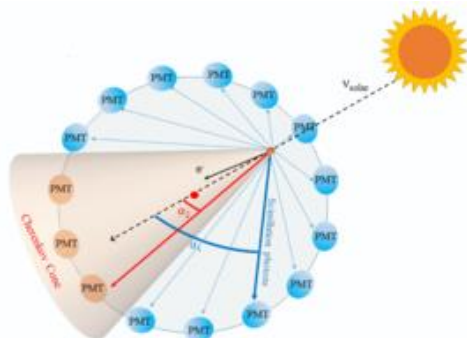
- Buffer consisting soln of the dimethylphthalate, DMP, $C_6H_4(COOCH_3)_2$ light quencher in PC



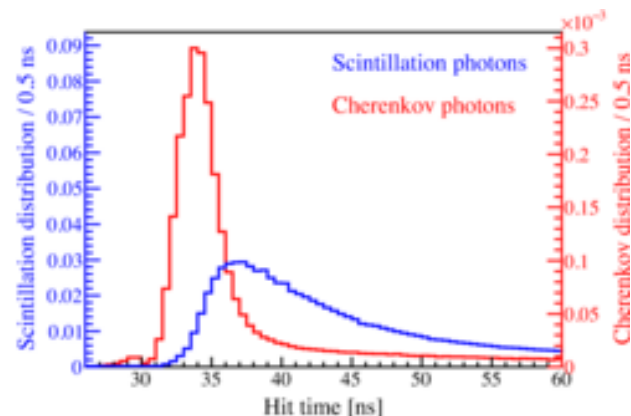
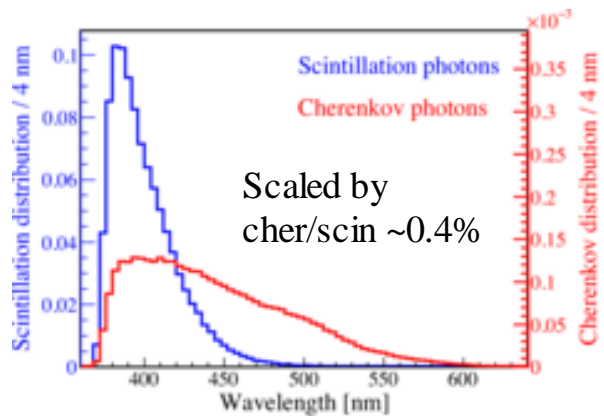
Spectra, Quantum efficiency, attenuation in scintillator



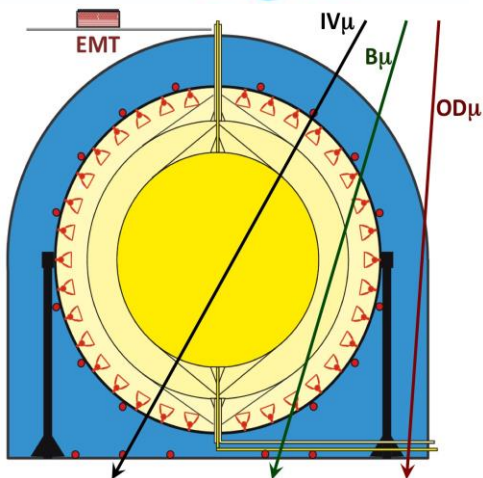
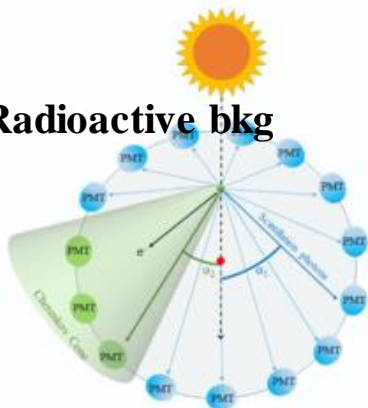
Signal and background events



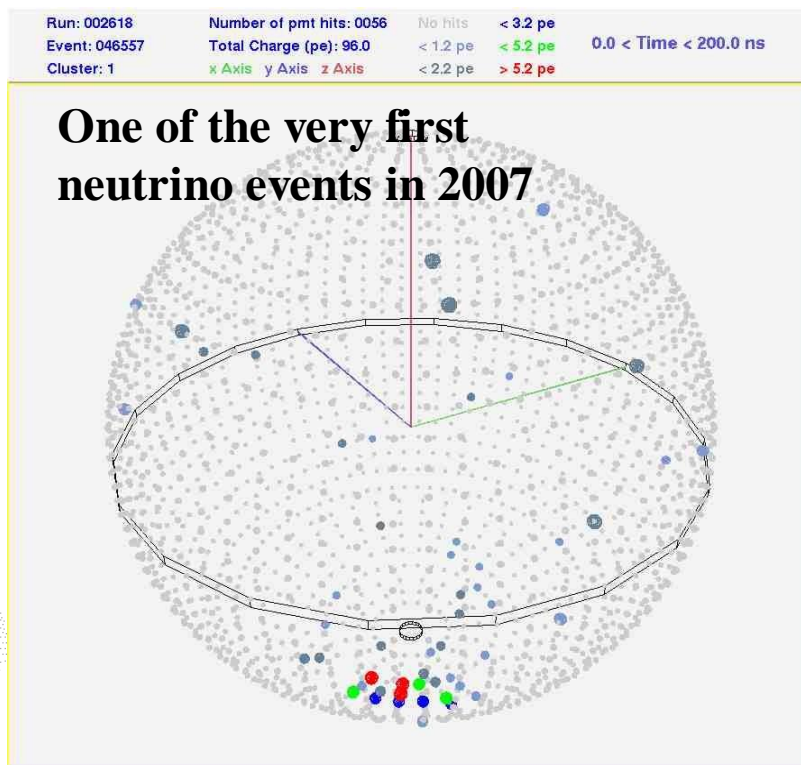
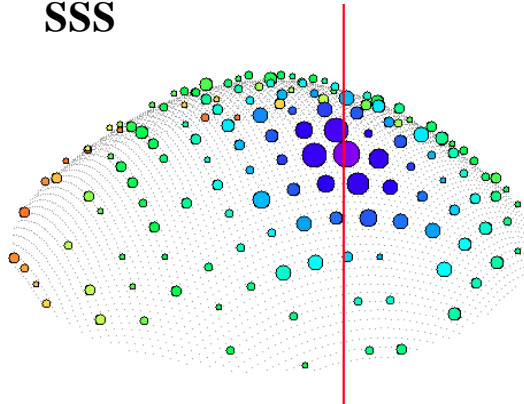
Solar neutrino events



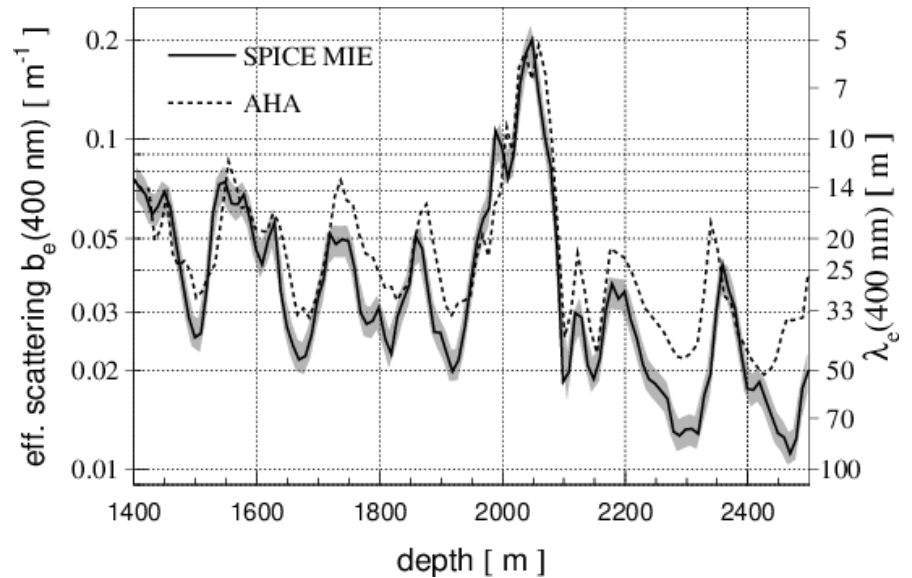
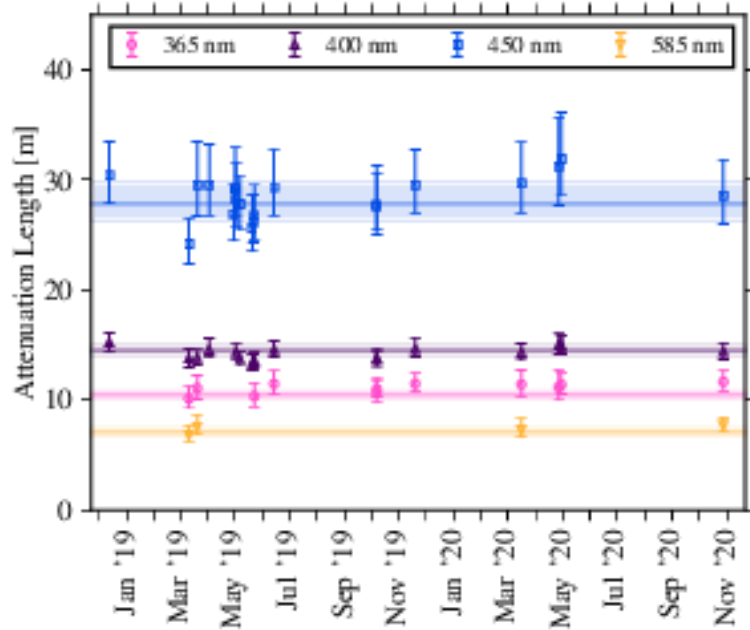
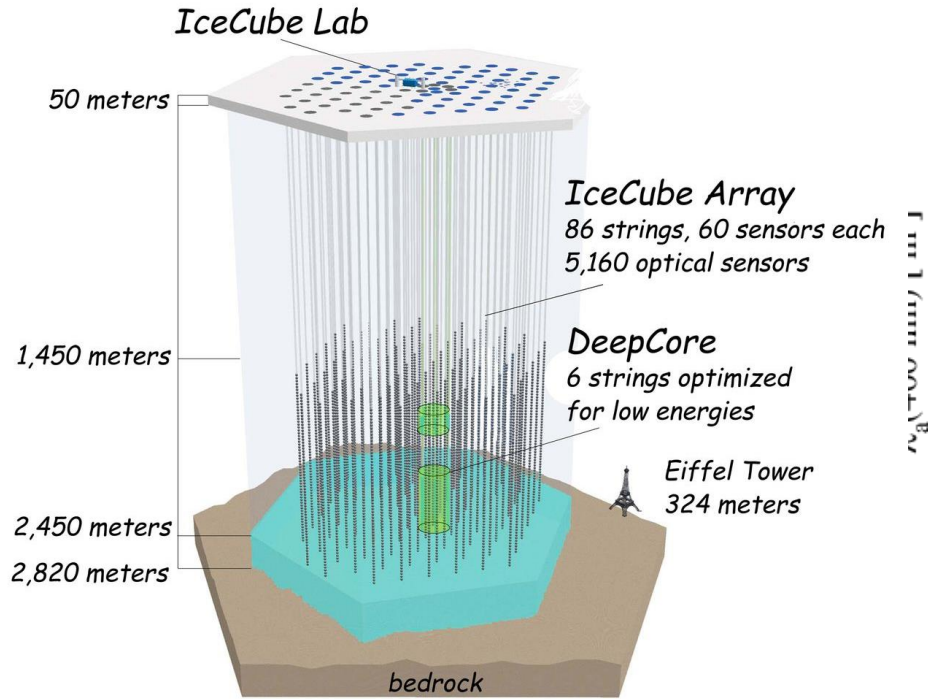
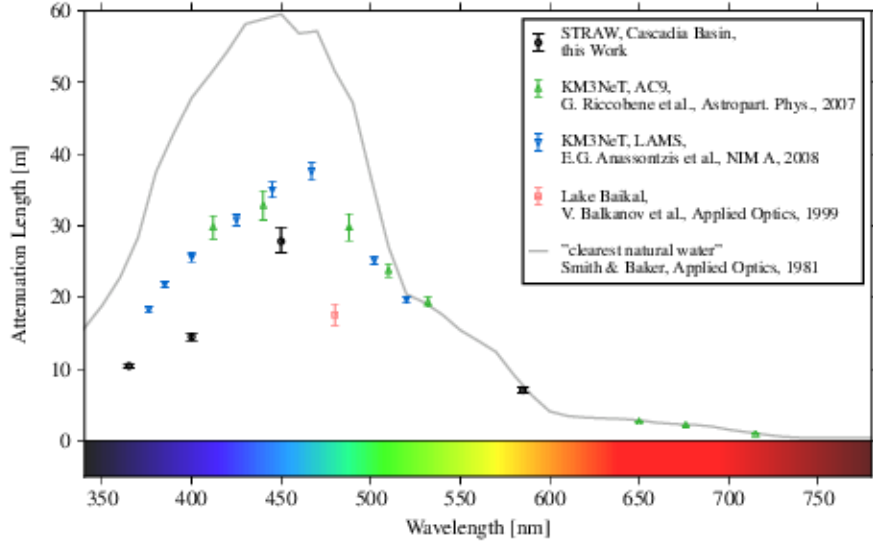
Radioactive bkg



the Cherenkov cone of a muon that is crossing the curved surface of the SSS

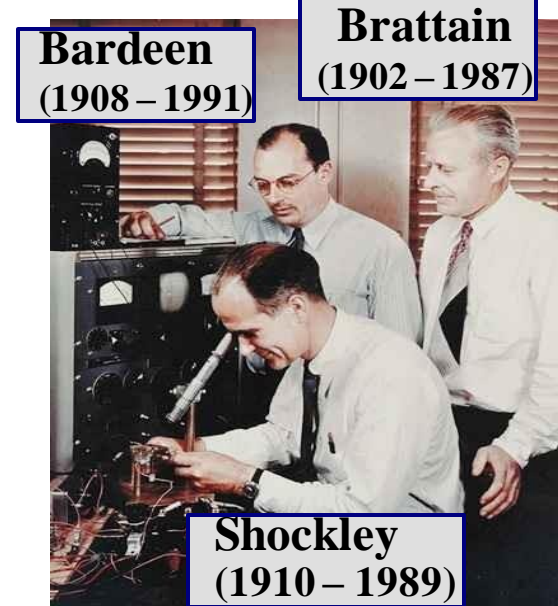


Light attenuation in water and ice

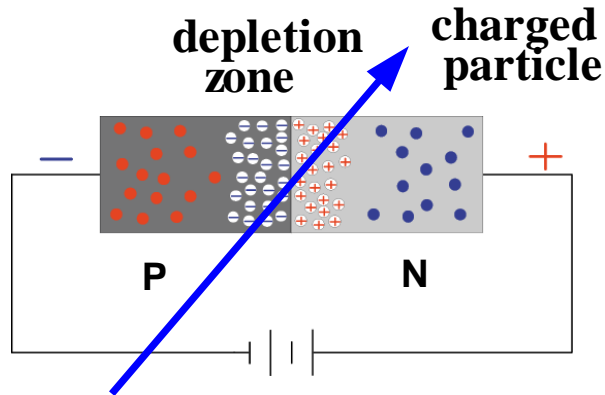


Solid State Detectors

- First transistor was invented 1947 by William B. Shockley, John Bardeen and Walter Brattain (Nobel Prize 1956)
- Transistors and diodes became common soon after
- Germanium diodes were used for particle detection
 - **p-type and n-type doped silicon material is put together and operated with reversed voltage**



more holes more electrons



- Around junction of p- and n-type material depletion zone is created

- Zone is free of charge carriers

- no holes, no electrons

- thickness of depletion zone depends on voltage, doping concentration ($V_{app} = \frac{q}{2\epsilon} |N_{eff}| D^2$)

Si (drift vel. of electron @ 150V/300 μ m)
 6.75×10^4 m/s

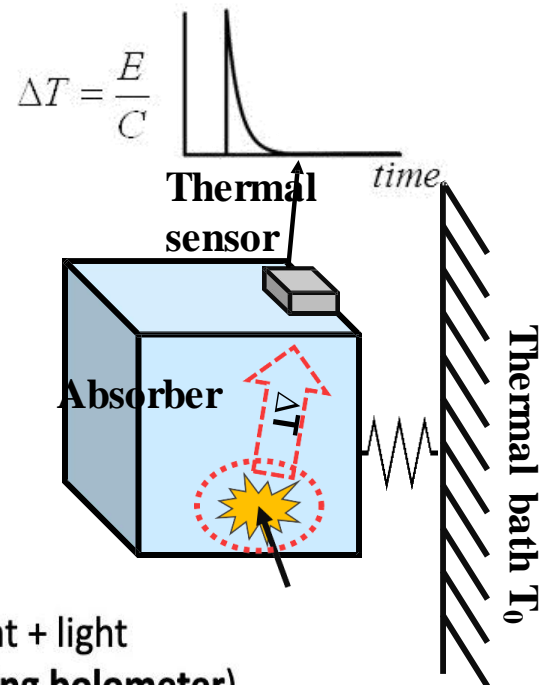
Drift velocity of electron in **Cu** $\sim 10^{-3}$ m/s (Thermal motion @ 300K $\sim 2 \times 10^2$ m/s)

A Charged particle typically creates 20k – 30k electron/hole pairs in 300 μ m thick material \rightarrow sufficient signal size

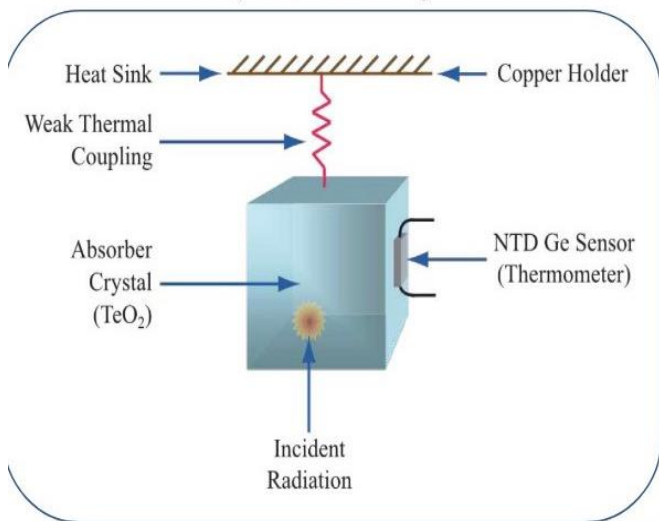
• All signals in particle detectors are due to induction by moving charges.
– Once the charges have arrived at the electrodes the signals are 'over'.

Thermal sensors

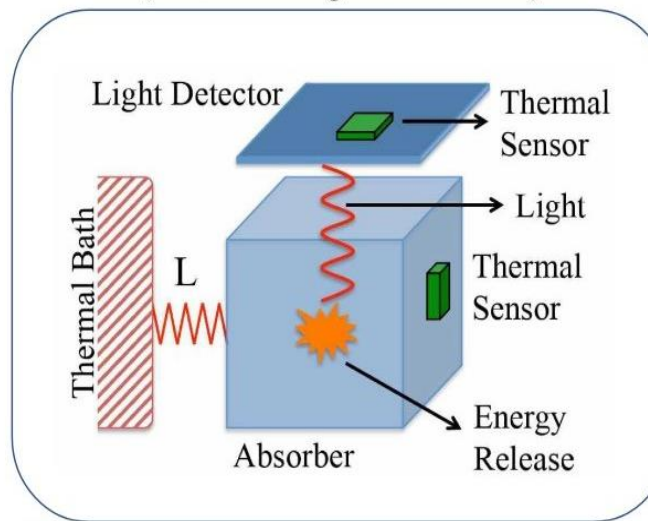
- TIPP slides



pure thermal detector
(bolometer)



heat + light
(scintillating bolometer)



Cherenkov Radiation

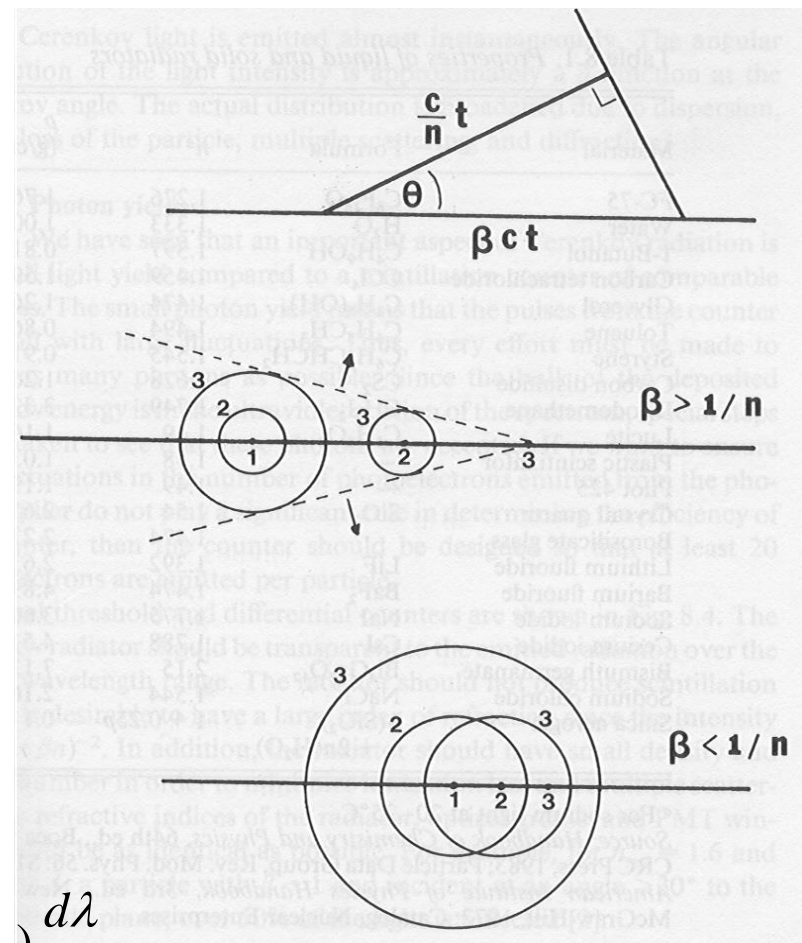
Occurs when the velocity of a charged particles exceeds the velocity of light in a dielectric medium. Polarisation of particles in the vicinity of trajectory. **Electromagnetic shock wave**

- The direction of emission of Cherenkov light, $\cos\theta = 1/n\beta$,
- Criteria : $n\beta \geq 1$ (or $\gamma > 1/(1-1/n^2)^{1/2}$)
- The amount of energy emitted per unit frequency interval $d\omega$ by a particle of charge Ze ,

$$\frac{dE}{dx d\omega} = \frac{Z^2 e^2}{c^2} \left(1 - \frac{1}{\beta^2 n^2}\right) \omega; \quad \frac{dN}{dx} = 2\pi\alpha \int_{\beta n > 1} \left(1 - \frac{1}{\beta^2 n^2}\right) \frac{d\lambda}{\lambda^2}$$

$$\frac{dN}{dx} = 2\pi\alpha \sin^2 \theta \left(\frac{1}{\lambda_1} - \frac{1}{\lambda_2} \right); \text{ for } 350 - 500 \text{ nm}; \quad \frac{dN}{dx} = 390 \sin^2 \theta \text{ photons/cm}$$

$$\frac{dN}{dx} \xrightarrow{\beta \approx 1} \begin{cases} 76/\text{cm in water/ice} \\ 0.15/\text{cm in air } (\sim 8\text{km}) \end{cases} \text{ for } 300\text{nm} \leq \lambda \leq 600\text{nm}$$

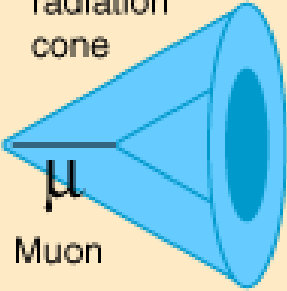


Cherenkov light

Cerenkov radiation cone

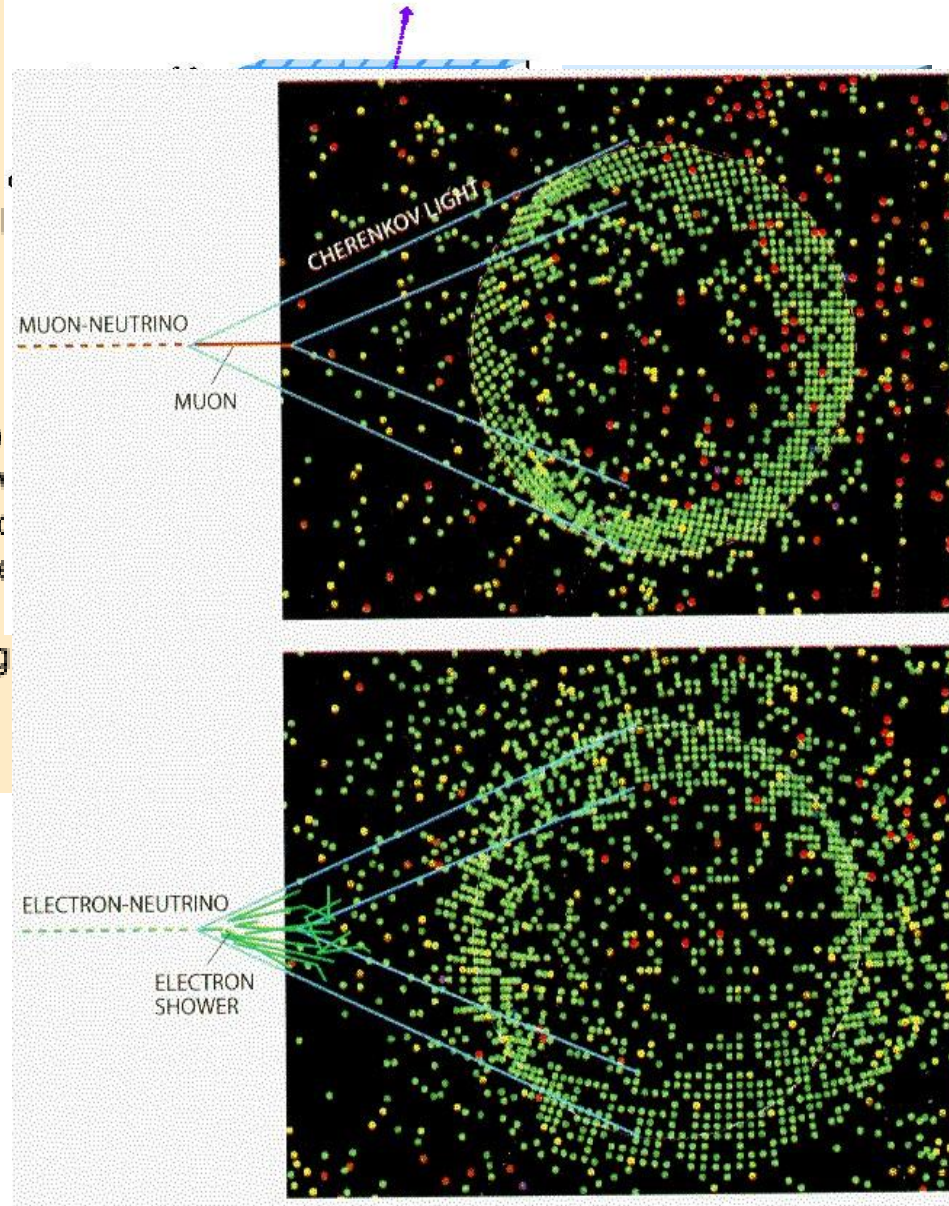
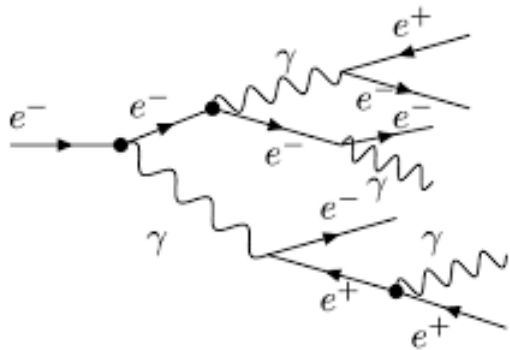
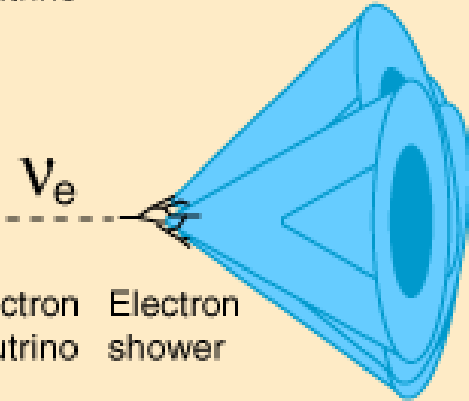
The Cerenkov radiation from a muon produced by a muon neutrino event yields a well defined circular ring in the photomultiplier detector bank.

ν_{μ} Muon neutrino
 μ Muon

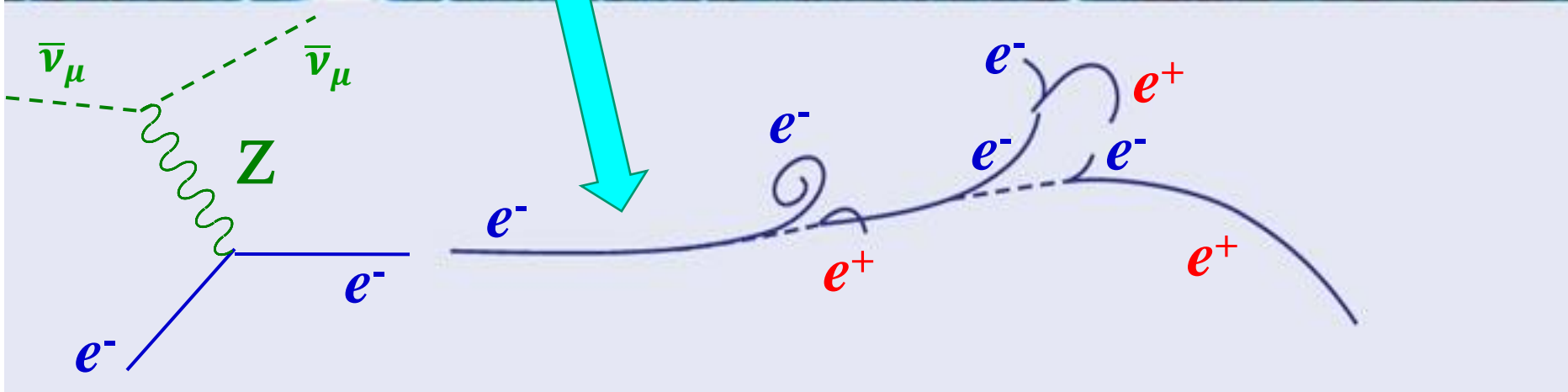
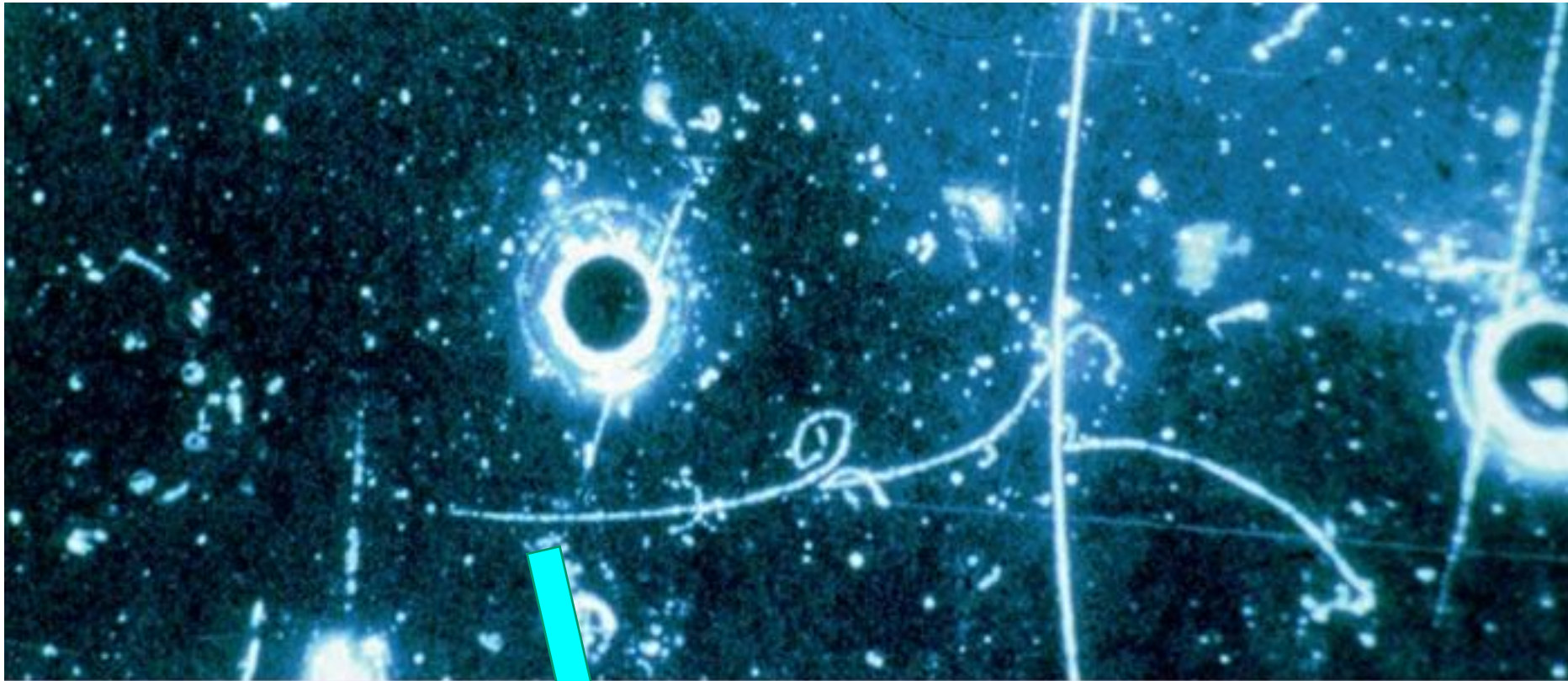


The Cerenkov radiation from the electron shower produced by an electron neutrino event produces multiple cones and therefore a diffuse ring in the detector array.

ν_e Electron neutrino
 Electron shower



Discovery of Neutral Currents (1973)

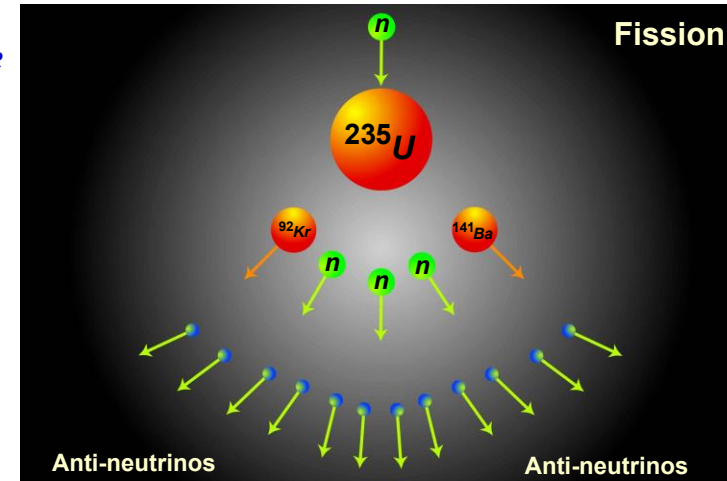


Production and Detection of Reactor Neutrinos 1801.05386

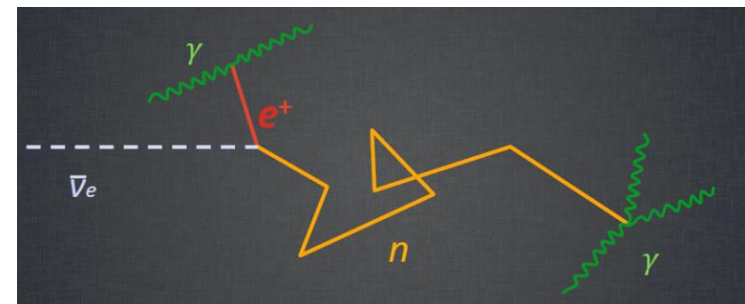
- **Beta decay** : $n \rightarrow p + e^- + \bar{\nu}_e \rightarrow e^+ + n \rightarrow p + \bar{\nu}_e$
- **Inverse Beta decay** : $\bar{\nu}_e + p \rightarrow e^+ + n$ ($E_{th}=1.806$ MeV)
- $E_{th} = 1.806$ MeV, almost all reactor neutrino expt, also use neutron capture, (n, γ) reaction to improve S/N. **Energy release on thermal neutron capture,**
- $E_{\bar{\nu}_e} \sim E_{e^+} + (m_n + m_e - m_p) \sim E_{e^+} + 1.806$ MeV (assuming K.E. of neutron is 0) $\rightarrow E_{\bar{\nu}_e} = E_{prompt} + 0.792$ MeV
- $E_{prompt} = E_{e^+} + 2 \times m_e = E_{e^+} + 1.022$ MeV

For 58%, 29%, 8%, and 5% for ^{235}U , ^{239}Pu , ^{238}U , and ^{241}Pu

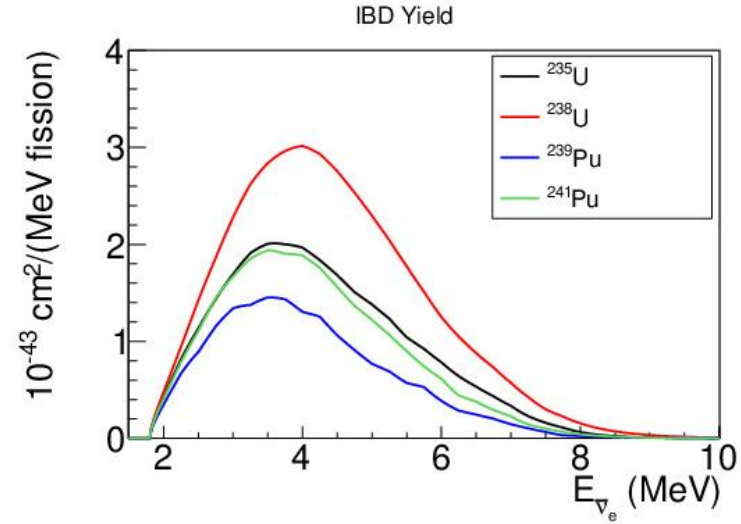
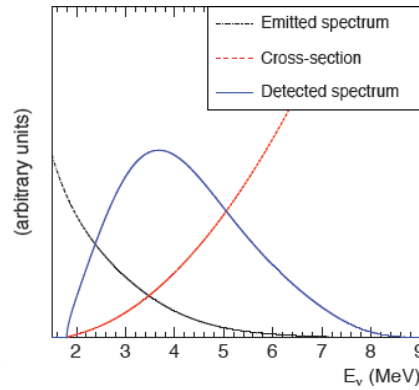
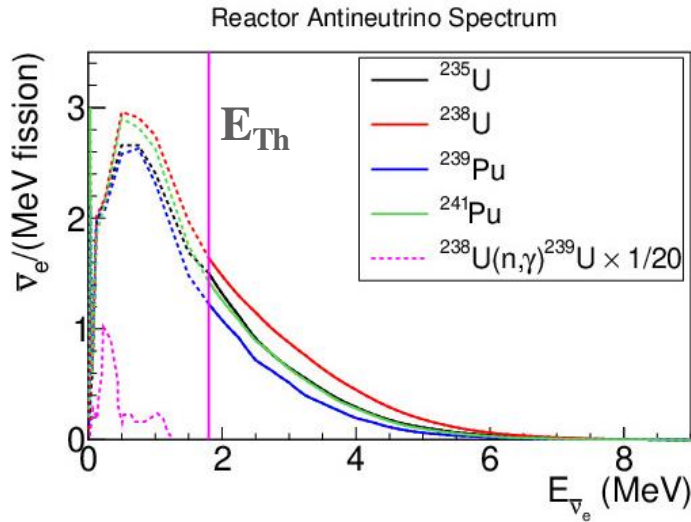
| Channel | Type | σ (10^{-44} cm ² /fission) | E_{th} (MeV) |
|---|-------|---|----------------|
| $\bar{\nu}_e + p \rightarrow e^+ + n$ | CC | ~63 | 1.8 |
| $\bar{\nu}_e + d \rightarrow e^+ + n + n$ | CC | ~1.1 | 4.0 |
| $\bar{\nu}_e + d \rightarrow e^+ + n + p$ | NC | ~3.1 | 2.2 |
| $\bar{\nu}_e + e^- \rightarrow \bar{\nu}_e + e^-$ | CC/NC | ~0.4 | 0 |
| $\bar{\nu}_e + A \rightarrow \bar{\nu}_e + A$ | NC | ~9.2 \times N ² | 0 |



For a typical reactor: $P_t = 3 \times 10^9$ W $\Rightarrow 5.6 \times 10^{20} \bar{\nu}_e / \text{s}$ (isotropic)
Continuous $\bar{\nu}_e$ energy spectrum - average energy ~ 3 MeV

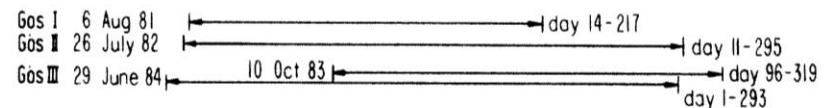
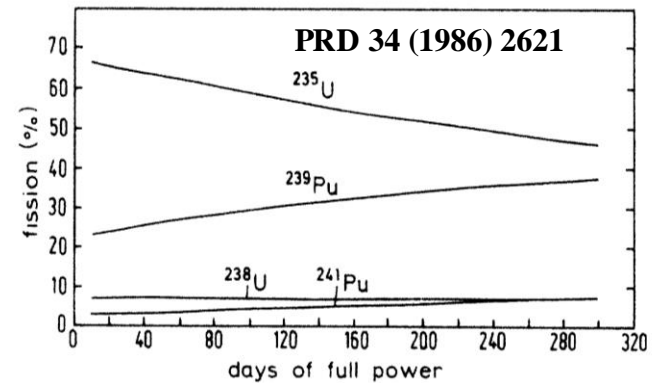


Production and Detection of Reactor Neutrinos 1801.05386

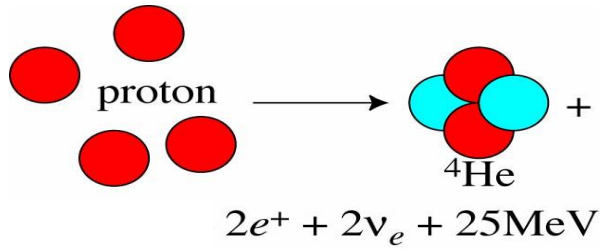


- IBD cross-section, $\sigma^{(0)} = \frac{G_F^2 \cos^2 \theta_c}{\pi} (1 + \Delta_{inner}^R) \cdot (f^2 + 3g^2) \cdot E_e^{(0)} \cdot p_e^{(0)}$, f and g are vector and axial coupling..... $f=1, g=1.27, \sigma^{(0)} \approx 9.52 \left(\frac{E_e^{(0)} \cdot p_e^{(0)}}{\text{MeV}^2} \right) \times 10^{-44} \text{ cm}^2$

In the commercial reactor neutrino flux spectrum change with time due to change in core material



Solar neutrino



$$L_{\text{sun}} \sim 4 \times 10^{26} \text{ W}$$

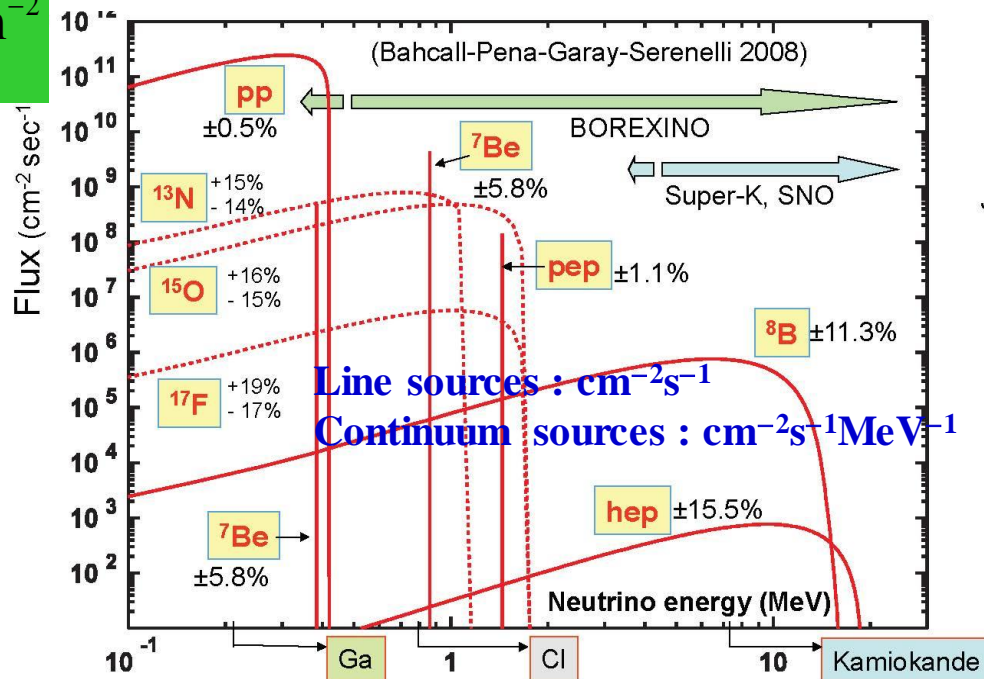
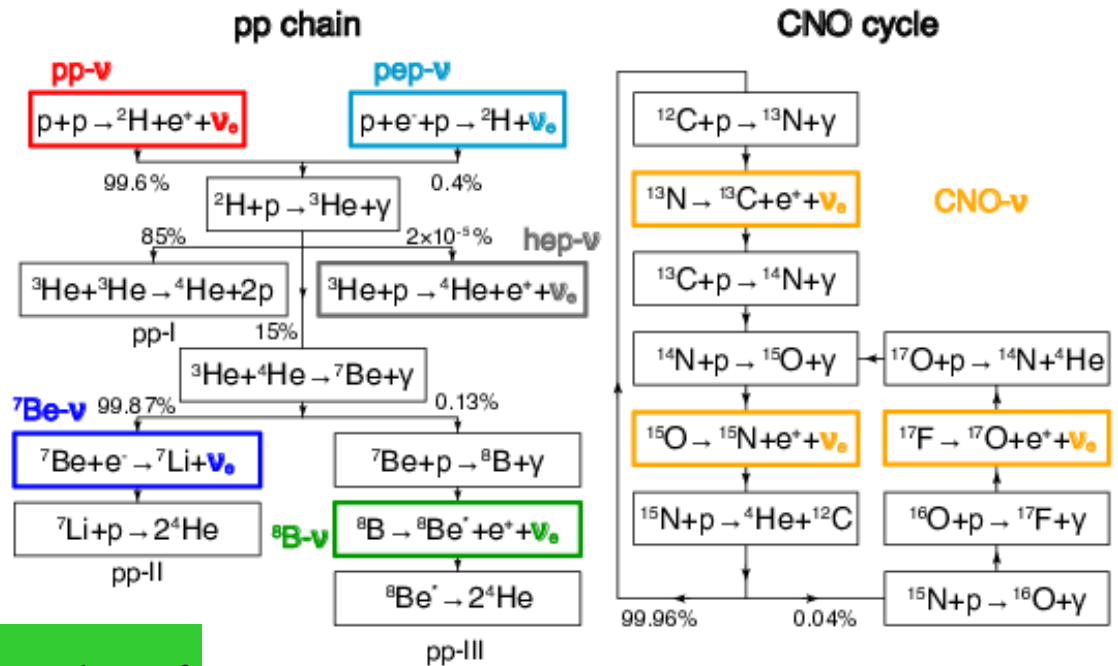
$$2 \times 10^{38} \text{ } \nu/\text{sec}$$

$$\Phi_{\nu} = \frac{2L_{\text{sun}}}{25\text{MeV}} \frac{1}{4\pi(1\text{AU})^2} = 7 \cdot 10^{10} \text{ sec}^{-1} \text{ cm}^{-2}$$

CNO cycle contributes only about 1% of the solar luminosity

${}^7\text{Be}$:
862 keV (90%, ground state)
384 keV (10%, excited state)

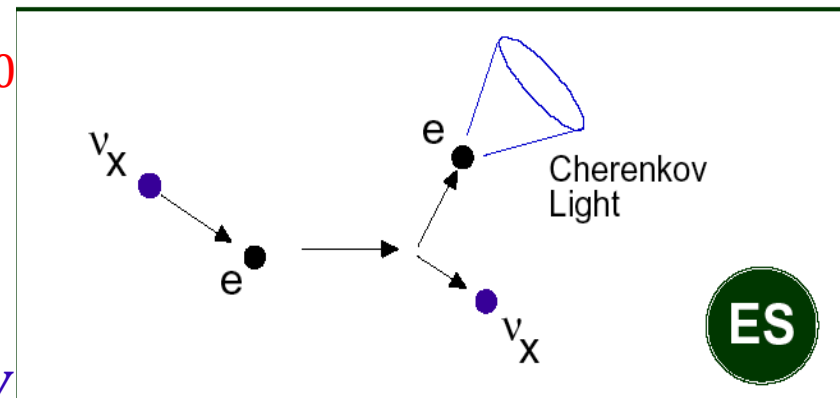
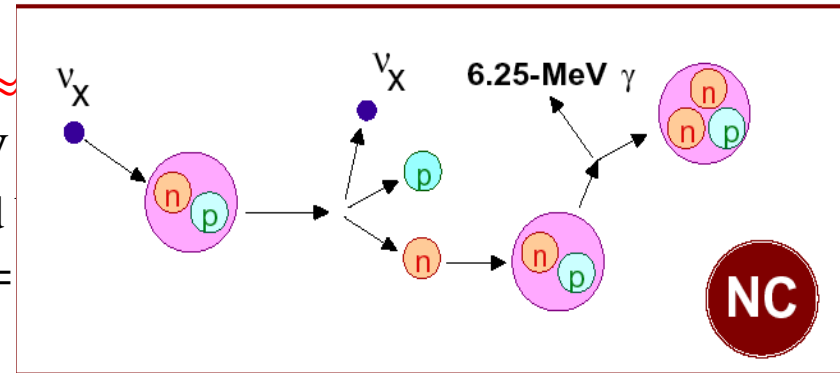
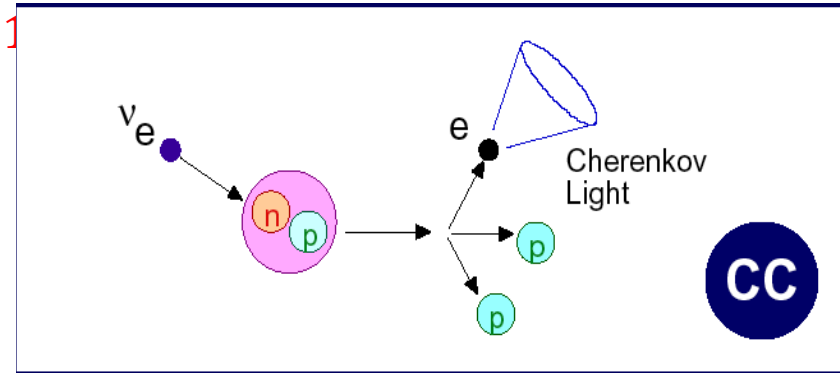
Only few tens of counts per days in 100t of scintillator



Measurement of both CC and NC events at the same time

Detect Cherenkov light from three different reactions : SNO

- Charge Current ($\nu_e + d \rightarrow p + p + e^-$) $E_{\nu_{th}} \approx 1.8$ MeV
 - Detect Cherenkov light from electron
 - Only sensitive to ν_e (above threshold)
 - Gives a measure of ν_e flux
 - CC Rate $\propto \phi(\nu_e)$
 - Measurement of ν_e energy spectrum
 - Weak directionality : $1 - 0.34 \cos\theta$
- Neutral Current ($\nu_x + d \rightarrow p + n + \nu_x$) $E_{\nu_{th}} \approx 2.2$ MeV
 - Neutron capture on a deuteron gives 6.25 MeV
 - Detect Cherenkov light from electrons scattered
 - Measures total neutrino flux, $\sigma(\nu_e) = \sigma(\nu_\mu) = \sigma(\nu_\tau)$
 - NC rate $\propto [\phi(\nu_e) + \phi(\nu_\mu) + \phi(\nu_\tau)]$
 - Measure total ^8B ν flux from the sun
- Elastic scattering ($\nu_x + e^- \rightarrow \nu_x + e^-$) $E_{\nu_{th}} \approx 0$ MeV
 - Detect Cherenkov light from electron
 - Sensitive to all neutrinos (NC part),
 - Low Statistics, but large cross section for ν_e
 - ES Rate $\propto [\phi(\nu_e) + 0.154\{\phi(\nu_\mu) + \phi(\nu_\tau)\}]$
 - Strong directionality : $\theta_e \leq 18^\circ$ ($T_e = 10$ MeV)



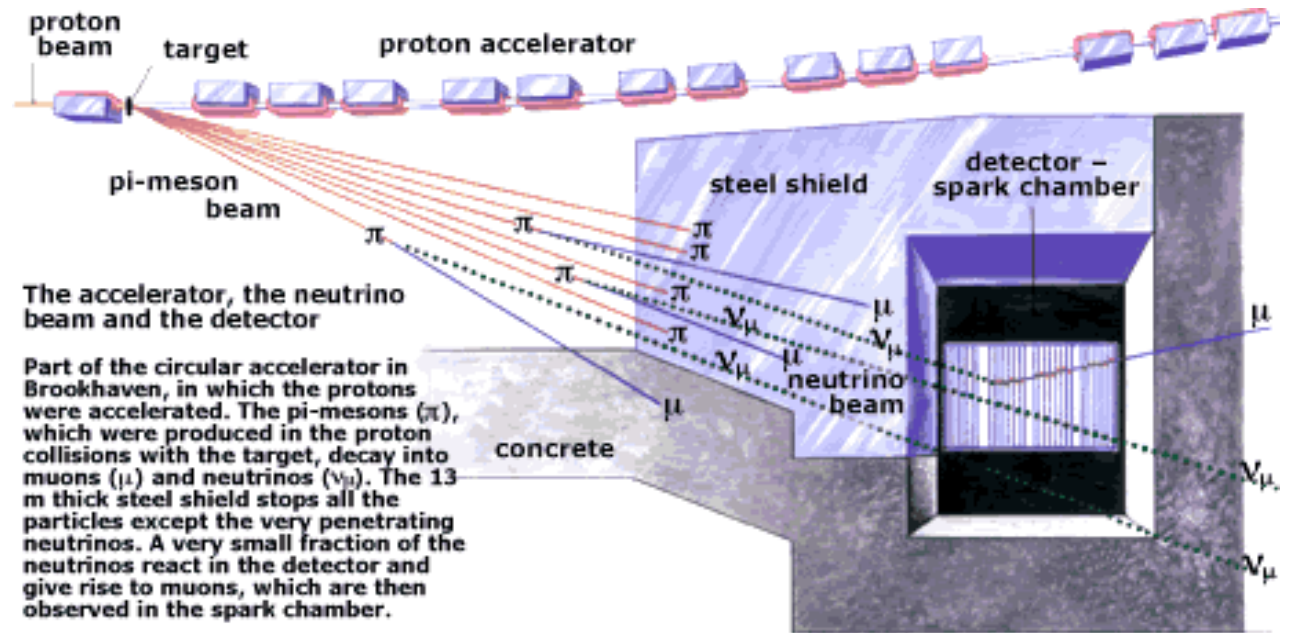
Neutrino Beam : Schematic of set up at AGS-BNL (1962)

$$\nu + n \rightarrow p + e^-$$

$$\bar{\nu} + p \rightarrow n + e^+$$

$$\nu + n \rightarrow p + \mu^-$$

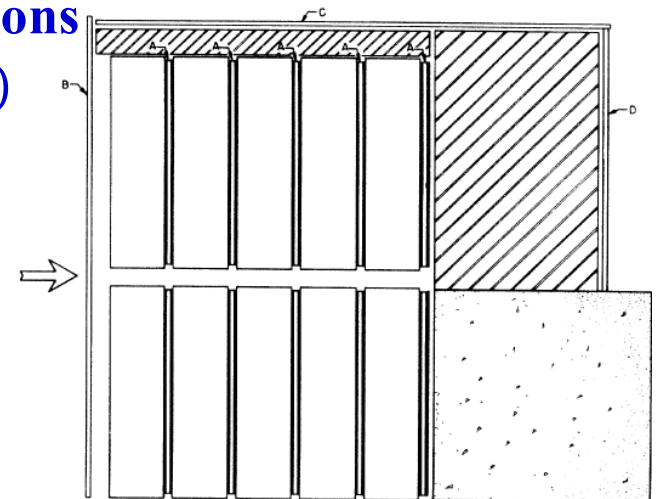
$$\bar{\nu} + p \rightarrow n + \mu^+$$



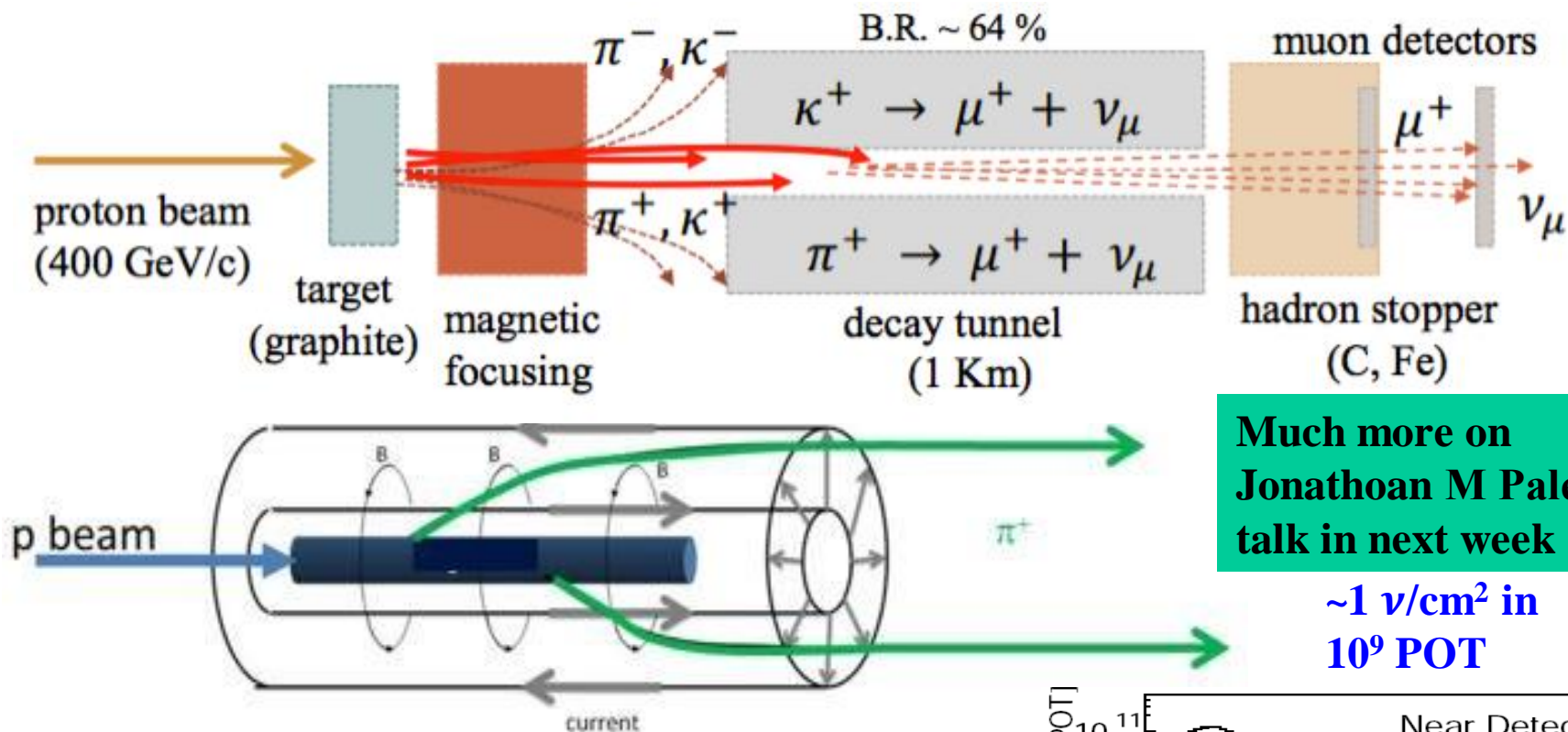
Based on a drawing in Scientific American, March 1963.

- 3" thick Be target in straight section, produces pions and kaons $\pi^\pm \rightarrow \mu^\pm + \nu_\mu (\bar{\nu}_\mu)$, $K^\pm \rightarrow \mu^\pm + \nu_\mu (\bar{\nu}_\mu)$
- Lifetimes: π (26 nsec), μ (2.2 μ sec), K (12.4 nsec)

- 13.5m steel shielding (deck plates of dismantled cruiser ship!) in front of a 10 ton Al spark chamber detector at 21m from the target. Stops penetrating muons.



Concept of focussing either +ve/-ve charge for $\nu_\mu/\bar{\nu}_\mu$ beam

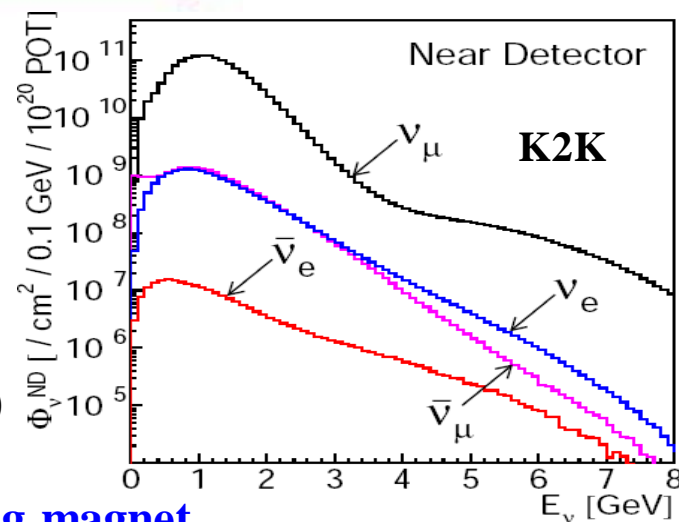


Much more on
Jonathoan M Paley's
talk in next week

~1 ν/cm^2 in
10⁹ POT

• But contaminations from

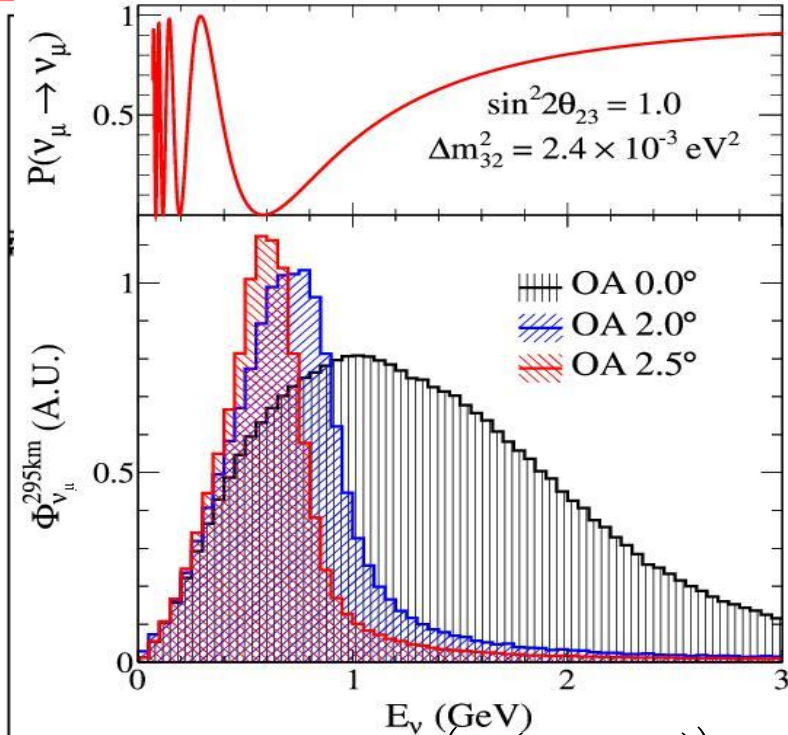
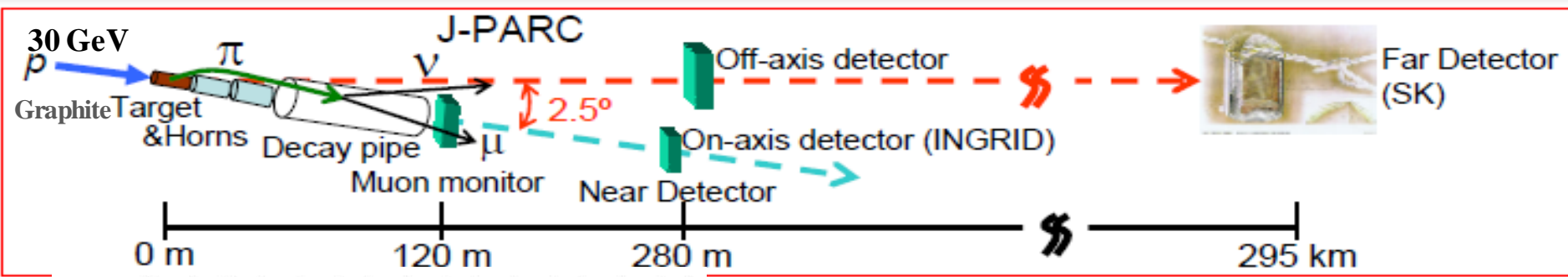
- Secondary decay of muon : $\mu \rightarrow e \nu_\mu \nu_e$ ($\beta \approx 100\%$)
- k_{e3}^+ decay of charged kaon : $K^\pm \rightarrow \pi^0 e \nu_e$ ($\beta \approx 5.07\%$)
- k_{e3}^0 decay of neutral kaon : $K_L^0 \rightarrow \pi^\pm e^\mp \nu_e$ ($\beta \approx 40.55\%$)
- $k_{\mu 3}^0$ decay of neutral kaon : $K_L^0 \rightarrow \pi^\pm \mu^\mp \nu_\mu$ ($\beta \approx 27.04\%$)



Relative fractions depends on beam energy and focussing magnet

Experimental apparatus and neutrino beam (T2K)

91.4cm Graphite target + 96m He-filled decay volume at downward angle -3.6° .



- ➔ Off-axis beam technique
 - ➔ Intense narrow band beam
- ➔ 2.5° off-axis
 - ➔ Energy peak tuned at oscillation max. ~ 0.7 GeV
- Projected 4km south and 12km below the SK
 - ➔ Statistics at Super-K
 - ➔ ~ 1600 ν_μ CC int./22.5kt/year (with 0.75kW beam, no oscillation case)
 - ➔ Pure ν_μ beam
 - ➔ Beam ν_e contamination $\sim 0.4\%$ at ν_μ peak energy

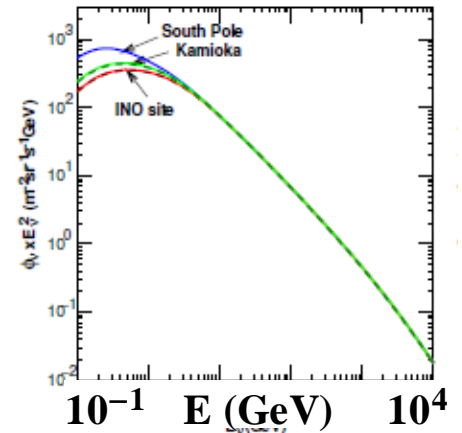
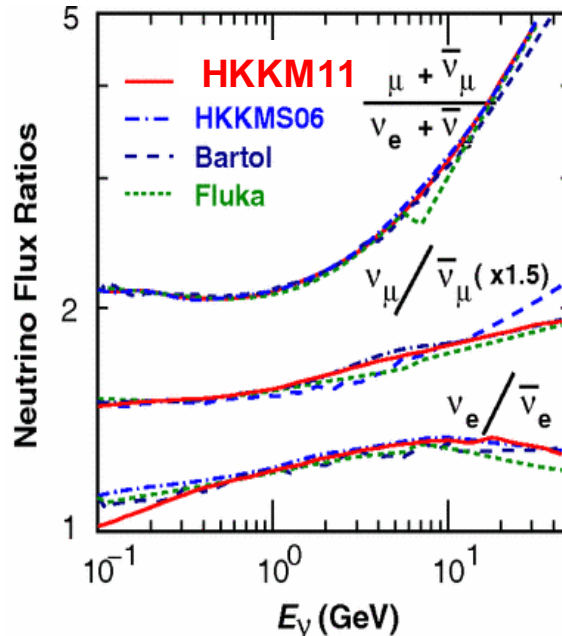
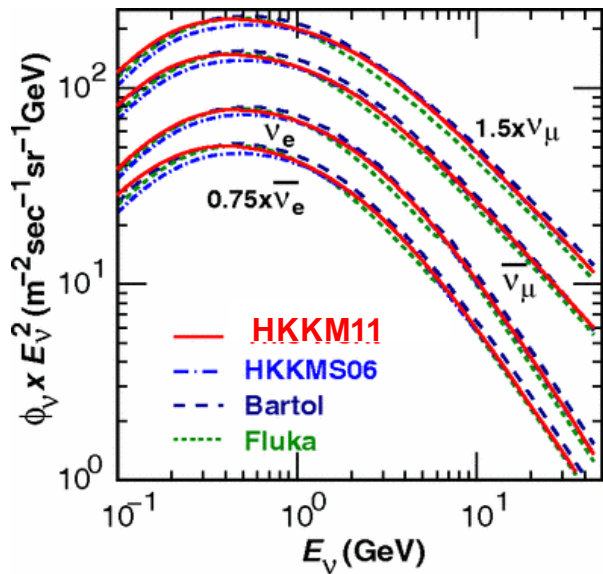
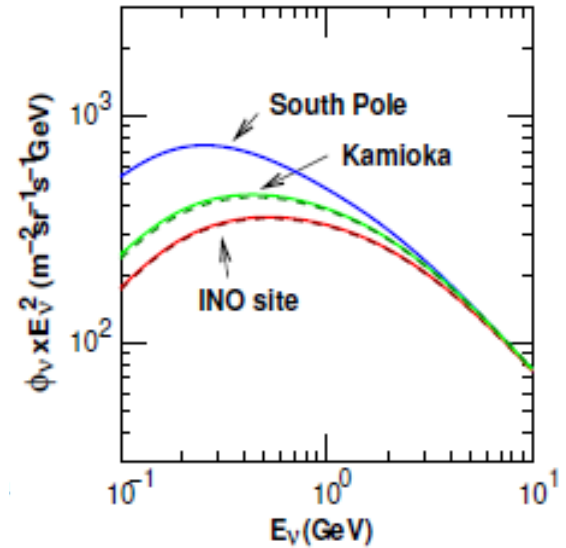
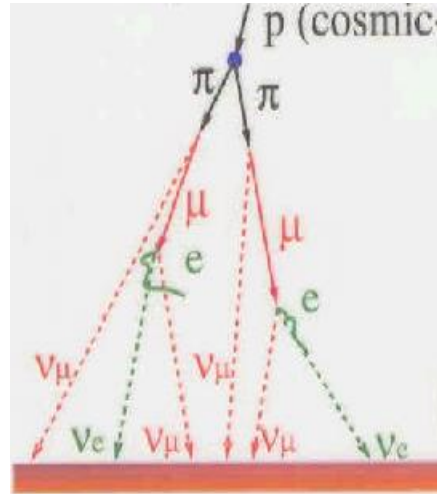
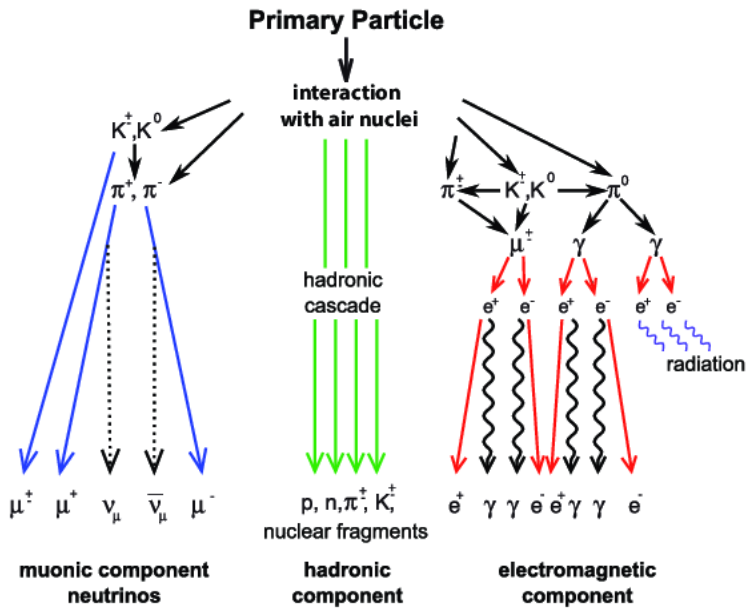
$$E_\nu = \frac{m_{\pi/k}^2 - m_\mu^2}{2(E_{\pi/k} - p_{\pi/k} \cos\theta)} \approx \frac{\left(1 - \left(m_\mu^2/m_{\pi/k}^2\right)\right) E_{\pi/k}}{1 + \gamma^2 \tan^2\theta} \approx \frac{0.43 E_\pi}{1 + \gamma^2 \theta^2} \text{ (for } \pi\text{)}$$

$$Flux = \left(\frac{2\gamma}{1 + \gamma^2 \theta^2} \right) \frac{A}{4\pi D^2}$$

Atmospheric Neutrino

- Cosmic neutrino, $R = \frac{\phi(\nu_\mu) + \phi(\bar{\nu}_\mu)}{\phi(\nu_e) + \phi(\bar{\nu}_e)} \approx 2$

- Sharply falling spectrum
 $\nu_e + \bar{\nu}_e + \nu_\mu + \bar{\nu}_\mu$



Threshold energy of neutrino interaction

- **Threshold production :** $\nu \text{ -----} \rightarrow \odot t$

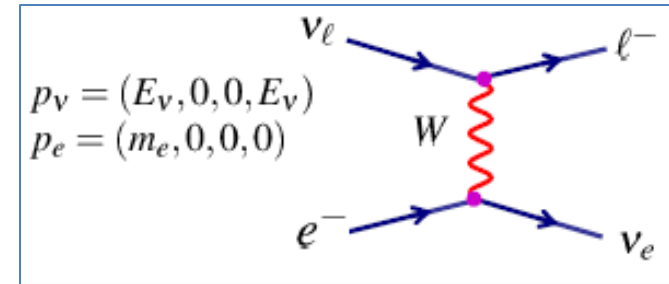
$$(E_\nu, 0, 0, +E_\nu) \ \& \ (m_t, 0, 0, 0) \rightarrow s = (E_\nu + m_t)^2 - E_\nu^2 = 2E_\nu m_t + m_t^2$$

$$= (m_\ell + m_{t'})^2 \Rightarrow E_\nu^{th} = \frac{(m_{t'}^2 - m_t^2) + m_\ell^2 + 2m_\ell m_{t'}}{2m_t}$$

- **CC on atomic electrons, $m_{t'} = m_\nu \approx 0$ (lab frame) :**

$$- E_\nu > \left[\left(\frac{m_\ell}{m_e} \right)^2 - 1 \right] \frac{m_e}{2}$$

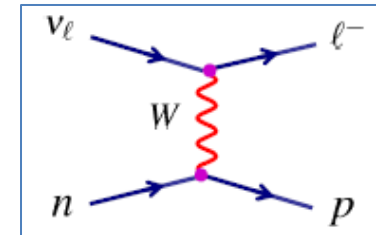
$$- E_{\nu_e} > 0, \quad E_{\nu_\mu} > 11 \text{ GeV}, \quad E_{\nu_\tau} > 3090 \text{ GeV}$$



- **CC on free nucleons (ν_ℓ at lab frame) :** $E_\nu > \frac{(m_p^2 - m_n^2) + m_\ell^2 + 2m_p m_\ell}{2m_n}$

$$\bullet E_{\nu_e} > 0, \quad E_{\nu_\mu} > 110 \text{ MeV}, \quad E_{\nu_\tau} > 3.454 \text{ GeV}$$

$$E_{\bar{\nu}_e} > 1.806 \text{ MeV}, \quad E_{\bar{\nu}_\mu} > 113 \text{ MeV}, \quad E_{\bar{\nu}_\tau} > 3.463 \text{ GeV}$$



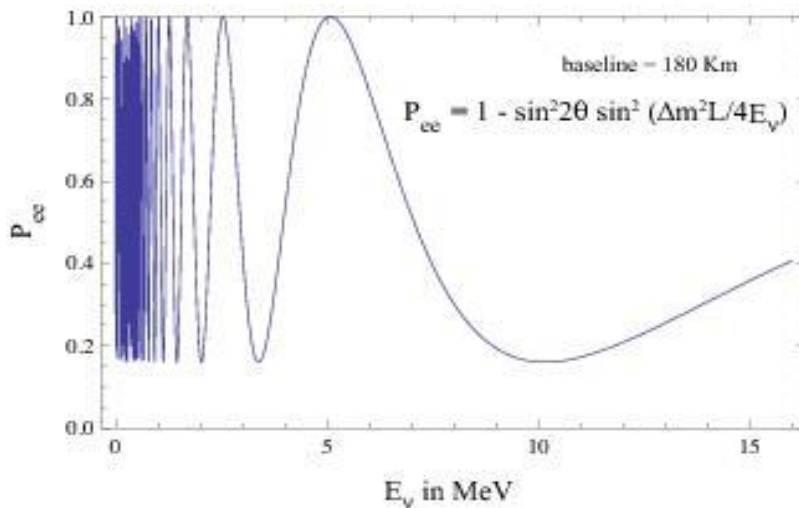
- **Electron neutrinos from the sun and nuclear reactors $E_\nu \sim 1 \text{ MeV}$ which oscillate into muon or tau neutrinos cannot interact via charged current interactions – “they effectively disappear”**

- **Atmospheric muon neutrinos $E_\nu \sim 1 \text{ GeV}$ which oscillate into tau neutrinos cannot interact via charged current interactions – “disappear”**

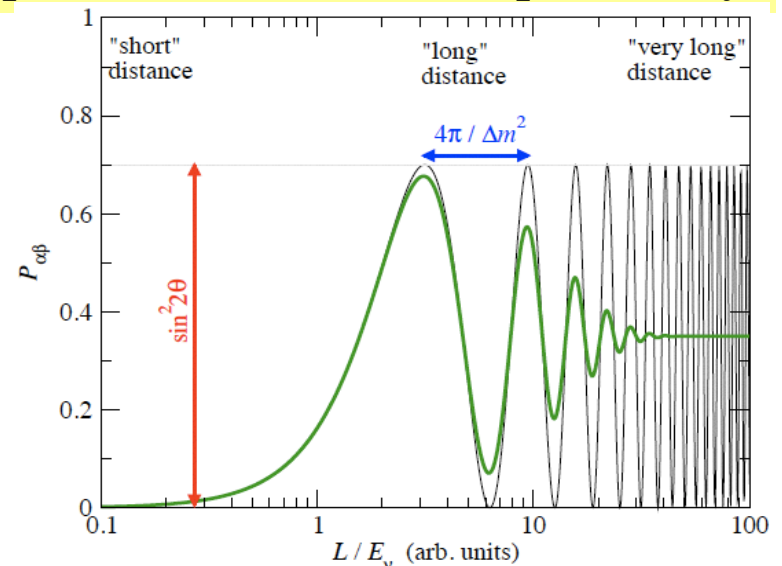
Neutrino oscillation

- $P(\nu_e \rightarrow \nu_e) = 1 - 4[|U_{e1}|^2|U_{e2}|^2 \sin^2 \Delta_{21} + |U_{e1}|^2|U_{e3}|^2 \sin^2 \Delta_{31} + |U_{e2}|^2|U_{e3}|^2 \sin^2 \Delta_{32}]$
 – Where $\Delta_{ij} = \frac{\phi_i - \phi_j}{2} = \frac{(m_i^2 - m_j^2)c^4 L}{4\hbar c E} = \frac{\Delta m_{ij}^2 (\text{eV}^2) L (\text{km})}{E (\text{GeV})} = \pi$ (for $L = \lambda_{osc}$)
 - $\rightarrow \lambda_{osc} (\text{km}) = 2.47 \left(E (\text{GeV}) / \Delta_{ij}^2 (\text{eV}^2) \right)$
- For solar neutrino, $E \sim 1 \text{ MeV} \rightarrow \lambda_{osc} (\text{km}) = 2.47 \frac{10^{-3}}{7.4 \times 10^{-5}} \sim 33 \text{ km}$ (for solar/reactor), but for shortbase line experiments, Δ_{31}^2 is important and $\lambda_{osc} (\text{km}) = 2.47 \frac{10^{-3}}{2.45 \times 10^{-3}} \sim \text{km}$
- For atmospheric neutrinos, $E \sim 1 \text{ GeV} \rightarrow \lambda_{osc} (\text{km}) = 2.47 \frac{1}{2.45 \times 10^{-3}} \sim 1000 \text{ km}$ (for $\mu \rightarrow \tau$), but for $(\mu \leftrightarrow e)$ $\lambda_{osc} (\text{km}) = 2.47 \frac{1}{7.4 \times 10^{-5}} \sim 33000 \text{ km}$, More than the diameter of the earth

Maximum deviation at $(\lambda_{osc} / 2)$



No phase (CPV) in survival probability

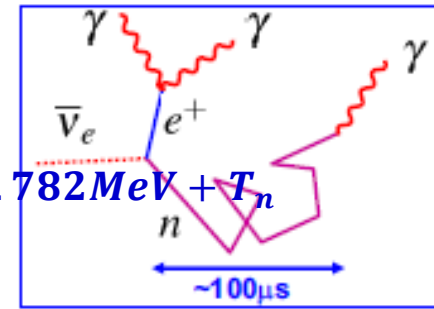


Neutrino detection

- **Reactor Neutrinos**

$$\bar{\nu}_e : E_{\bar{\nu}_e} < 5 \text{ MeV}$$

- **Liquid Scintillator**, e.g., Kamland, Daya Bay, JUNO, $E_{\bar{\nu}_e} \approx E_{\text{prompt}} + 0.782 \text{ MeV} + T_n$
 - **Low energy** → large radioactive background
 - **Dominant reaction** : $\bar{\nu}_e + p \rightarrow e^+ + n$
 - **Prompt position annihilation signal + delayed signal from n** (space/time correlation reduced background)
 - **Electrons produced by photons excite scintillator** which produces light or cherenkov signal



- **Solar Neutrino**

$$\nu_e : E_{\nu_e} < 20 \text{ MeV}$$

- **Water Cherenkov** : e.g., Super Kamiokande
 - **Detect Cherenkov light** from electron produced in $\nu_e + e^- \rightarrow \nu_e + e^-$
 - **Because of background from neutral radioactivity limited to $E_\nu > 5 \text{ MeV}$**
 - **Because Oxygen is a double magic nucleus don't get $\nu_e + n \rightarrow e^- + p$**
- **Liquid Scintillator**, e.g., BOREXINO,
- **Heavy water**, e.g., SNO
- **Radio Chemical**, e.g., Homestake, SAGE, GALEX
 - **Use inverse beta decay process**, e.g., $\nu_e + {}^{71}\text{Ga} \rightarrow e^- + {}^{71}\text{Ge}$, or ${}^{37}\text{Cl} + \nu_e \rightarrow {}^{37}\text{Ar} + e^-$
 - **Chemically extract produced isotope and count decays** (only gives a rate)

- **Atmospheric/Beam Neutrinos**

$$\nu_e, \nu_\mu, \bar{\nu}_e, \bar{\nu}_\mu : E_\nu \geq \text{GeV}$$

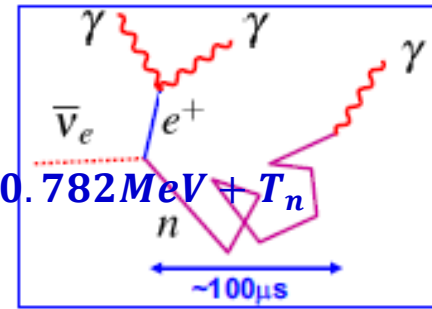
- **Water Cherenkov** : e.g., Super Kamiokande, KM3NeT, IceCube
- **Iron Calorimeter**, e.g., MINOS, ICAL, CDHS..
- **Liquid Argon detector**, e.g., ICARUS, MicroBooNE, DUNE
 - **Produce high energy charged lepton** → relatively easy to detect

Neutrino detection

- **Reactor Neutrinos**

$$\bar{\nu}_e : E_{\bar{\nu}_e} < 5 \text{ MeV}$$

- Liquid Scintillator, e.g., Kamland, Daya Bay, **JUNO**, $E_{\bar{\nu}_e} \approx E_{\text{prompt}} + 0.782 \text{ MeV} + T_n$
 - Low energy \rightarrow large radioactive background
 - Dominant reaction : $\bar{\nu}_e + p \rightarrow e^+ + n$
 - Prompt position annihilation signal + delayed signal from n (space/time correlation reduced background)
 - Electrons produced by photons excite scintillator which produces light or cherenkov signal



- **Solar Neutrino**

$$\nu_e : E_{\nu_e} < 20 \text{ MeV}$$

- Water Cherenkov : e.g., **Super Kamiokande**
 - Detect Cherenkov light from electron produced in $\nu_e + e^- \rightarrow \nu_e + e^-$
 - Because of background from neutral radioactivity limited to $E_\nu > 5 \text{ MeV}$
 - Because Oxygen is a double magic nucleus don't get $\nu_e + n \rightarrow e^- + p$
- Liquid Scintillator, e.g., BOREXINO,
- Heavy water, e.g., SNO
- ~~Radio Chemical, e.g., Homestake, SAGE, GALEX~~
 - Use inverse beta decay process, e.g., $\nu_e + {}^{71}\text{Ga} \rightarrow e^- + {}^{71}\text{Ge}$, or ${}^{37}\text{Cl} + \nu_e \rightarrow {}^{37}\text{Ar} + e^-$
 - Chemically extract produced isotope and count decays (only gives a rate)

- **Atmospheric/Beam Neutrinos**

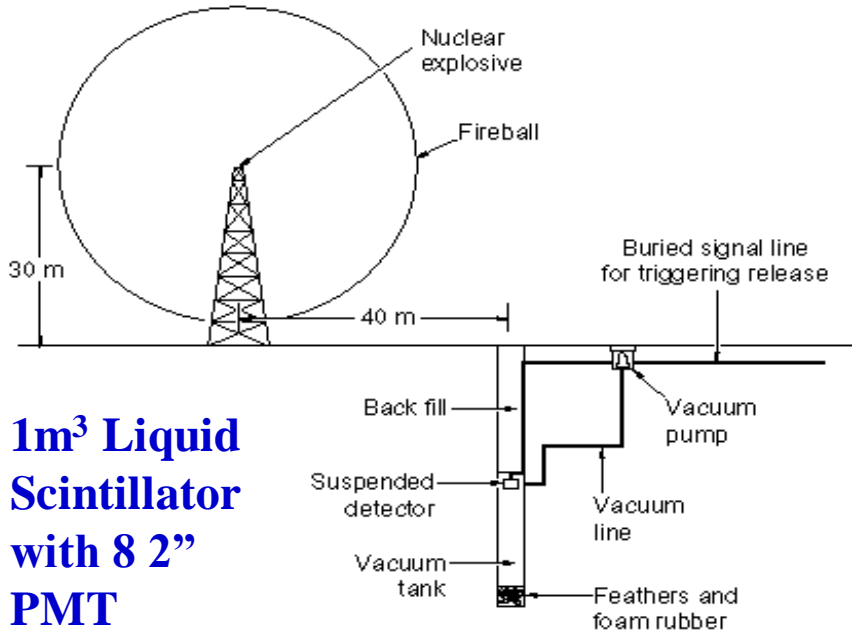
$$\nu_e, \nu_\mu, \bar{\nu}_e, \bar{\nu}_\mu : E_\nu \geq \text{GeV}$$

- Cherenkov : e.g., Super Kamiokande, KM3NeT, IceCube
- Iron Calorimeter, e.g., MINOS, ICAL, CDHS..
- Liquid Argon detector, e.g., ICARUS, MicroBooNE, **DUNE**
 - Produce high energy charged lepton \rightarrow relatively easy to detect

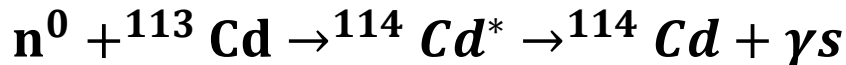
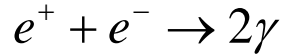
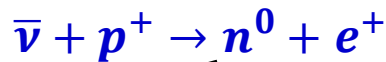
First detector to detect neutrino

- Initial plan was to put a detector (free fall to avoid any vibration) near nuclear bomb

Detector at Hanford 300l LS viewed by 90 2" PMT

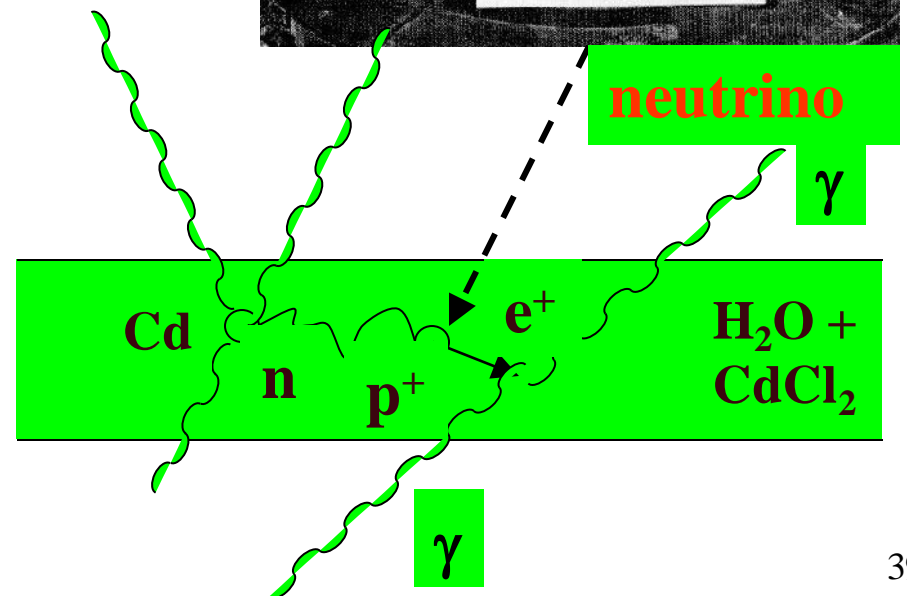
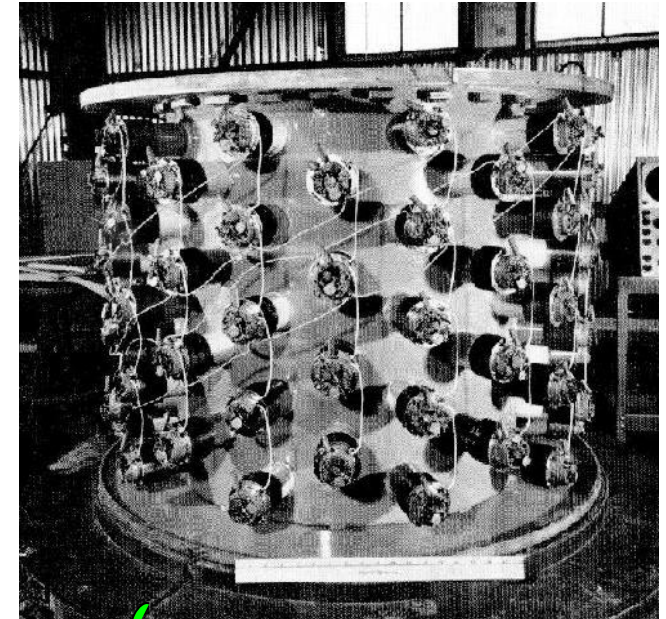


1m³ Liquid Scintillator with 8 2" PMT



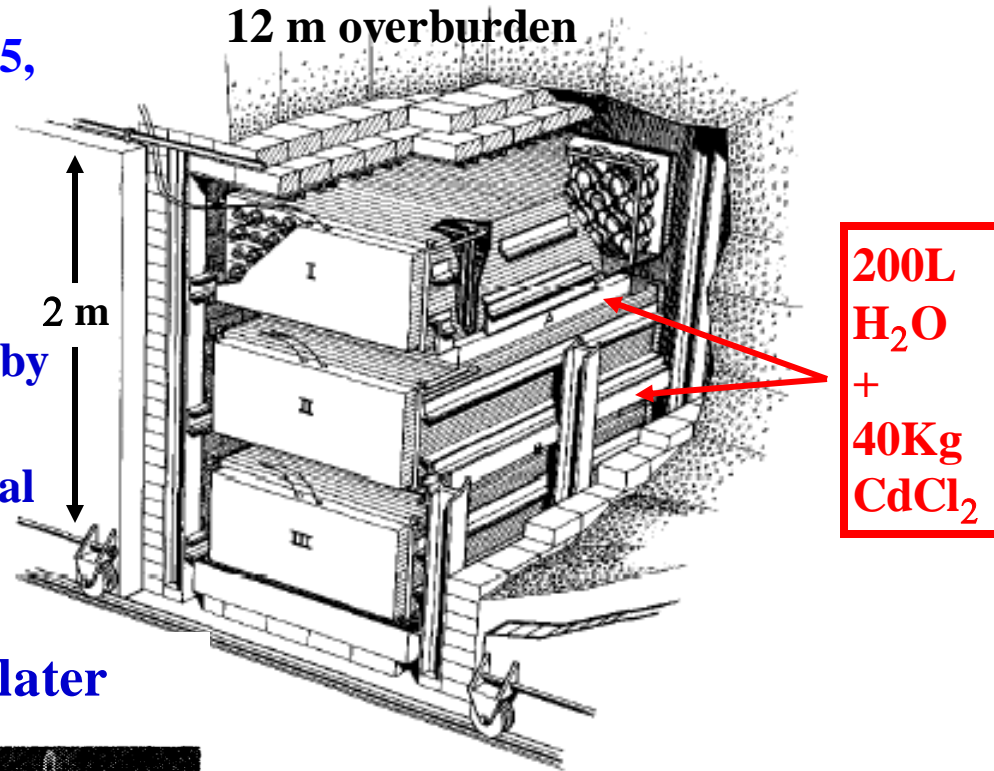
Experiment attempted at Hanford in 1953, too much background (Signal 0.4 ± 0.2 evt/min dominated by background).

Signal 2γ , then several γ ~few (30) μs later

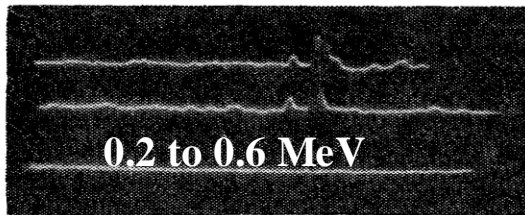


First detection of reactor neutrino

- Final detector at Savannah reactor 1955,
- Reactor power 700 MW
- Distance 11m
- Flux: 10^{13} neutrinos/(cm² s) reactor
- I,II,III : 1400l LS (Total), Each viewer by 55 PMT
- Rate : 3.0 ± 0.2 evt/hour, where accidental coincidence rate : 0.2 ± 0.7 evt/hour



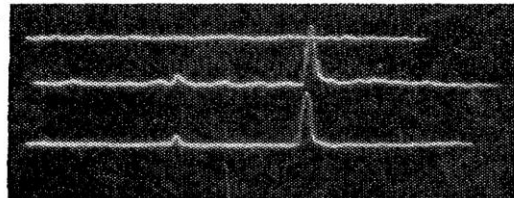
Signal 2γ , then several γ ~few (30) μ s later



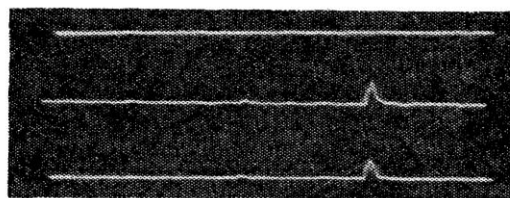
β^+ scope



n scope

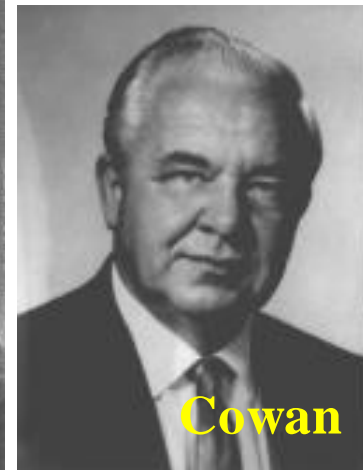
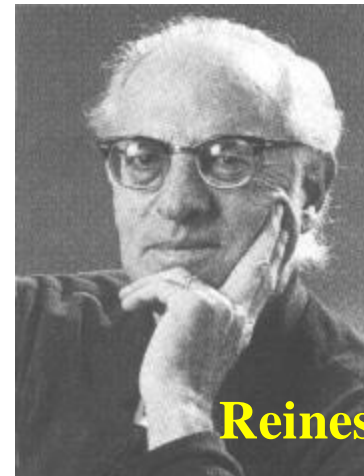


β^+ scope



n scope

F. Reines won the Nobel prize in Physics in 1995



Detector of Nobel Prizes

- **Masatoshi Koshiha (2002)** : "for pioneering contributions to astrophysics, in particular for the detection of cosmic neutrinos"



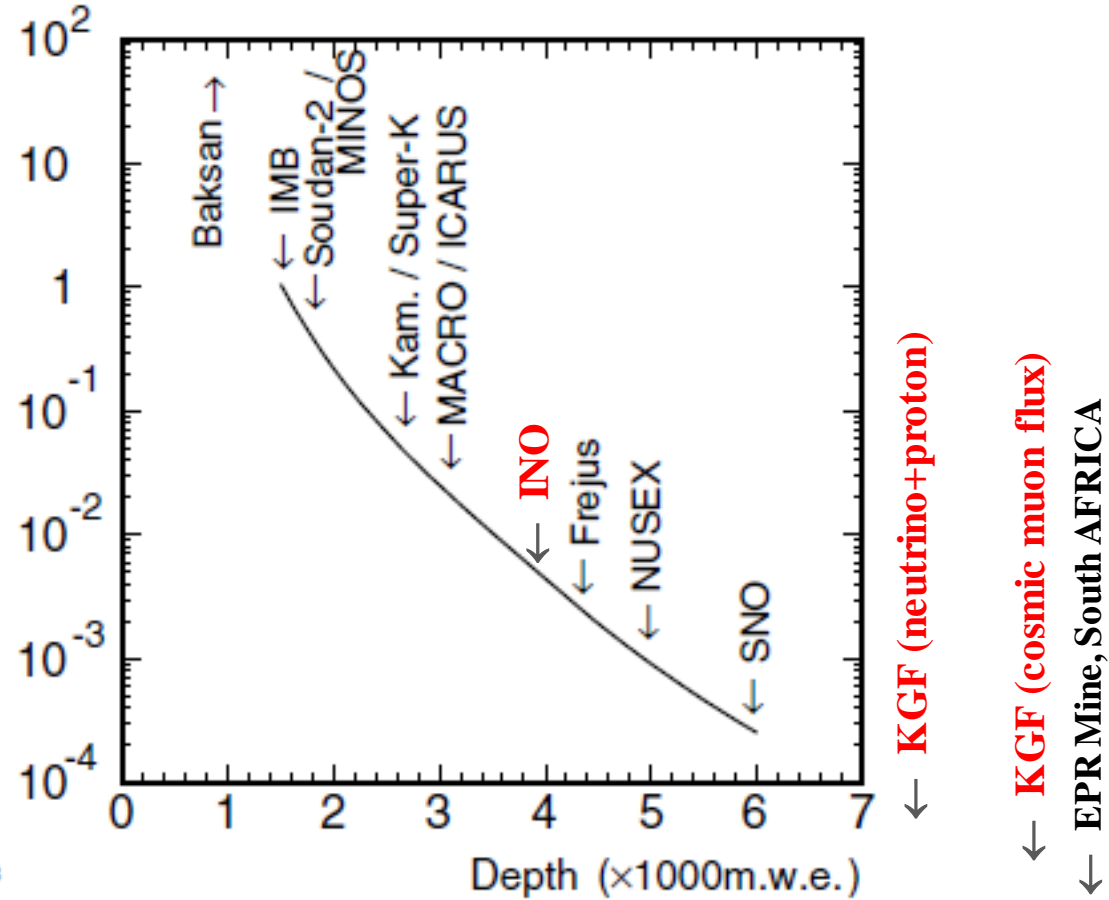
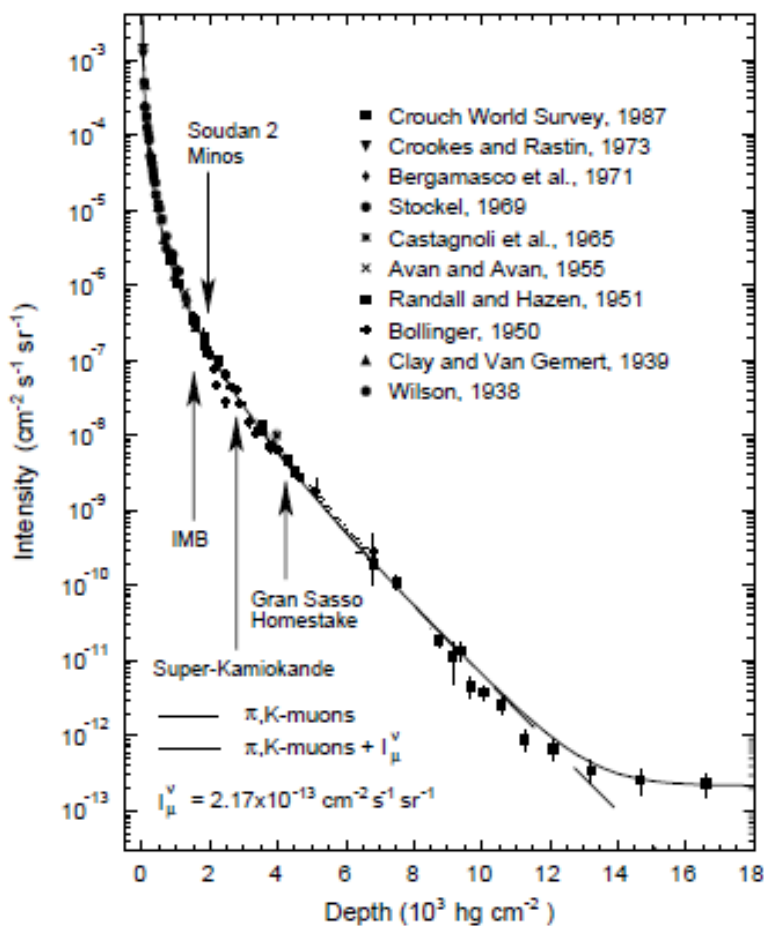
- **Takaaki Kajita (2015)** : "For the discovery of neutrino oscillations, which shows that neutrinos have mass"



- **XXX (20yy)**: "For the discovery of"

Underground lab

- The rate of the atmospheric neutrino interactions is about $200 \text{ kt}^{-1} \text{ year}^{-1}$.
- Rate at the surface due to cosmic ray particles is very frequent, namely $\sim 200 \text{ m}^{-2} \text{ s}^{-1}$,



Deepest experimental halls :

EPR Mine in South Africa : 8800 m.w.e

KGF : Deepest : 8400m.w.e (whereas atmospheric neutrino discovery at 7500m.w.e

Kamioka Observatory Underground Labs



KamLAND (Tohoku Univ.)
 1000ton liquid scintillator detector
 Reactor, geo neutrinos ^{136}Xe double beta decay



Super-Kamiokande 50,000 ton water Cherenkov detector
 Atmospheric, solar, supernova neutrinos
 Proton decay, indirect dark matter search
 Far detector for T2K



CANDLES

CaF₂ scintillation detector for ^{48}Ca double beta decay



KamLAND

1000m

Gravitational-wave CLIO
 100m×100m prototype
 Geophysics 100m×100m Laser strainmeter

Lab.A

Super-K dome

clean room

XMASS

Direct dark matter search experiment

Lab.E/IMPU

Lab.2

water system

EGADS

200t Gd test tank

Lab.G

Atotsu entrance

IMPU
 Lab.1

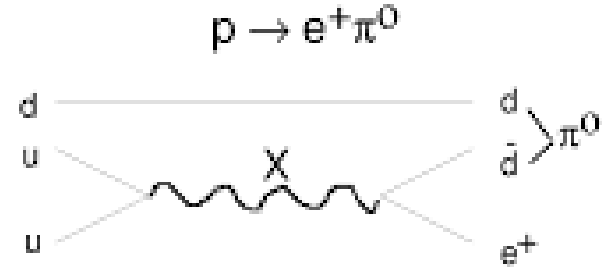
100m

NEWAGE Direction dark matter experiment



GUTs (Grand Unified Theories)

- At the beginning of the Kamiokande experiment, the main purpose was examination of Grand Unified Theories.
- In the end of 1970s, GUTs were proposed by many theorists.
- Grand Unified Theory (GUT) merges the electromagnetic, weak, and strong forces (the three gauge interactions of the Standard Model) into a single force at high energies.
- SU(5) model : 24 generators, 12 new gauge bosons,....
 - Baryon and lepton numbers are not conserved



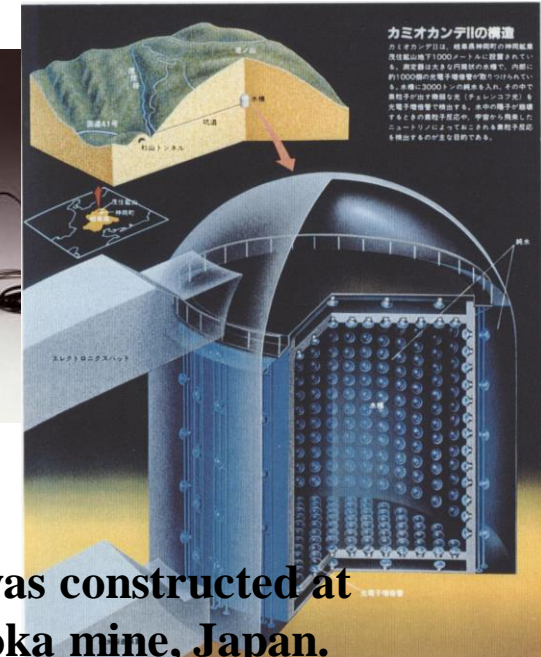
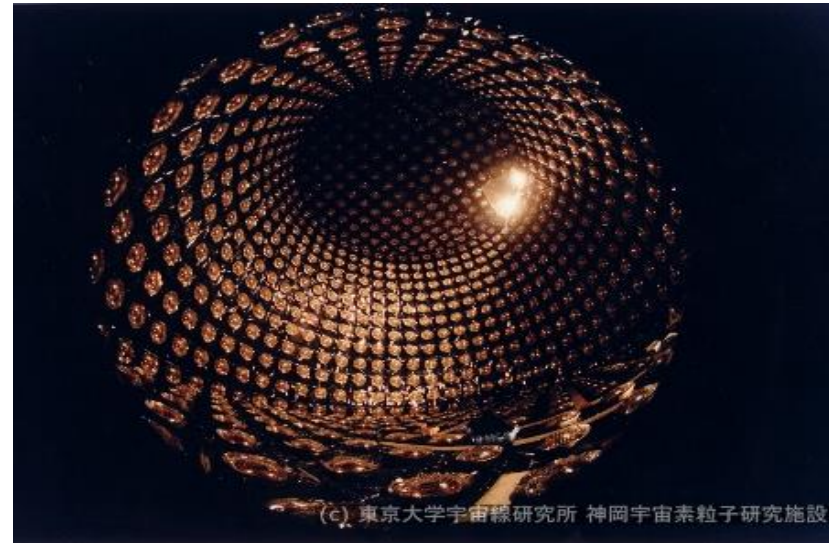
Kamioka Neutron Decay Experiment

- To search for nucleon decay, a huge number of nucleons must be 'viewed'.
- Water Cherenkov detectors are one of the best solutions for nucleon decay search.

1. Water is very cheap and transparent.
2. Assume that the nominal size of the detector is R . The volume is in proportional to R^3 , but number of photo sensor on the wall is in proportional to R^2 . It is effectively cheaper for larger detectors.

- In February 1979, the first unofficial proposal of Kamiokande was presented.
- In December 1980, the design of 20-inch photomultiplier tube (PMT) was fixed.
- In July 1983, the experiment started.

- A large water Cherenkov detector (15.6m Φ \times 16m height) was constructed at **1000 m** (2400 meter water equivalent) underground in Kamioka mine, Japan.
- **3000 tons** of pure water (**Fiducial vol 1040t**) are viewed by **1000 20-inch Φ** PMTs.



Nucleon decay and atmospheric neutrino background

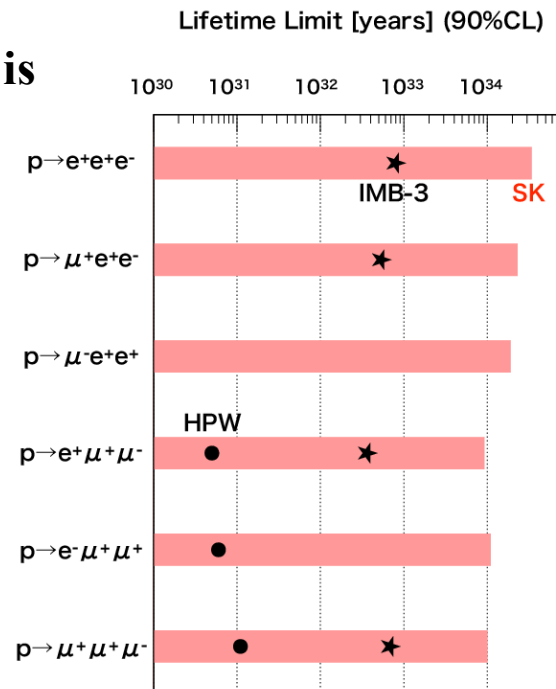
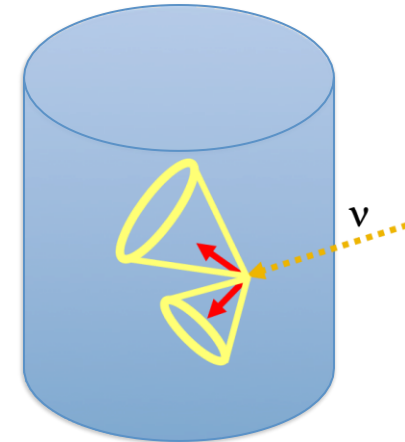
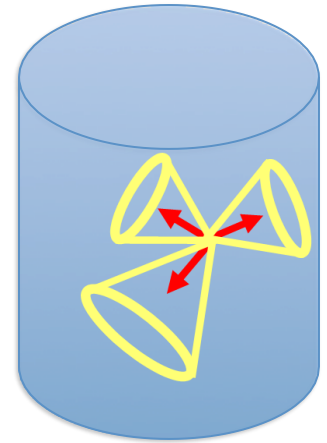
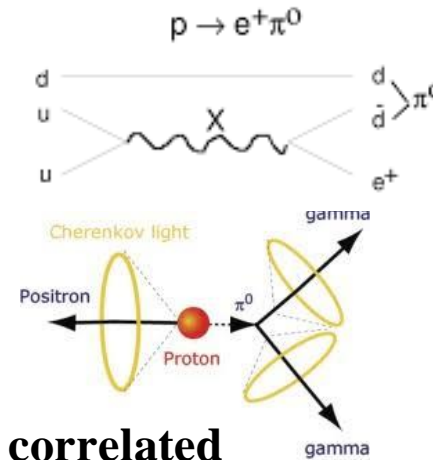
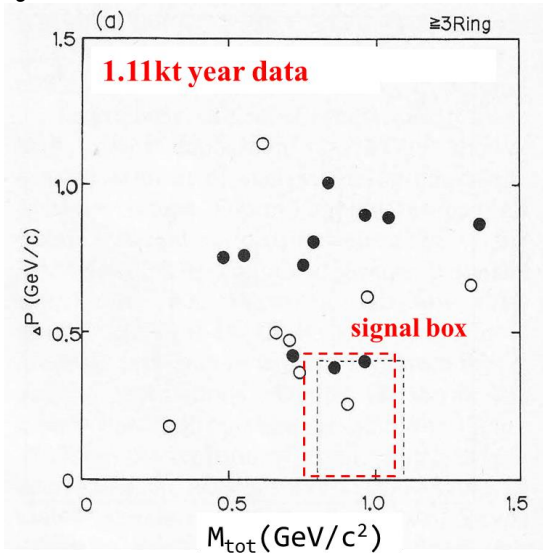
Nucleon decay

- Invariant mass (M_{tot}) from all generated particle agrees with the mass of nucleon ($M_p = 938.3 \text{ MeV}/c^2$ or $M_n = 939.6 \text{ MeV}/c^2$).
- Since a nucleon at rest decays, momentum imbalance $\Delta P = \sum \vec{p} \sim 0 \text{ MeV}/c$.

Atmospheric neutrino

- Invariant mass and momentum imbalance are correlated with initial neutrino energy and travel direction.

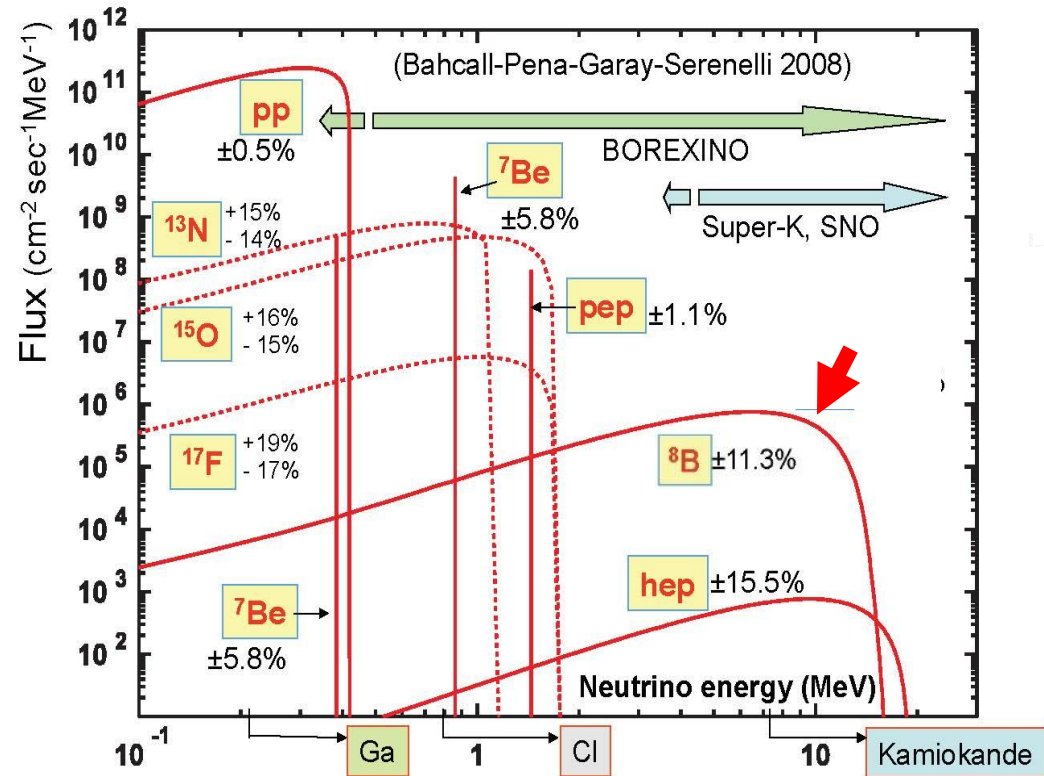
Possible nucleon decay can be examined in the M_{tot} vs ΔP plane. “Back to back” is a key feature of a nucleon decay event.



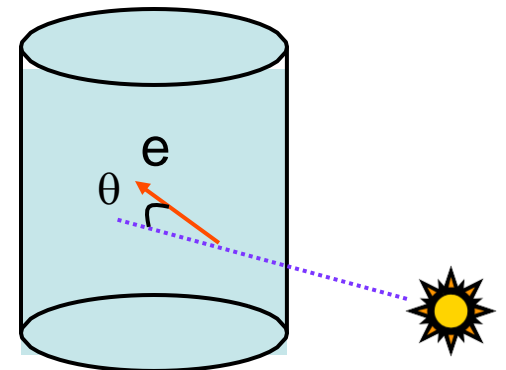
Solar neutrinos in water Cherenkov detector

- In water Cherenkov detector, only **^8B neutrinos** whose nominal energy is **$\sim 8 \text{ MeV}$** can be detected.
- Elastic scattering between neutrinos and orbital electrons are employed.

$$\nu_e + e^- \rightarrow \nu_e + e^-$$
- Recoil electrons keep energy and directional information of initial neutrinos
- Interactions with hydrogen and oxygen nuclei do not occur because the energy of solar neutrinos are too low.



- It was impossible to use existing Kamiokande-I for this study
- Required extensive work to achieve the goal

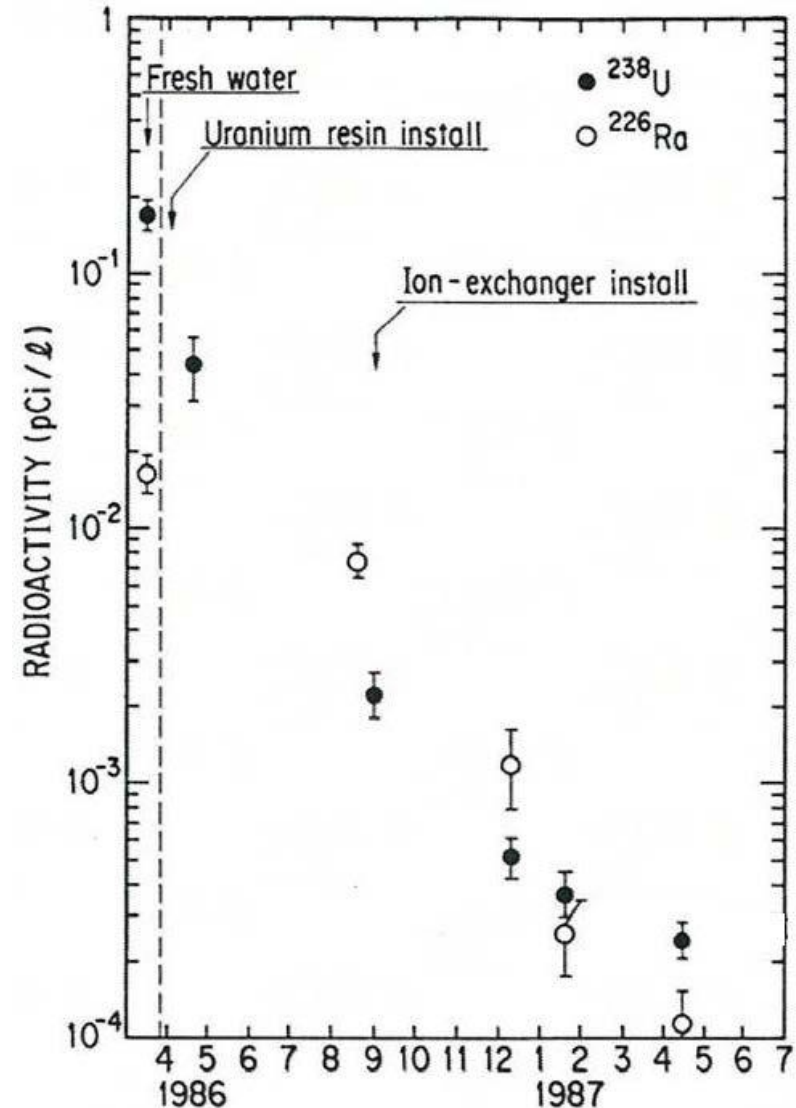


Kamiokande-II

- **KAM-I:** trigger threshold of 110 photoelectrons (p.e.), which corresponds to **30 MeV/c** (at 50% efficiency) and **37 MeV/c (90%)** for electrons (3.4 p.e.=1 MeV for electrons), and **205 MeV/c (50%)** and **220 MeV/c (90%)** for muons.
- This threshold was low enough to detect nucleon decay mode $p \rightarrow \nu K^+ (\mu^+ \nu)$, which records the smallest energy deposit in the detector.
- To detector **^8B solar neutrinos**, the trigger threshold of the detector should be reduced to be around **~ 8 MeV**.
 - **KAM-II :** **7.6 MeV/c (50%)** and **10 MeV/c (90%)** for electrons, and **165 MeV/c (50%)** and **180 MeV/c (90%)** for muons
- In addition to the trigger threshold, background events in the low energy range should be reduced.
- **From fall 1984 to the end of 1986**, many detector upgrades to observe **^8B solar neutrinos** were done. They are:
 - **Removal of radioactive sources in water**
 - **Construction of anticounter**
 - **Installation of New electronics**
- After these upgrades, **Kamiokande-II** started in early 1987.

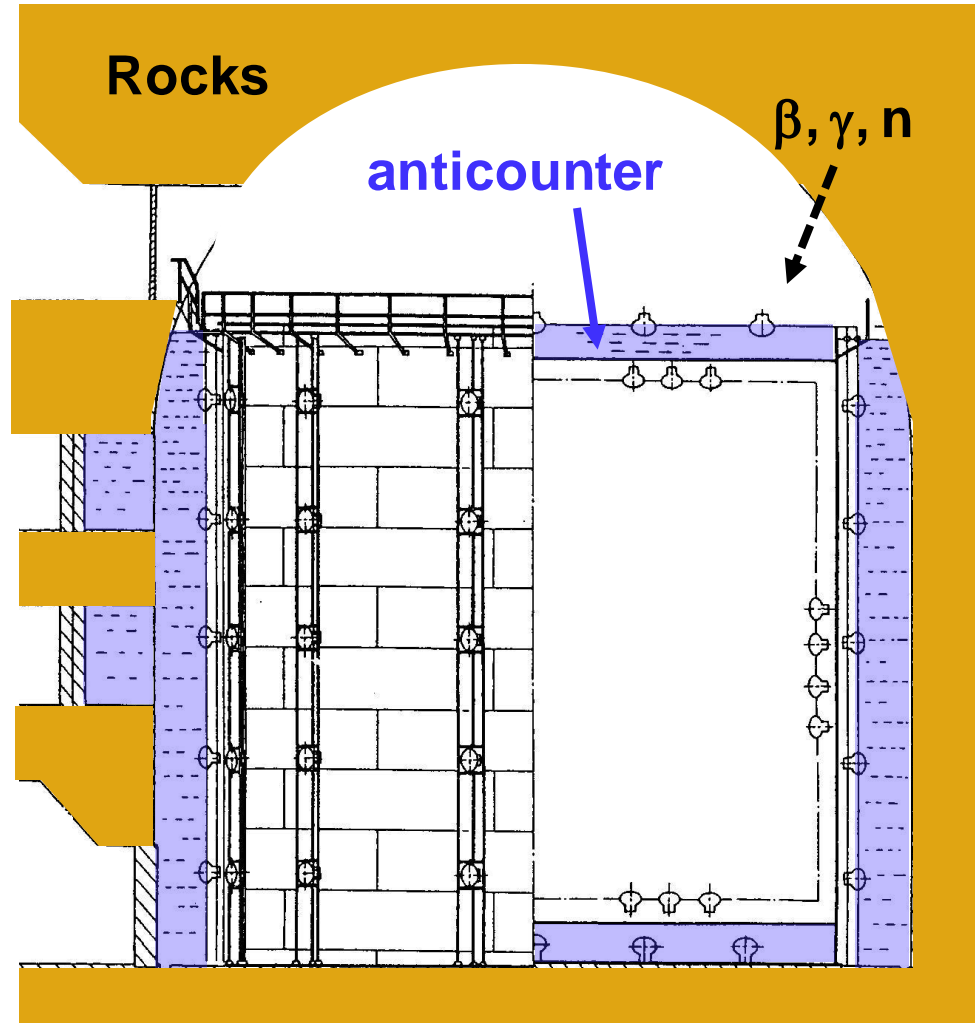
Removal of radioactive sources in water

- The most serious background were the β -decay products in the **Uranium-Radium** series. Note that nominal energy of them is **< several MeV**.
- Fresh water from the mine contains large concentration of Radon. Supplying the fresh water was stopped and closed circulation mode was employed. A Radon-free water generation system was also installed.
- In the water circulation system, **Uranium resin** and **Ion-exchanger** were added.
- To prevent contact of water and Radon-rich mine air, an **air-tight** ceiling on the top of the tank were made. Other components in the water circulation system were also made air-tightened.
- **Finally, the radioactivity was reduced by 3 orders of magnitudes.**



Anticounter

- The anticounter layer surrounding the inner detector was constructed until fall 1985.
- It was also water **Cherenkov detector with >1.4 m water thickness** and 123 20-inch Φ PMTs.
- The main purpose of the anticounter layer is to identify entering/exiting charged particles such as cosmic ray muons.
- The anticounter water layer effectively absorbs radio activities from surrounding rocks and air.

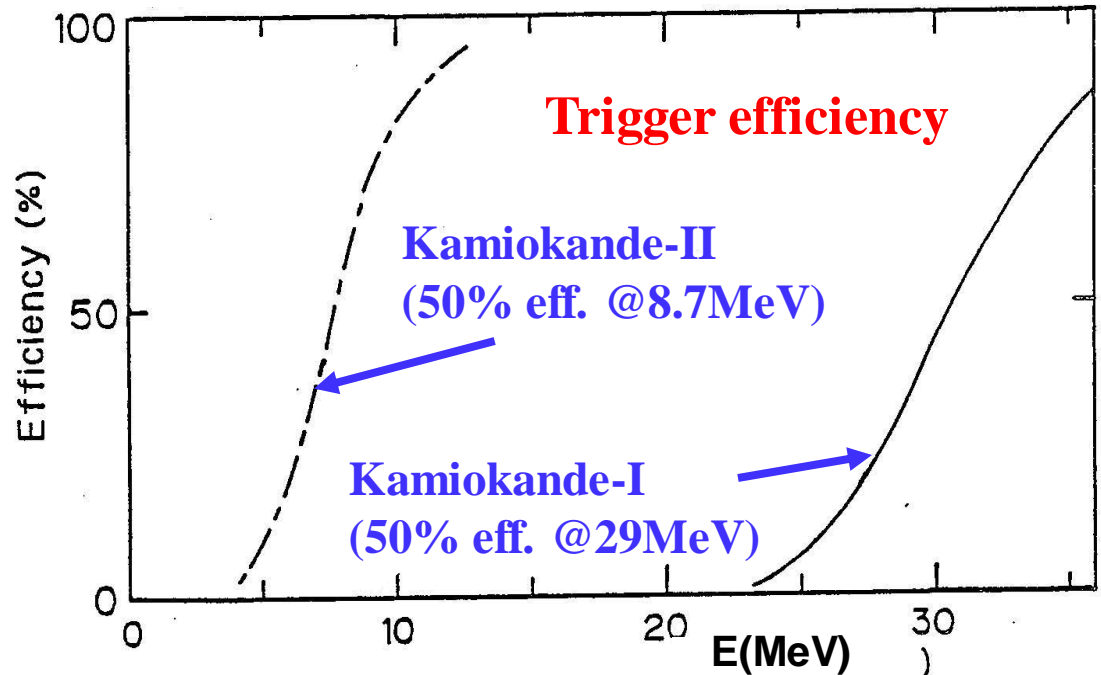


New electronics

Design of the new electronics

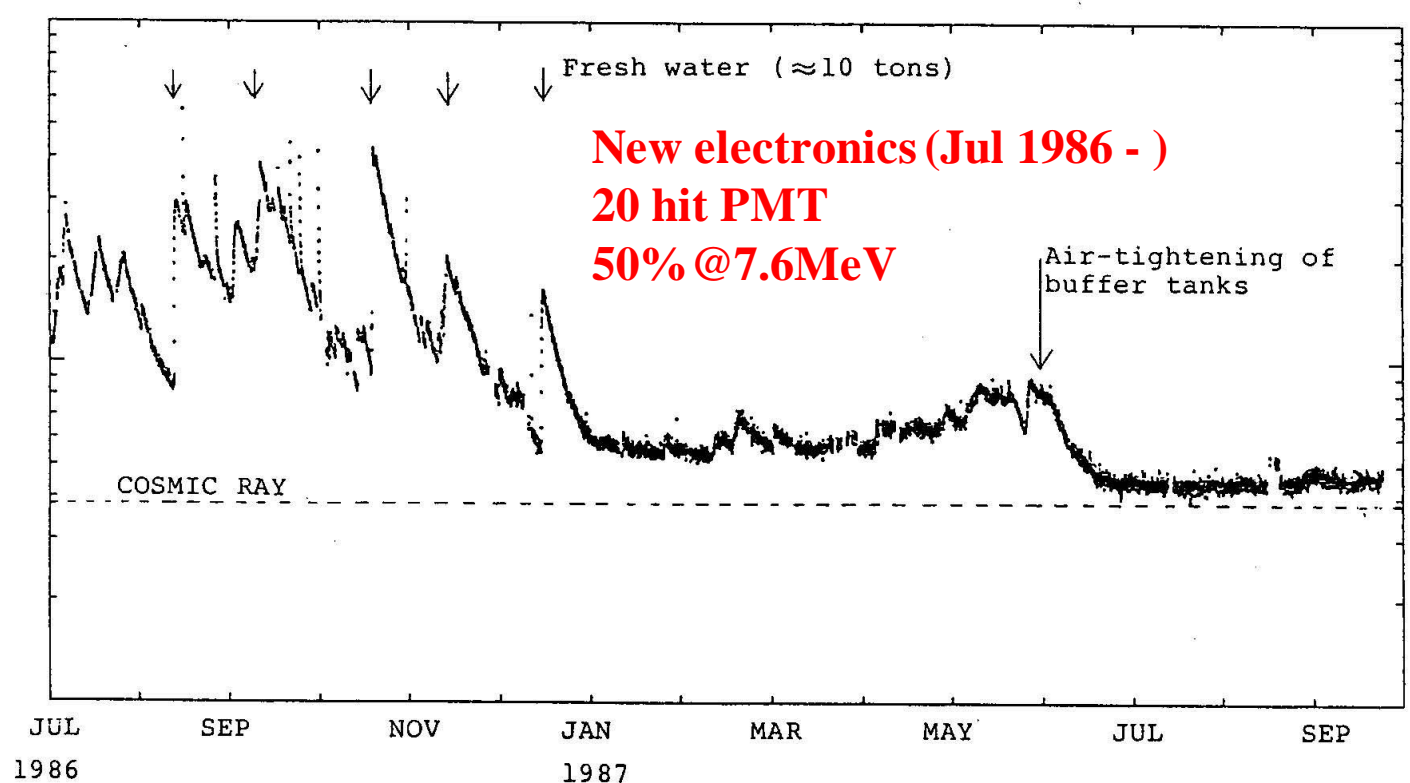
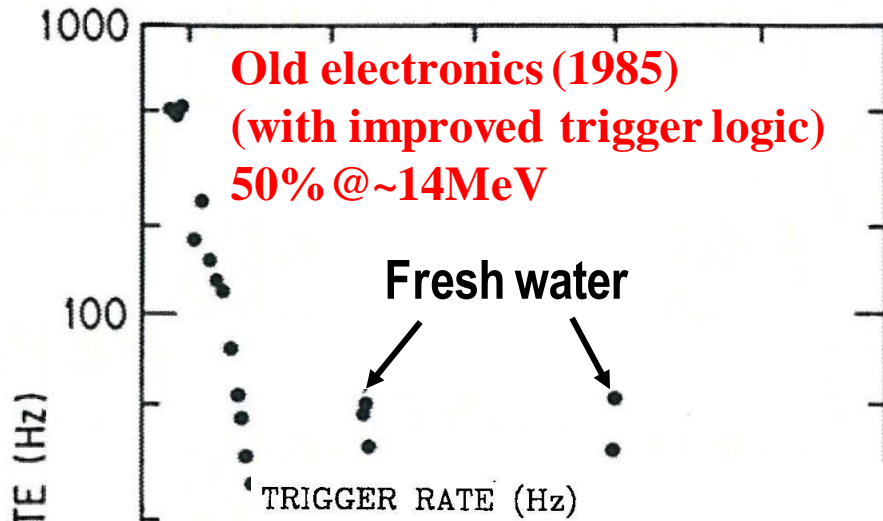
- Charge and timing information of PMTs are digitized in PMT by PMT basis.
- Discrimination is also in PMT by PMT basis.
“Number of hit PMT” signal is made from the sum of the discriminator outputs, and used for the trigger logic.

- The new electronics was operated with the condition $N_{\text{hit}} \geq 20$, which corresponds to **7.6MeV** energy threshold.



Lower the trigger rate !

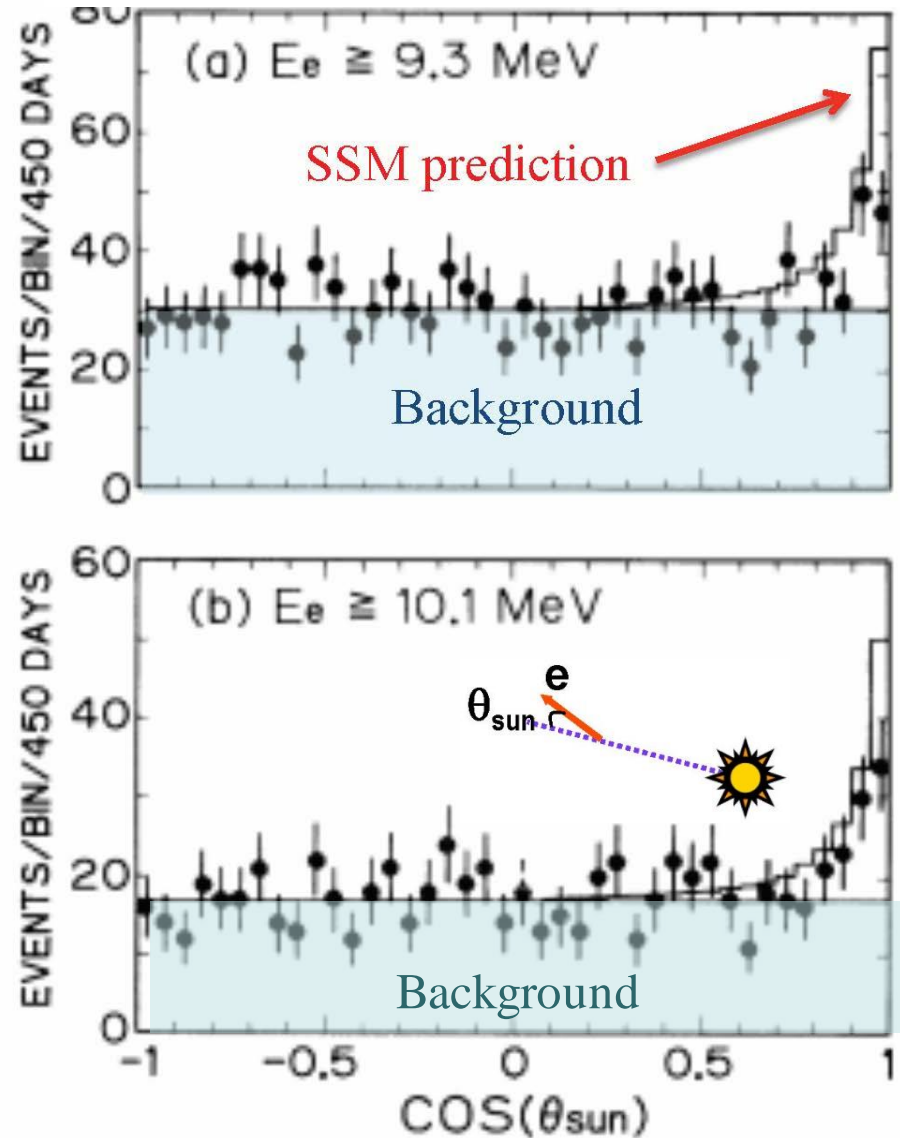
Finally, the trigger rate of low energy events were reduced by more than 3 orders of magnitudes.



Observation of solar neutrinos in Kamiokande-II

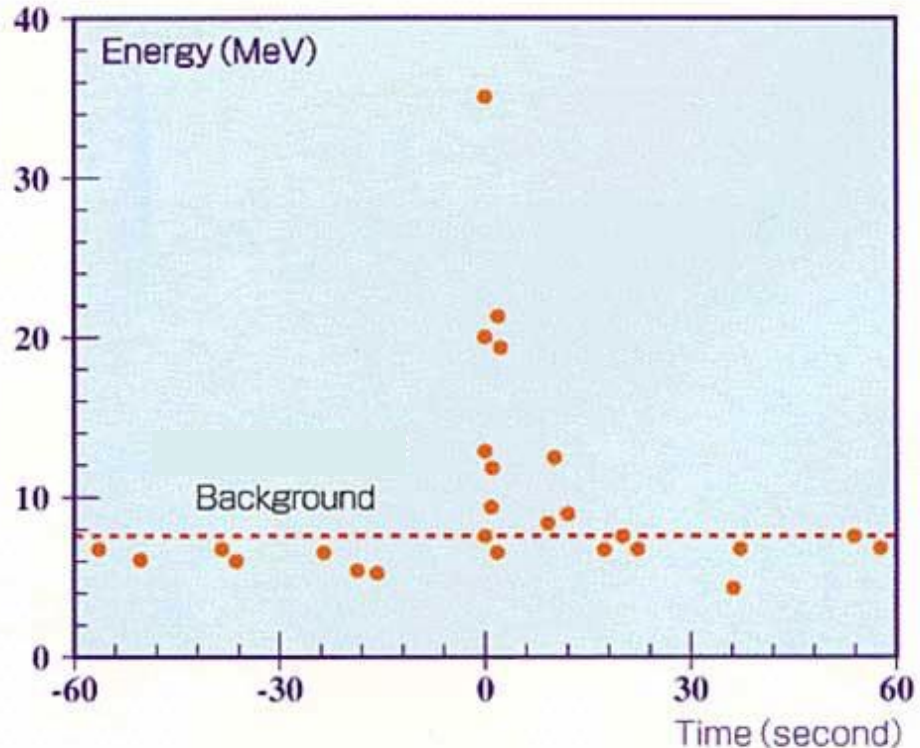
- **The first real-time, directional neutrino signal from the direction of the Sun.**
- The observed neutrino flux is $0.46 \pm 0.13(\text{stat.}) \pm 0.08(\text{sys.})$ of SSM prediction
- The observation is certainly smaller than the SSM prediction. However, the discrepancy is not consistent with Homestake.
- Homestake : $\sim 1/3$ of SSM
Kamiokande-II : $\sim 1/2$ of SSM
- Measurements with different energy thresholds became key issues for other new experiments.

K.S.Hirata et al., Phys. Rev. Lett. 63, 16(1989)



SN1987A

- In Kamiokande, observation of solar neutrinos started in early January 1987. The detector was ready for observation of low energy neutrinos.
- In February 25, 1987, they received a news of a supernova explosion in Large Magellanic Cloud, which is only 160k light-year away from our solar system.
- Kamiokande immediately analyzed the data, and found a clear **11 neutrino events** in 13 seconds from **February 23, 07:35:35UT (± 1 min)**.
- The birth of neutrino astronomy.
- Due to power failure, the KGF detector was off during that time !!!



Atmospheric neutrino oscillation in early 1990s

- In the first result, the statistics were poor, and the up/down asymmetry was not clear. The straightforward impression was "Number of muon neutrino events were little low..."
- Some of the experiments reported negative results. Kamiokande/IMB results are not widely believed.
- To claim "**Neutrino Oscillation**" was a big and risky challenge.

If it is not true, all Kamiokande/IMB members would lose their confidence as high energy physicists.

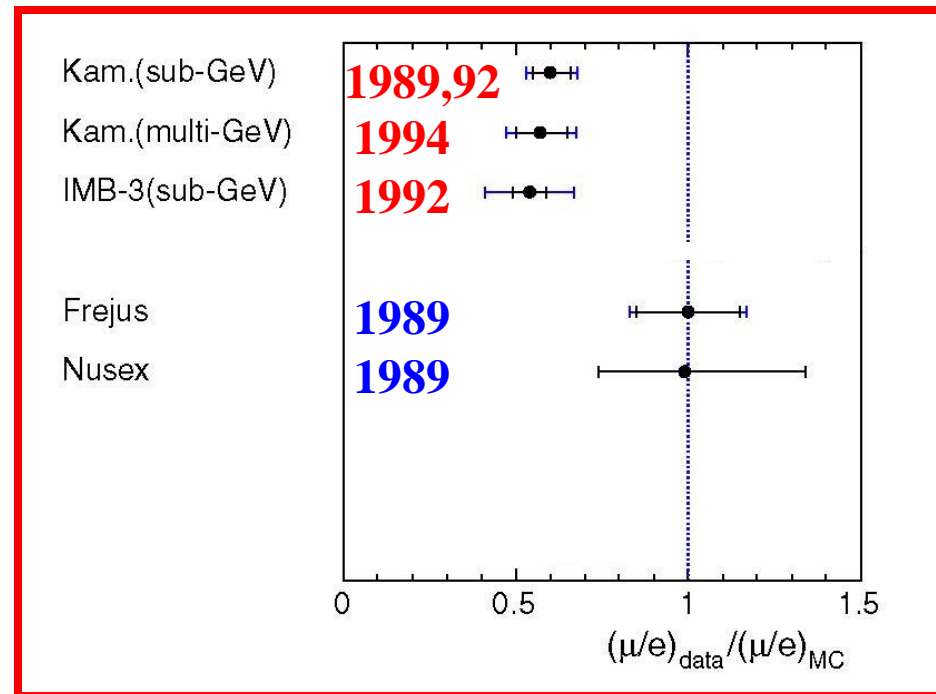
They had hesitated to use the word "neutrino oscillations".

They had frequently used "muon neutrino deficit" or "atmospheric neutrino anomaly", instead.

Were there any discrepancies in e/μ separation in data and MC ??

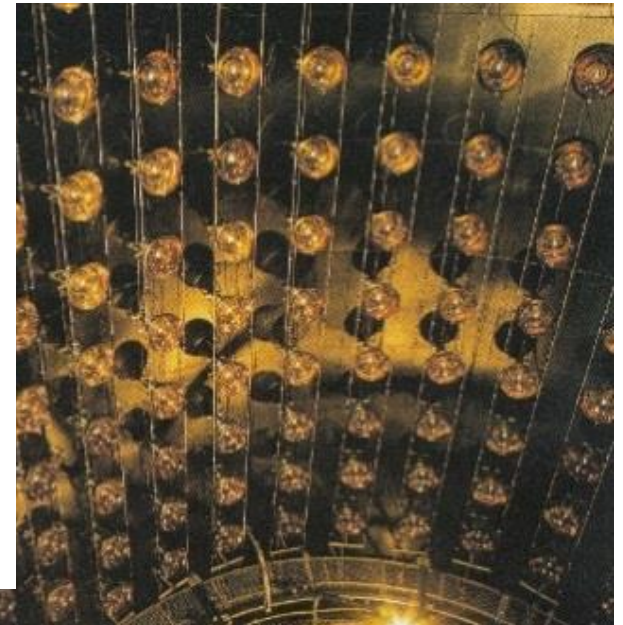
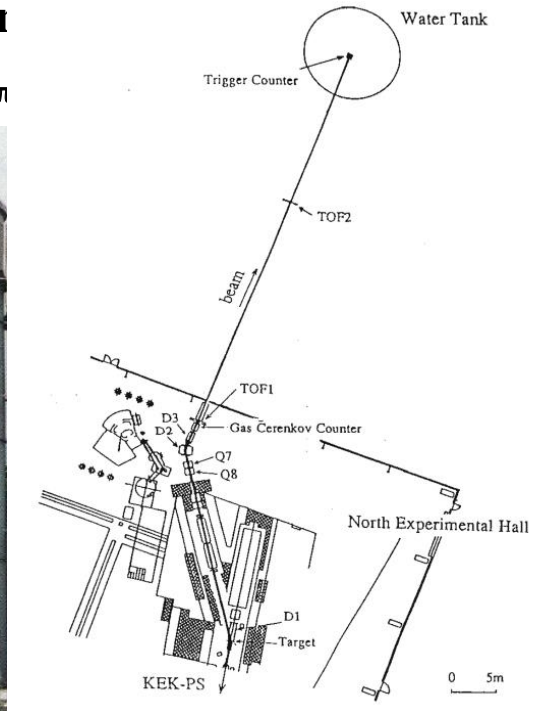
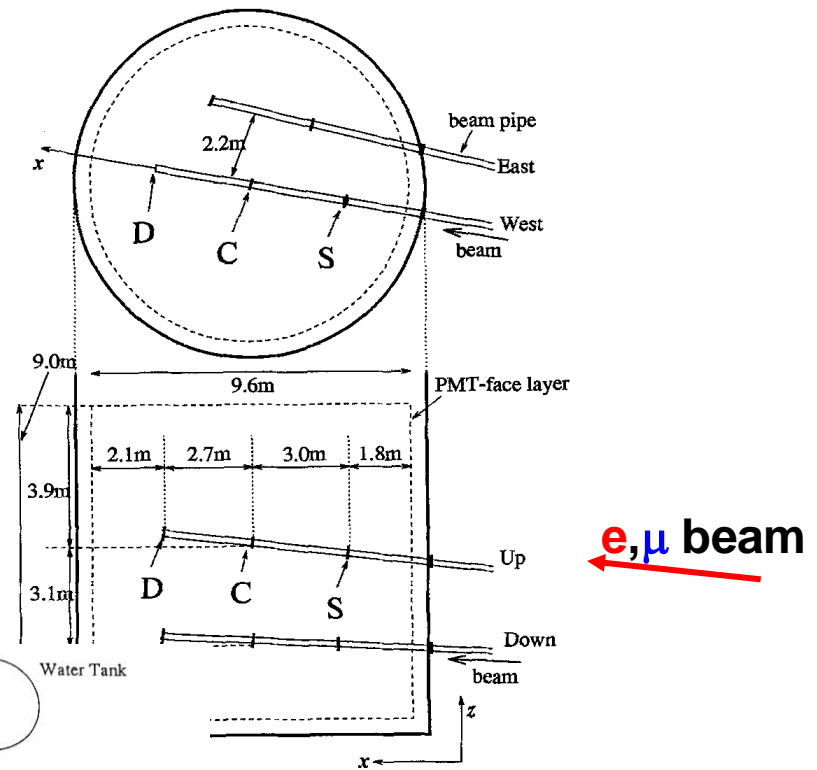
Build a new detector to verify that

From a review article "Atmospheric Neutrinos" by T. Kajita
New Journal of Physics 6, 194(2004) **Water Cherenkov Tracker**



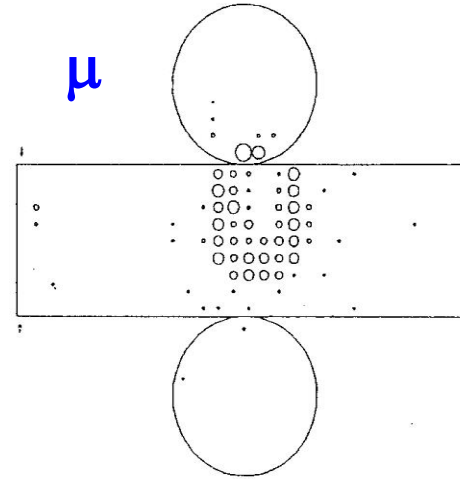
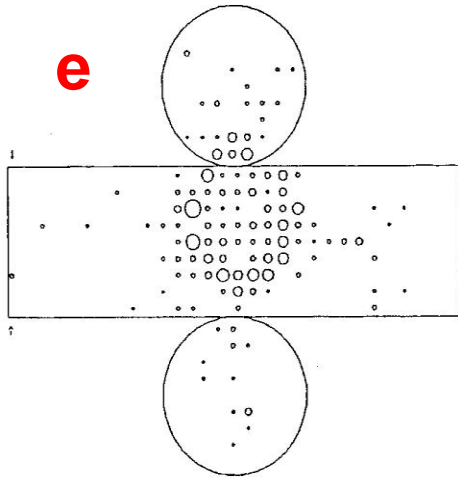
KEK Proton Synchrotron E261A (1992-1994)

- 1kt water Cherenkov detector was built in KEK North counter hall (380 20"-PMT) Electrons and muons from 12 GeV proton Synchrotrons were injected.
- A gas Cerenkov counter, TOF counters to identify particle over momentum range 100 MeV/c - 1000 MeV/c.
- Rejection of pion : Decayed in opposite direction, $p_{\mu} \sim 0.57P_{\pi}$



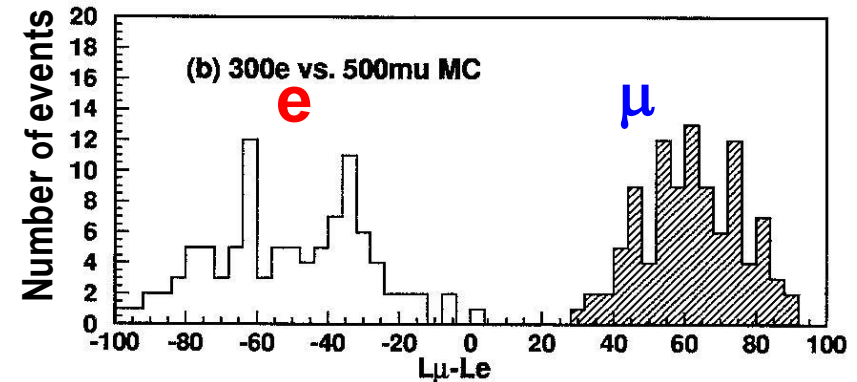
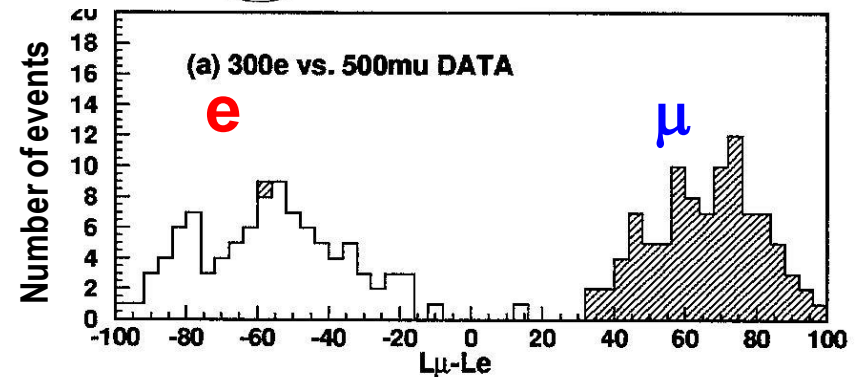
Beam test for the particle identification

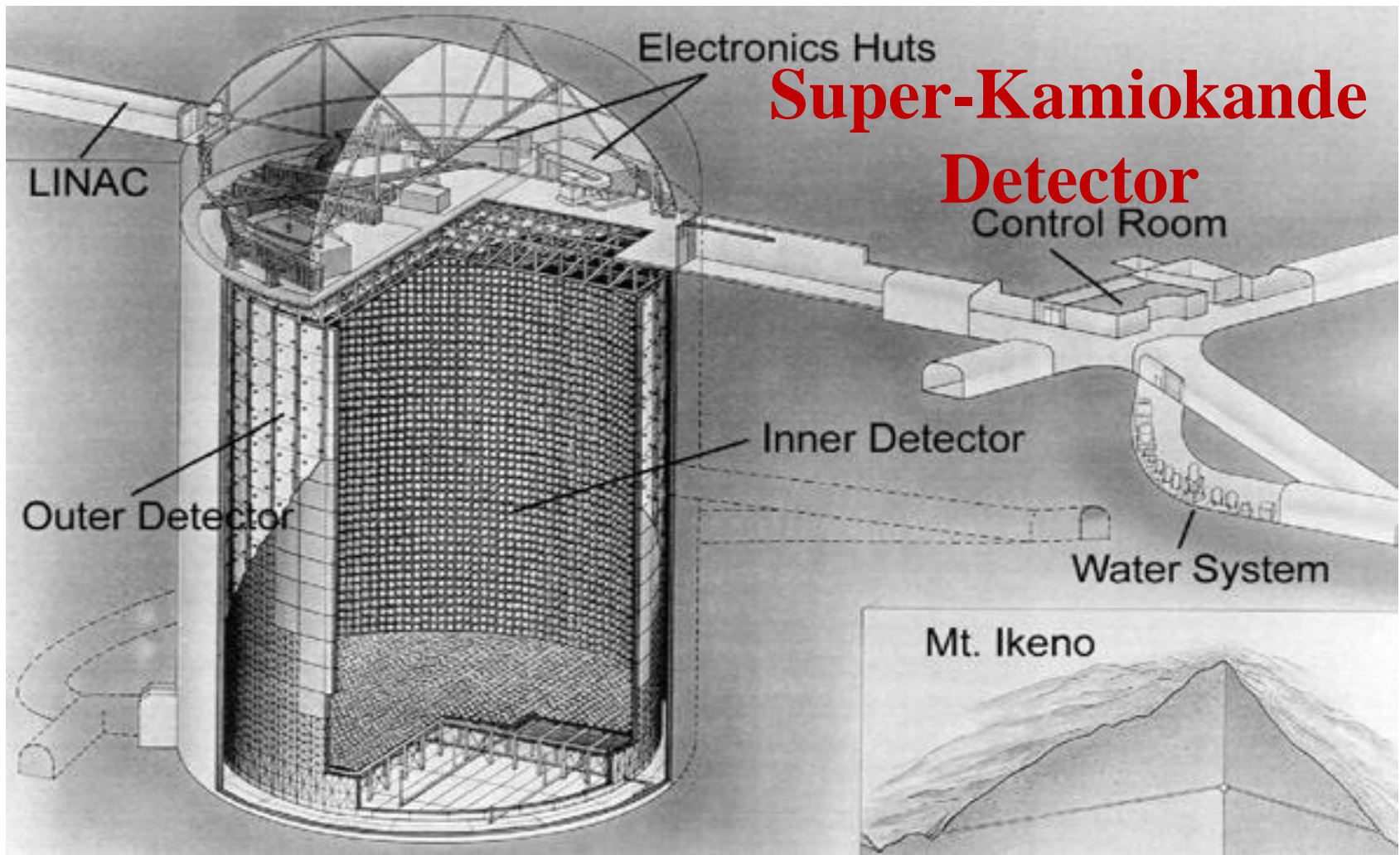
- Fuzzy edge for e event and clear edge for μ event are confirmed.



Phys. Lett. B374
(1996) 238

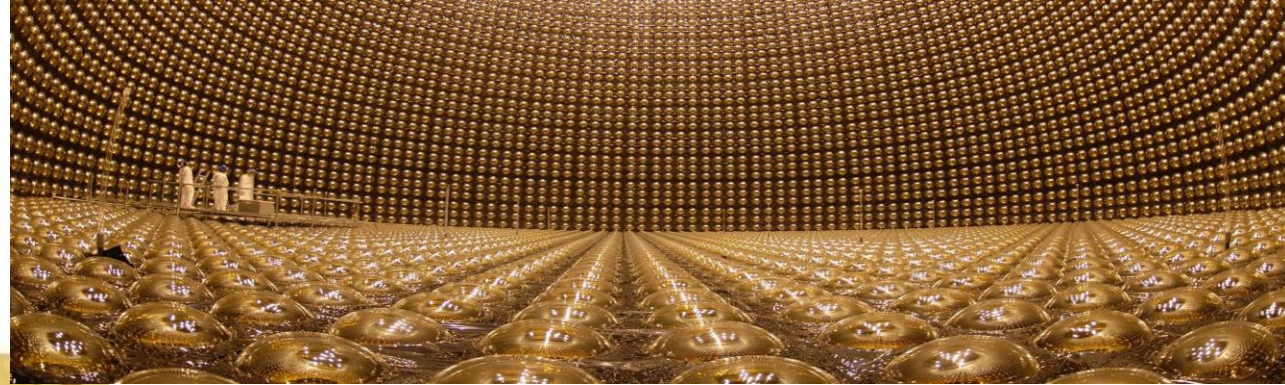
- e -likelihood (L_e) and m -likelihood (L_μ) are calculated. From a comparison between L_e and L_μ , particle id are judged.
- The algorithm clearly separates e beam events and m beam events.
- It was experimentally verified that the e/μ identification capability is better than 99%.





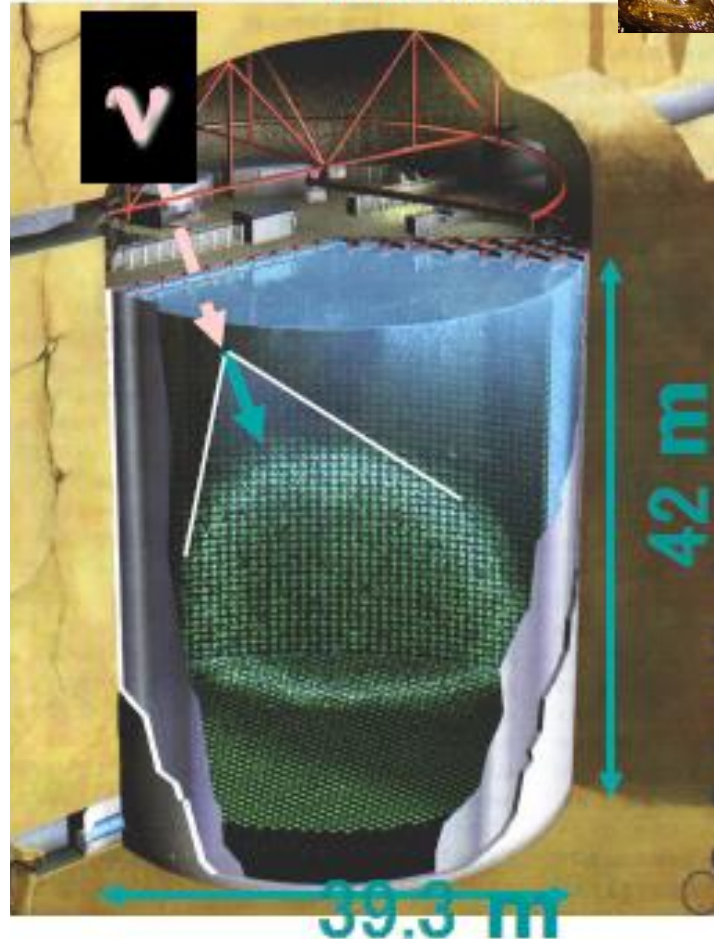
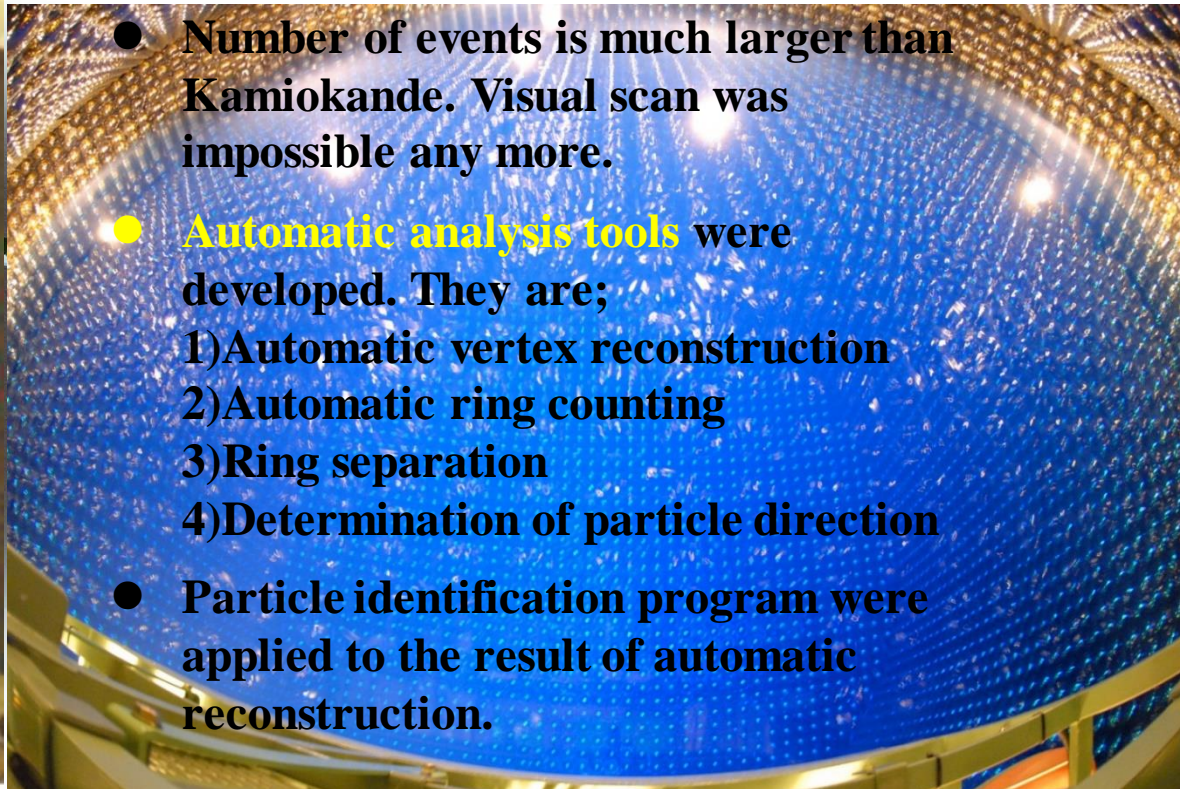
- **Inner cylinder** : 33.3m in dia and 36.2m in height : **Readout by 11129 20" inward facing PMT (40%)** acceptance, empty part is covered by black sheet
- **Outer cylinder** : 39m in dia and 42m in height : **Readout by 1885 8" outward facing PMT (from IMB)**, empty part and other wall are covered by tyvek
- **Muon rate** ~ 2Hz, whereas neutrino events, 9/day, **muon background** $\sim 2 \times 10^4$
- **50kton water**, but **fiducial volume is** $\sim 22.5\text{kton}$

Super-Kamiokande (1996 -)



Software upgrade in Super-Kamiokande

- Number of events is much larger than Kamiokande. Visual scan was impossible any more.
- **Automatic analysis tools** were developed. They are;
 - 1) Automatic vertex reconstruction
 - 2) Automatic ring counting
 - 3) Ring separation
 - 4) Determination of particle direction
- Particle identification program were applied to the result of automatic reconstruction.



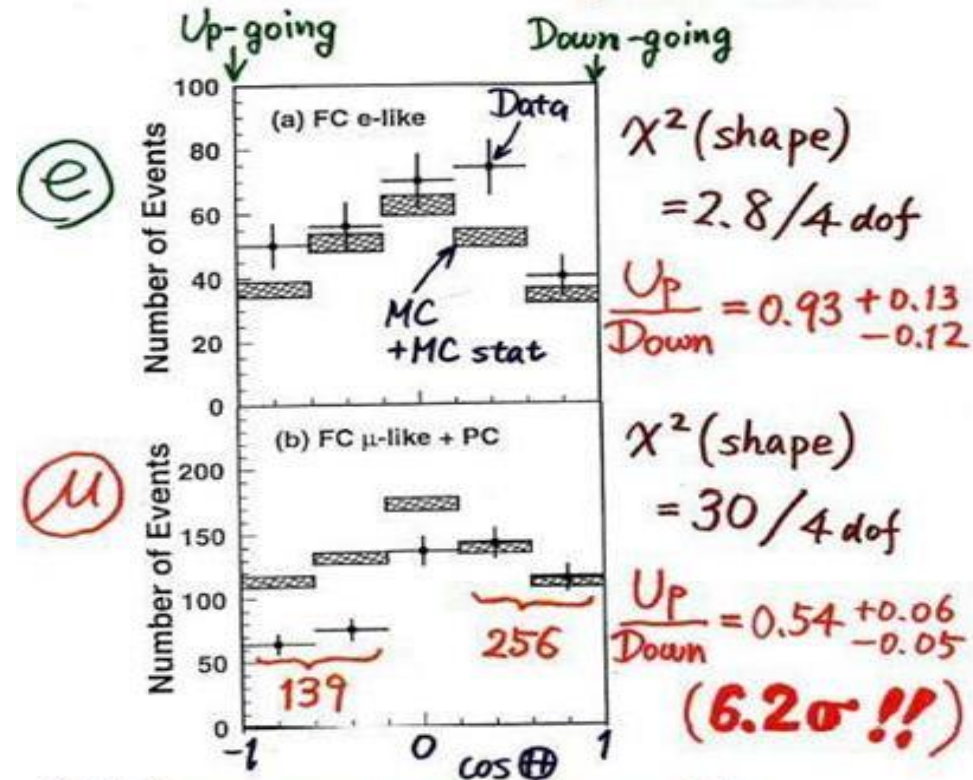
Discovery of atmospheric neutrino oscillation in Super-Kamiokande

At **NEUTRINO 1998** Conference
in Takayama, discovery of $\nu_\mu - \nu_\tau$
oscillation was reported by
Prof. T. Kajita, on behalf of
Super-Kamiokande collaboration.



Nobel Prize in 2015

Zenith angle dependence
(Multi-GeV)



* Up/Down syst. error for μ -like

Prediction (flux calculation $\lesssim 1\%$
1km rock above SK 1.5%) 1.8%

Data (Energy calib. for $\uparrow\downarrow$ 0.7%
Non ν Background < 2%) 2.1%

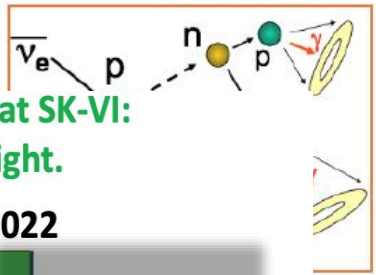
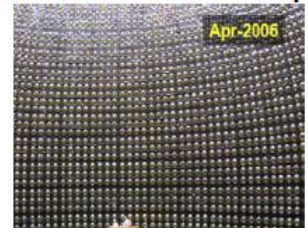
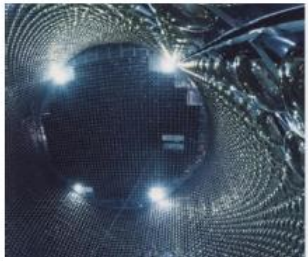
Super Kamiokande, K2K, T2K

1996 2002 2006 2008 2018

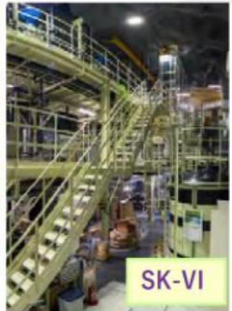
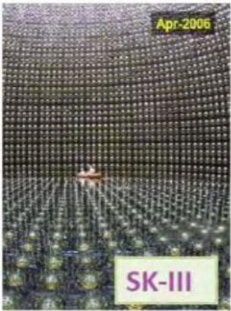
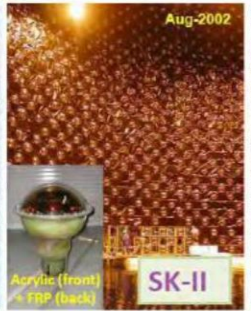
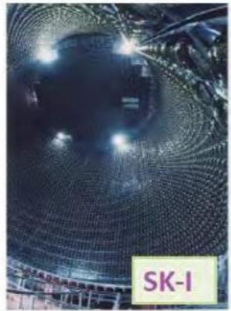


Photo coverage 40%

Accident Full reconstruction Replace electronics & DAQ system Preparation for SK-Gd



1996 2002 2006 2008 2018 2019 2020 2022



“SK-Gd”



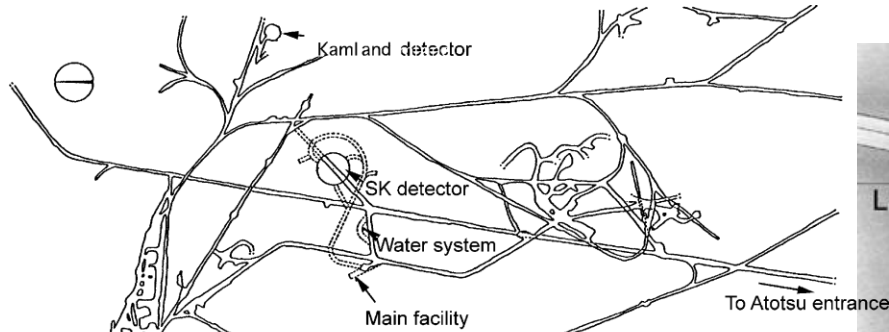
Pure water
6,511 days live-time



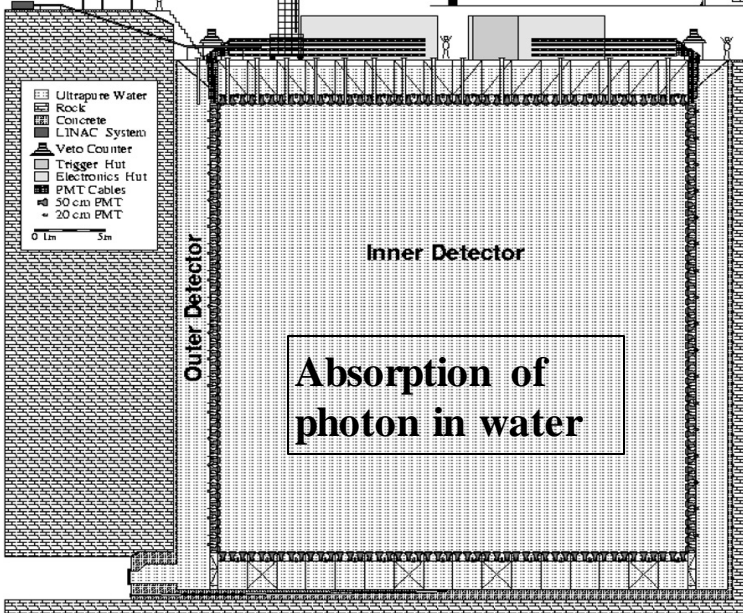
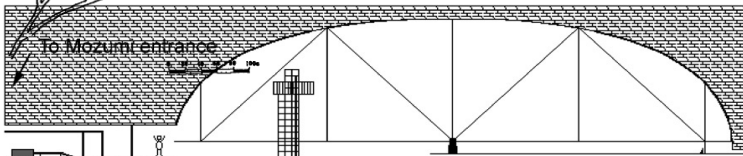
Gd-loaded water
583.3 days + the future...

Calibration of SuperKamiokande detector

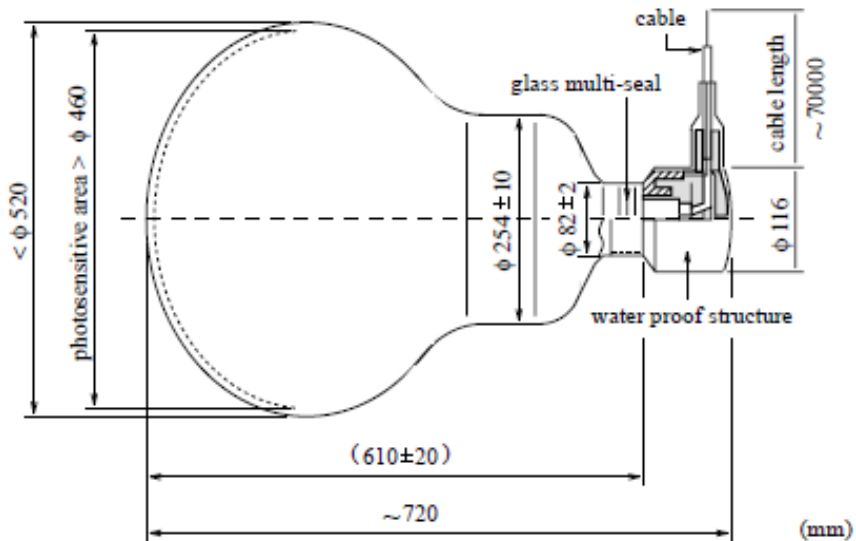
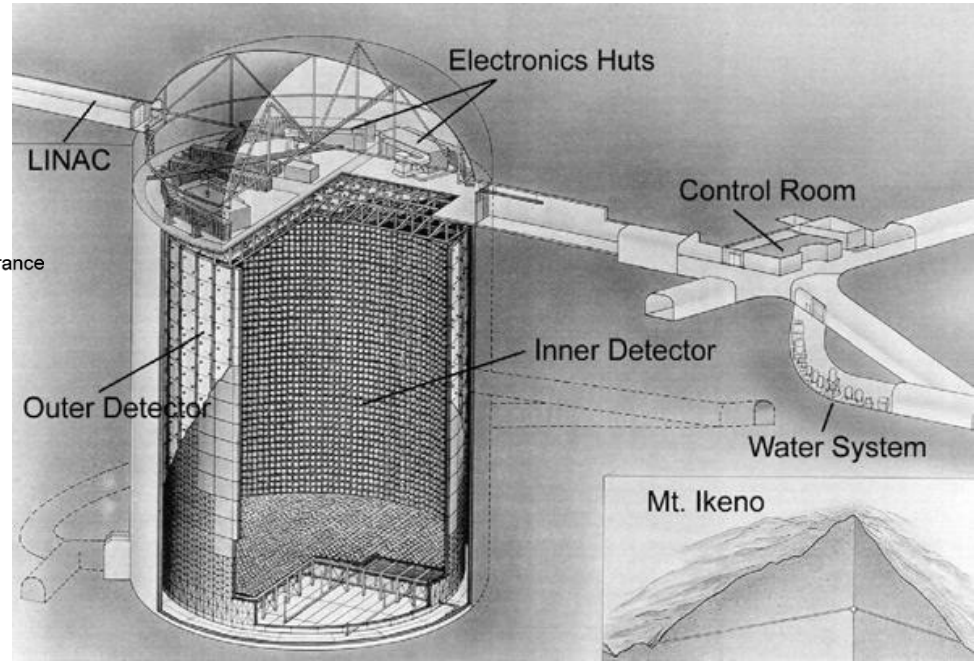
NIMA 501 (2003) 418



Water & air purification



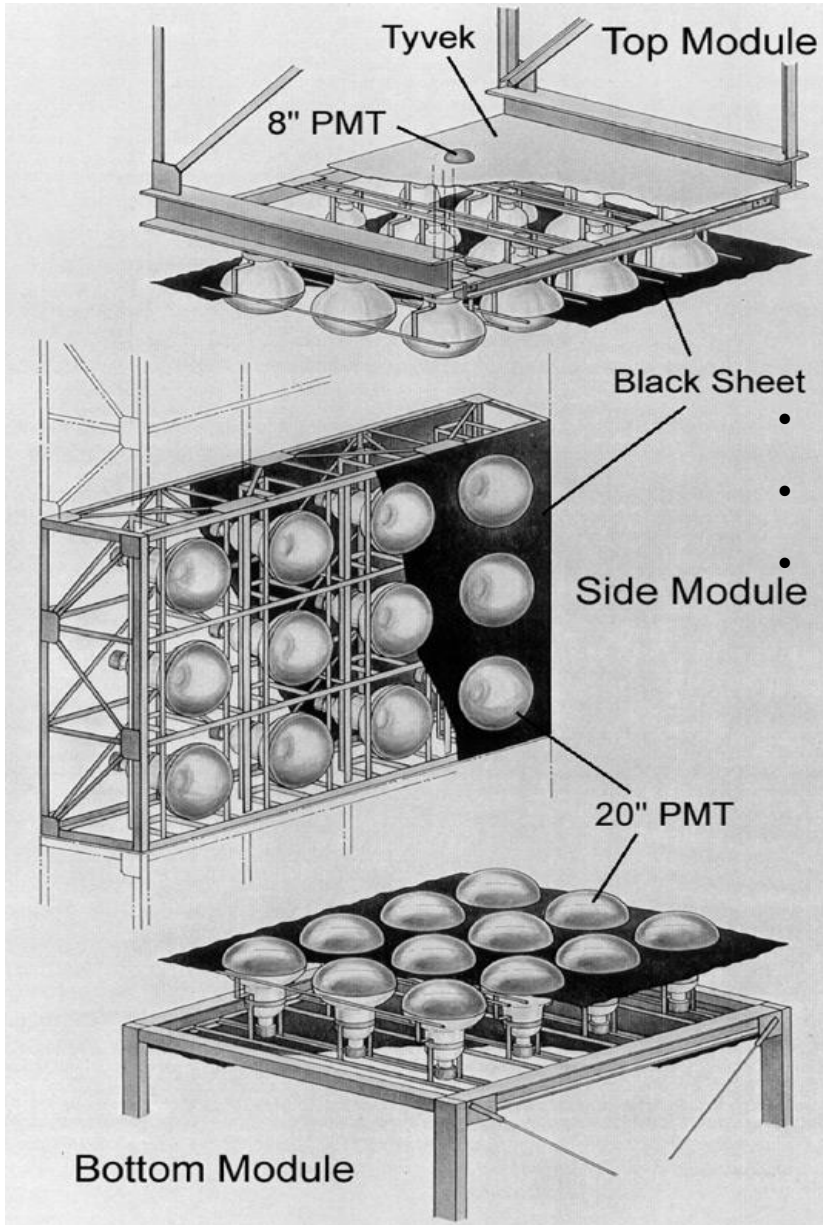
Absorption of photon in water



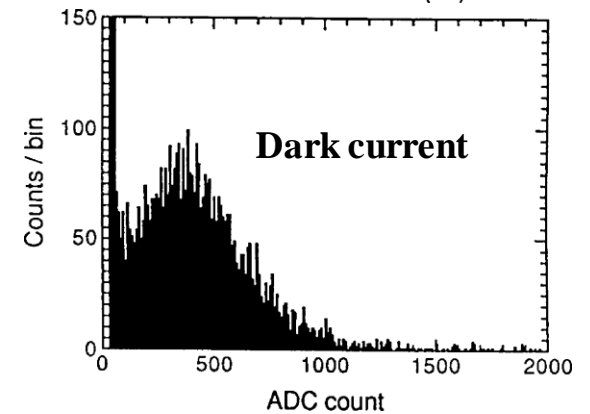
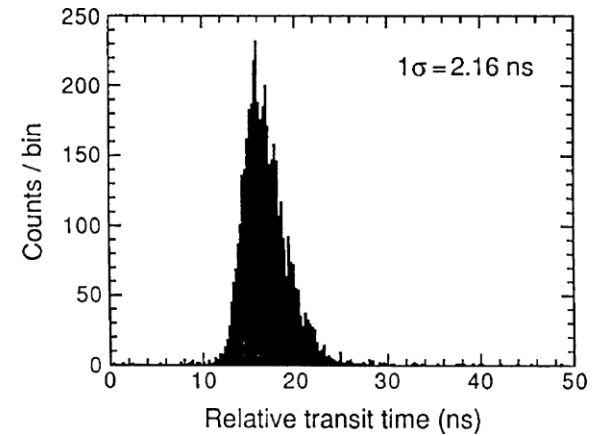
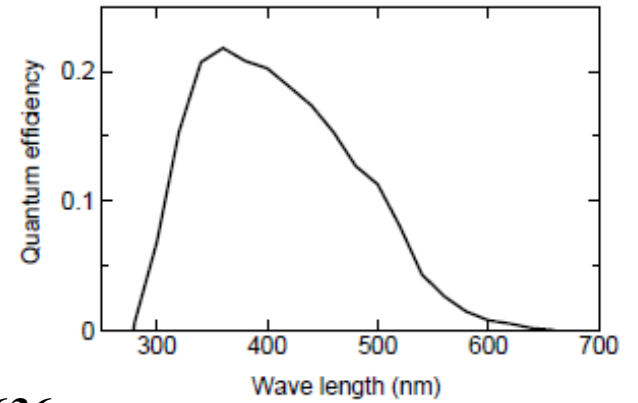
Mag field

Q.E. (θ)

Photomultipliers at SK



- NIMA 458 (2001) 636
- NIMA 501 (2003) 418
- NIMA 737 (2014) 253



SK : Target of calibration system

- Charge determination at the level of 1%, and the timing resolution of 2.1 ns at the one-photoelectron charge level and 0.5 ns at the 100- photoelectron charge level.
- To prevent further accidents, all ID-PMTs were encased in fibre-reinforced plastic (FRP) cases with acrylic front windows
- TAC : dynamic range –300 to 1000ns with resolution 0.4ns (stored data upto 32μs)
- QAC : 1 p.e. ~ 2.5pC
- ADC/TDC pedestal/offset is linear with Temp and is less than 3count/°C (0.6pC/°C)/2 count/°C (0.8ns/°C)
- Water purification : $\rho=18.24 \text{ M}\Omega\text{-cm}$, concentration of Rn (@ supply tank 2mBq/m^{-3} and $0.4 \pm 0.2 \text{ mBq/m}^{-3}$ at outlet), though it is $\sim 2000\text{-}4000\text{Bq/m}^{-3}$ at mine and $^{40}\text{Bq/m}^{-3}$ (dome air, circulated from outside)

| Range | Region | Resolution/count |
|--------|----------|-------------------|
| Small | 0-51pC | 0.1pC (0.04p.e.) |
| Medium | 0-357pC | 0.7pC (0.26 p.e.) |
| Large | 0-2500pC | 4.9pC (1.8 p.e.) |

- Other backgrounds :
- $I_{\mu} = 6 \times 10^{-8} \text{ cm}^{-2} \text{ s}^{-1} \text{ sr}^{-1}$
- Signal : $I_{\mu}^{\nu} = 2.17 \times 10^{-13} \text{ cm}^{-2} \text{ s}^{-1}$

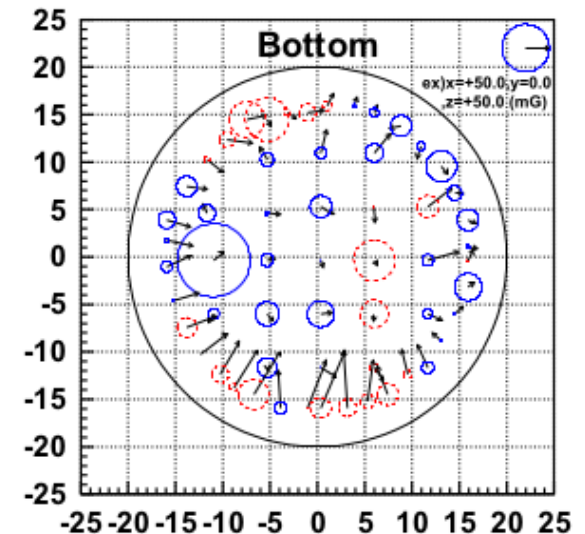
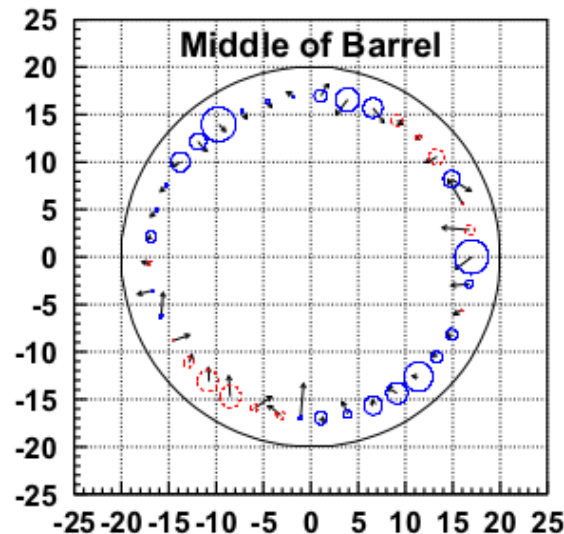
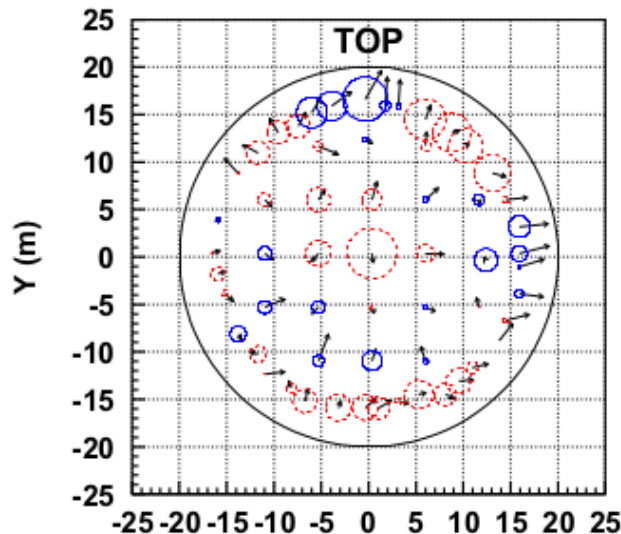
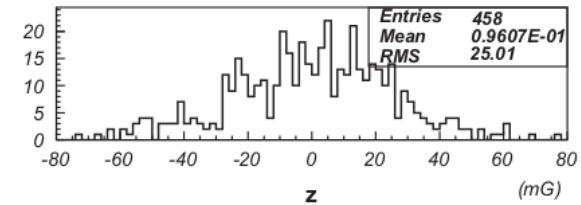
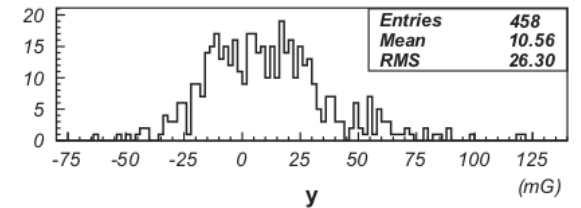
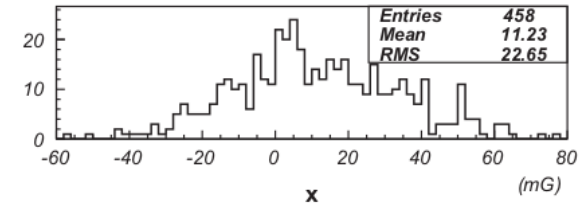
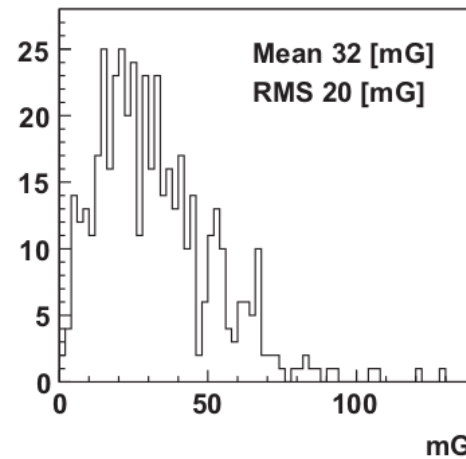
| Particle | Energy Range | Rate ($\text{cm}^{-2}\text{s}^{-1}\text{sr}^{-1}$) |
|----------------|--|--|
| γ -rays | $E_{\gamma} > 0.5 \text{ MeV}$ | 0.1 |
| | $E_{\gamma} > 5 \text{ MeV}$ | 2.7×10^{-6} |
| Neutrons | $E_n \leq 5 \times 10^{-2} \text{ eV}$ | 1.4×10^{-5} |
| | $5 \times 10^{-2} < E_n \leq 2.5 \times 10^6 \text{ eV}$ | 2.5×10^{-5} |
| | $2.5 \times 10^6 < E_n \leq 2.5 \times 10^7 \text{ eV}$ | 0.33×10^{-5} |

Trigger threshold
29 p.e. \equiv 5.7 MeV electron
Also 4.6 MeV trigger (SLE)

SK : Magnetic field & PMT performance

Geomagnetic field inside the tank :

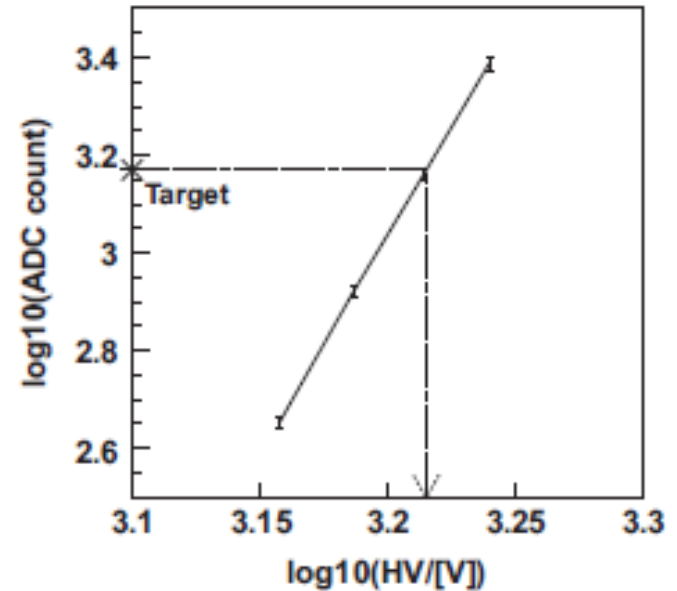
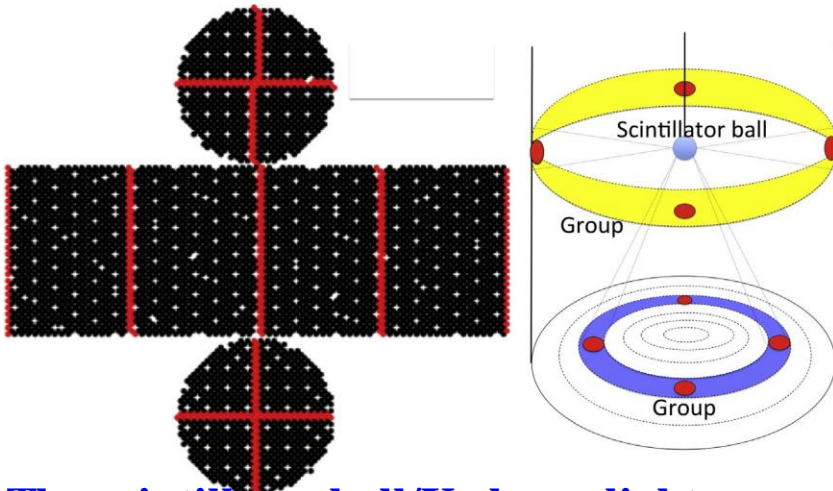
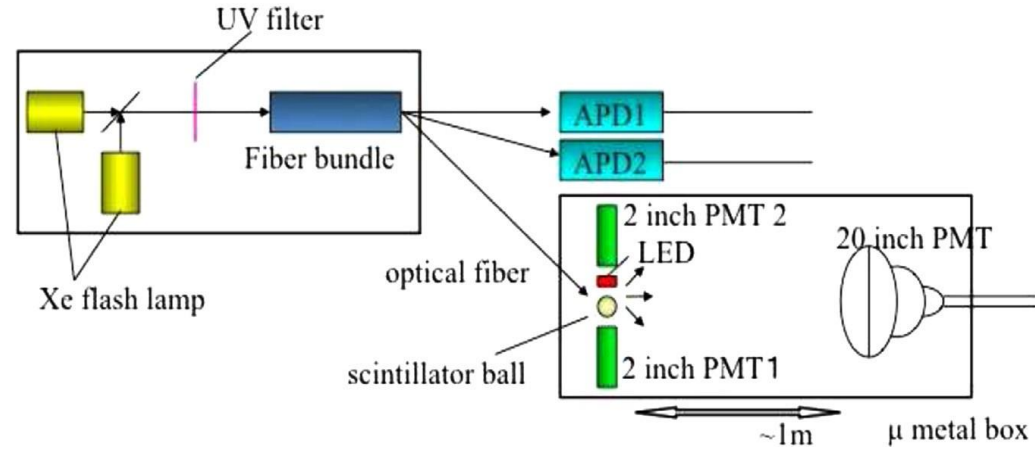
- A **100mG** field parallel to axis of 20" PMT → Reduction of **hit collection by 10%**
- the compensation coils on the outer OD wall provide enough magnetic field correction, maximum field is **32mG** (reduction in $\epsilon \sim 1-2\%$)



X (m)

PMT and electronics (pre)calibration

- Prepare 400 PMTs with precise gain measurement before the SK starts
 - Adjust HV to have the same gain at 30 p.e. level
- Set them in geometrically uniform to SK
- Adjust HV of other PMTs to these PMTs (done with in 1.3% precision)
 - The “QE × gain” for each PMT is adjusted : First step of calibration



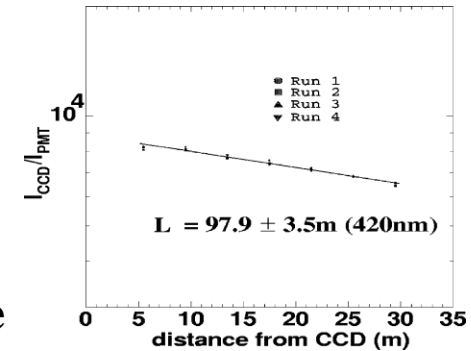
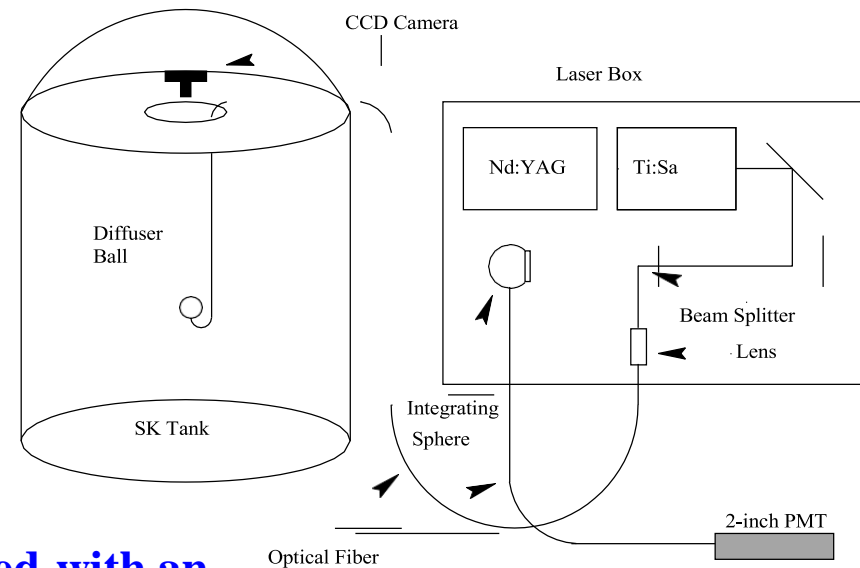
The scintillator ball/Xe lamp light source remains permanently at the center of the ID for real-time as well as long-term monitoring of ID-PMT gains.

Calibration : Water transparency measurement

- The optical attenuation length in water represents the combined effects of scattering (Rayleigh and Mie) and absorption on the intensity of light

$$- I = I_0(1/l) \exp(-l/L_{att}) \text{ with } L_{att} = (1/(\alpha_{abs} + \alpha_{scat}))$$

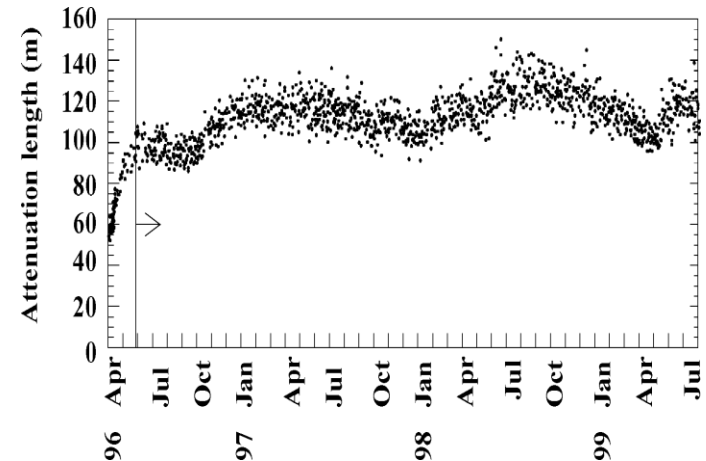
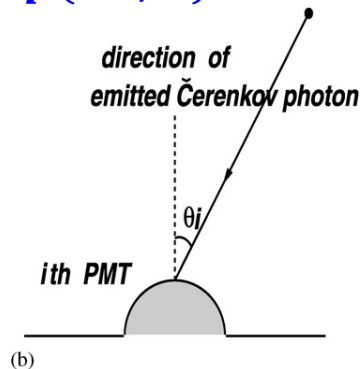
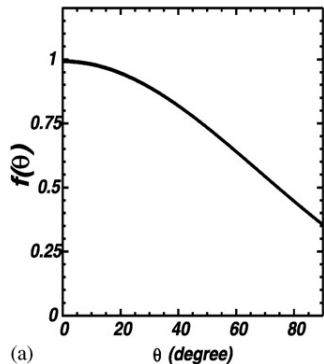
- The tunable titanium-sapphire laser is pumped with an Nd:YAG laser, which can provide output energies of 2–3 mJ per pulse at a wavelength of 420 nm and using second harmonic generator attenuation length within 350 to 500nm is measured



- Indirect measurement with cosmic rays as constant light source

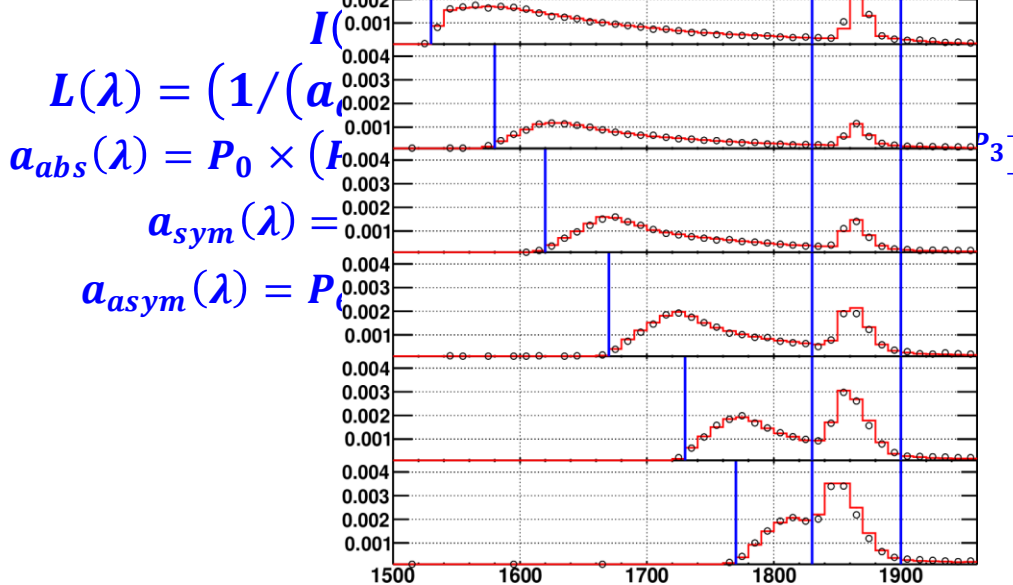
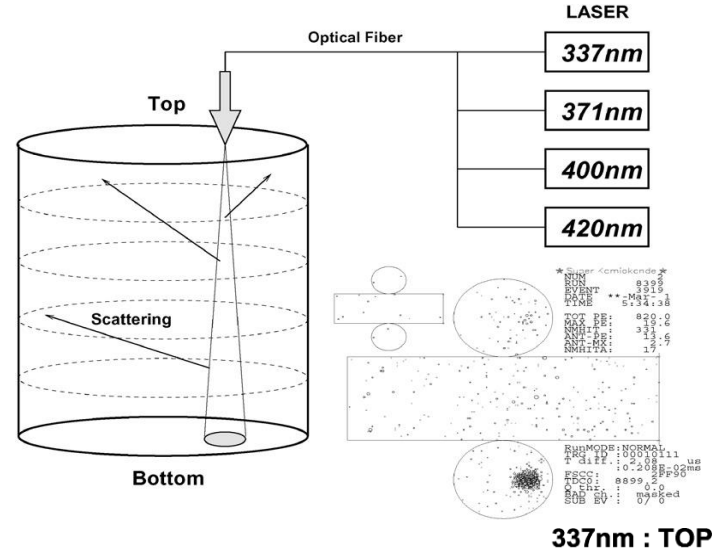
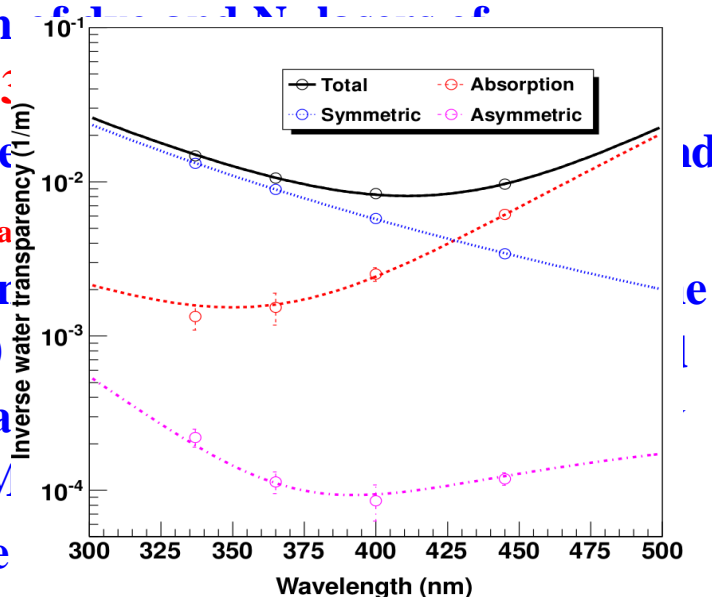
Cannot measure λ -dependent attenuation

$$Q = Q_0(f(\theta)/l) \exp(-l/L)$$



Calibration : Light scattering measurement

- A combination of wavelengths sources are used for absorption measurement
- Total charge in peak near 730 nm is the second peak in the bottom PM
- Each laser fire taking

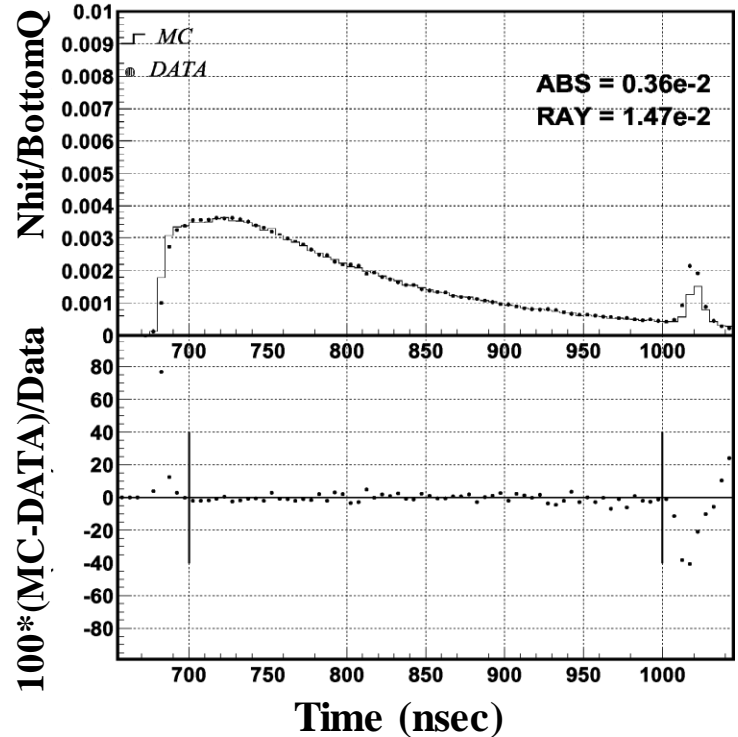


$$L(\lambda) = \frac{1}{\alpha(\lambda)}$$

$$\alpha_{abs}(\lambda) = P_0 \times I(\lambda)$$

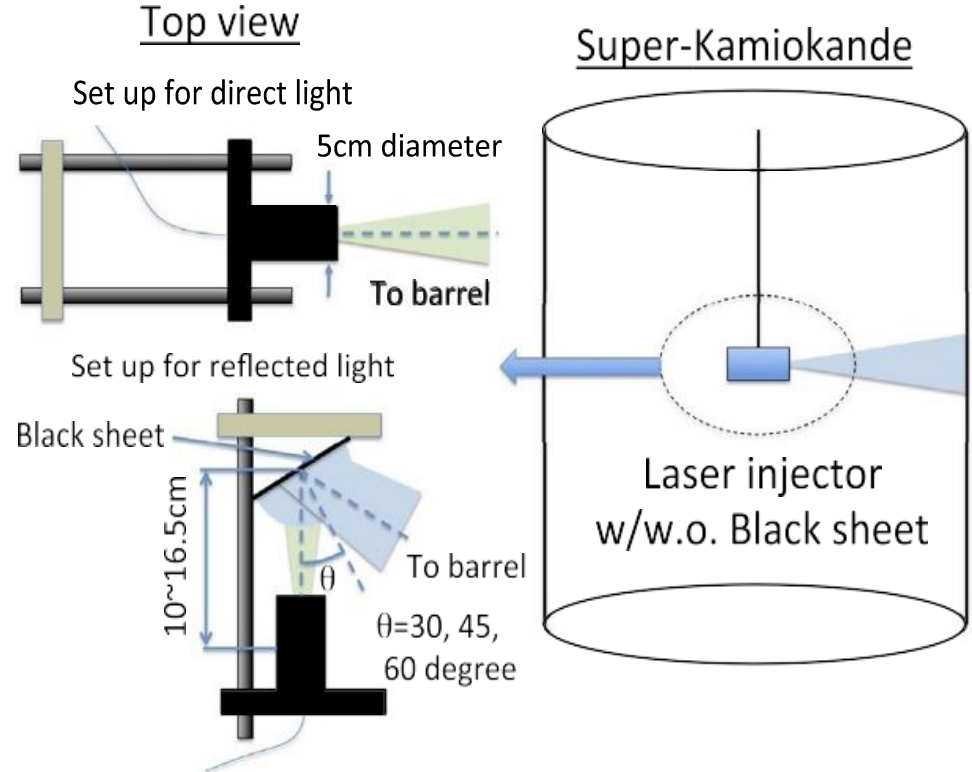
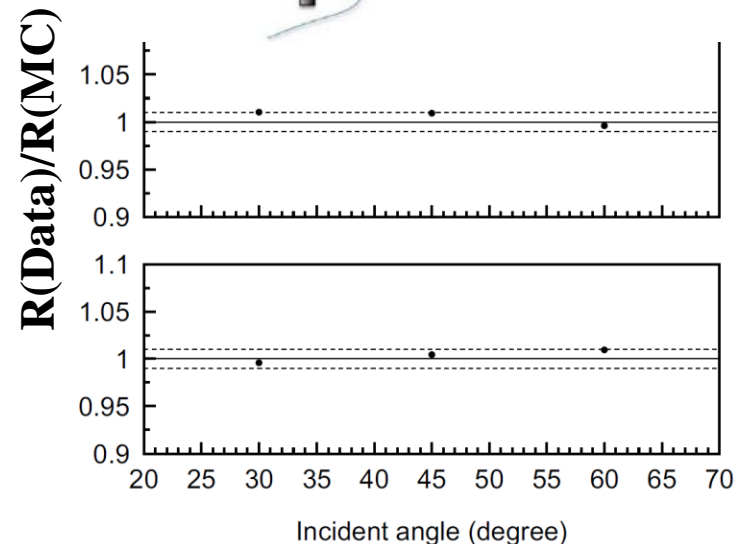
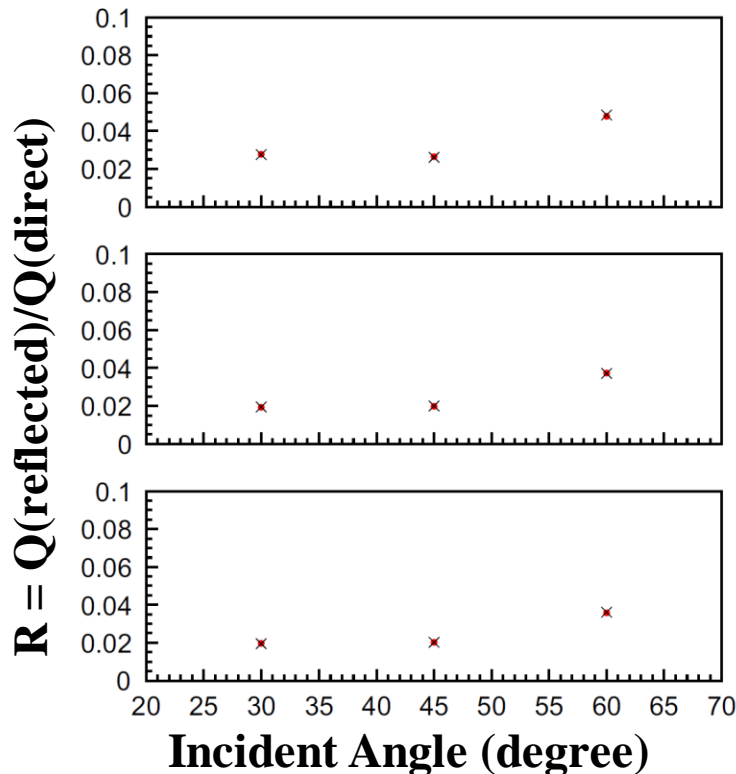
$$\alpha_{sym}(\lambda) = P_1 \times I(\lambda)$$

$$\alpha_{asym}(\lambda) = P_2 \times I(\lambda)$$



Light reflection at PMT and black sheet

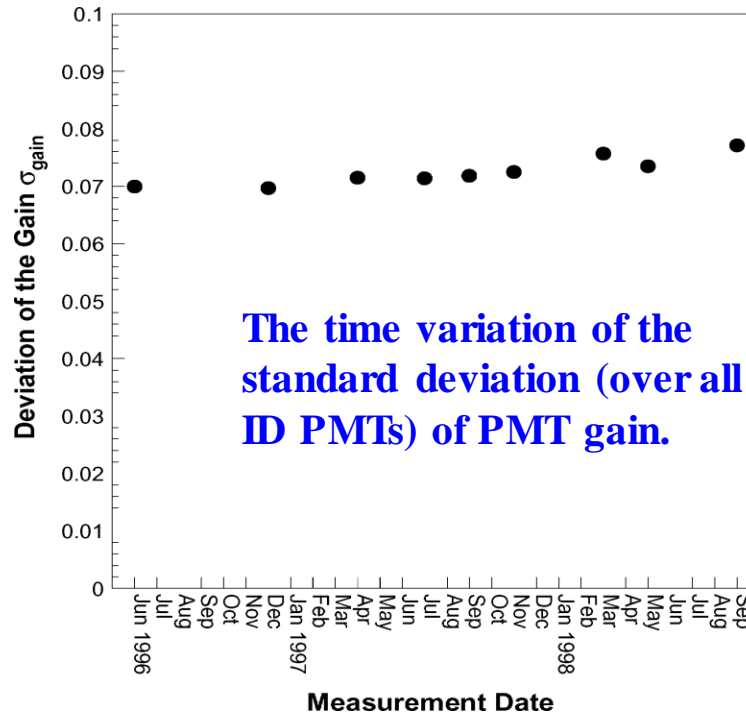
- $n_{\text{water}} = 1.33$
- $n_{\text{glass}} = (1.472 + 3670/[\lambda(\text{nm})]^2)$
- $n_{\text{bialkali}} = n_{\text{real}} + i \cdot n_{\text{img}}$
- **Best fit value from scattering ($n_{\text{real}} = 1.667$ and $n_{\text{img}} = 1.31, 2.69, 3.06, 3.24$ for $\lambda = 337, 363, 400$ and 420 nm)**



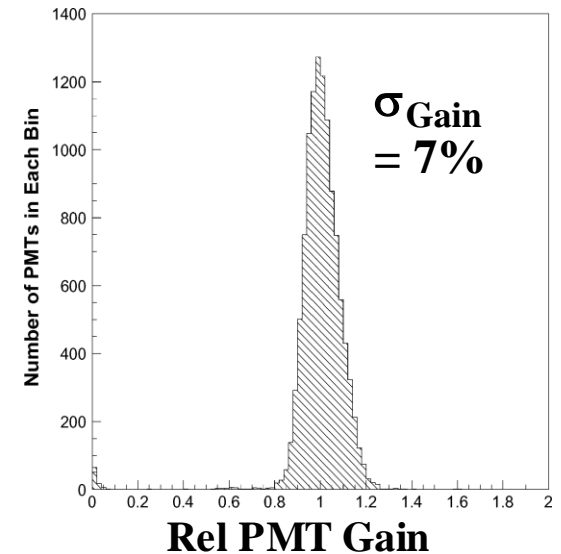
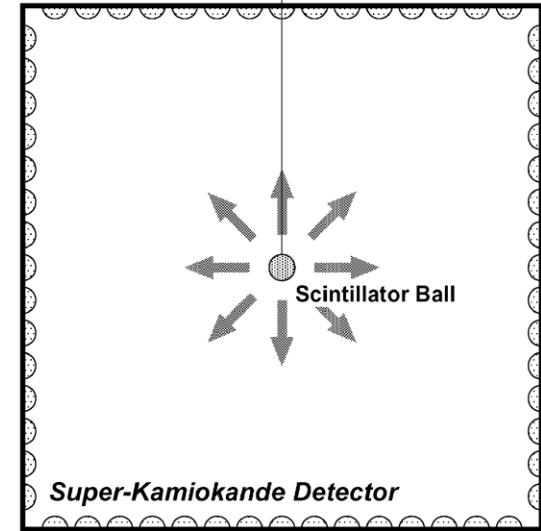
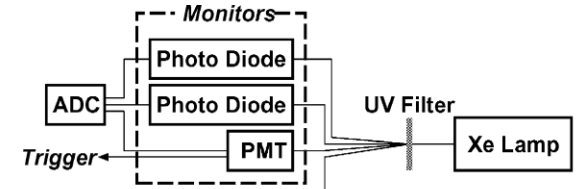
Relative Gain Calibration

- Light generated by a Xe lamp is passed through an ultraviolet (UV) filter and injected into a scintillator ball (acrylic ball with BBOT wavelength shifter with emission peak at 440nm and MgO powder diffuser) via an optical fiber.

- Relative Gain, $G_i = \frac{Q_i}{Q_0 f(\theta)} l_i \exp\left(\frac{l_i}{L}\right)$

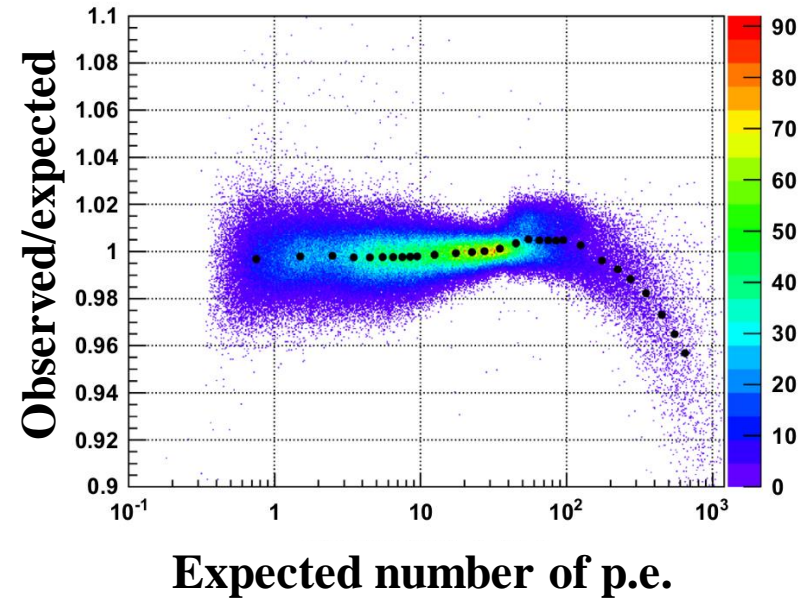
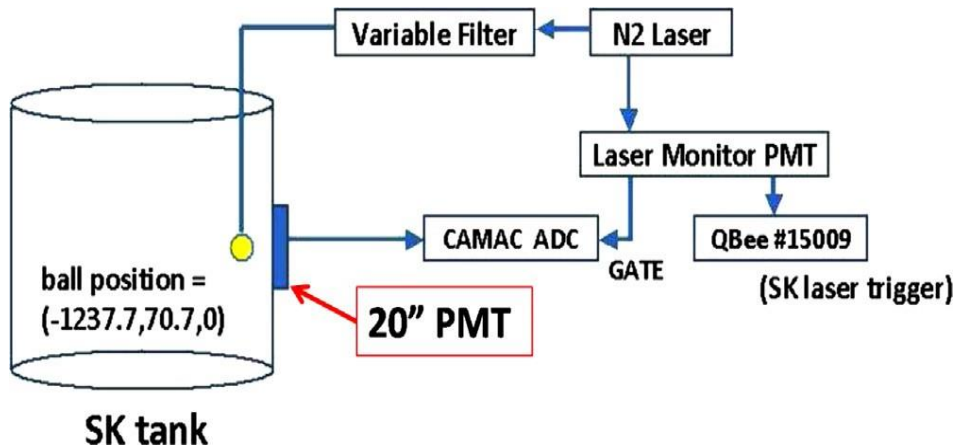


The relative gain distribution measured just after recalibration and adjustment, in June, 1996.



Linearity of charge measurement

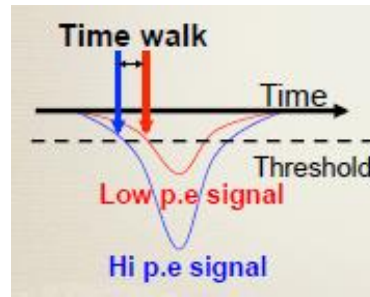
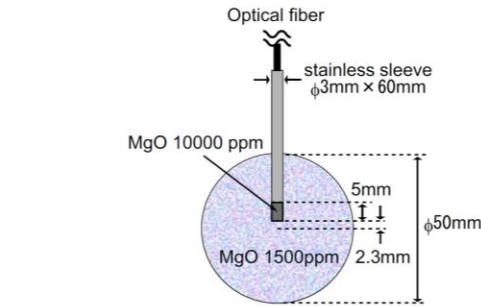
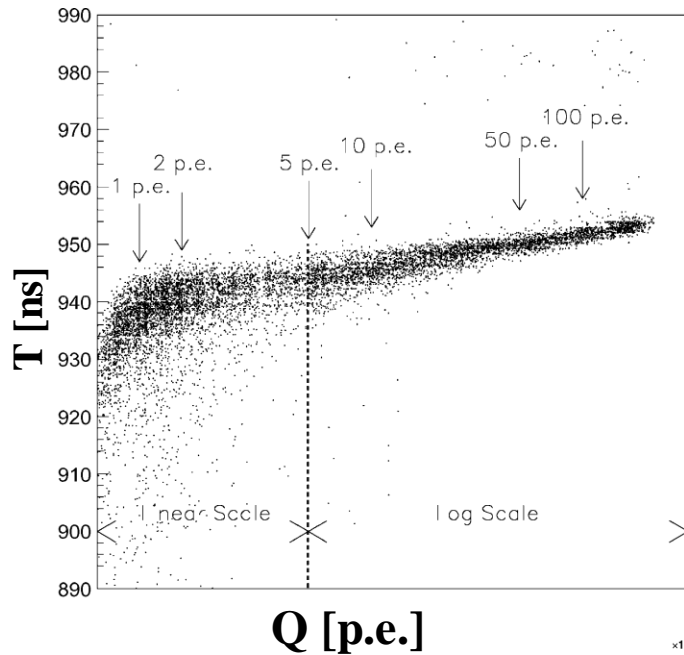
- Thirty different laser intensities were injected into the diffuser balls
- Each PMT is self normalised with 30p.e. signal (HV setting for that)



- 1% variation at 200 p.e. and 10% at 1000 p.e.

Relative Timing Calibration

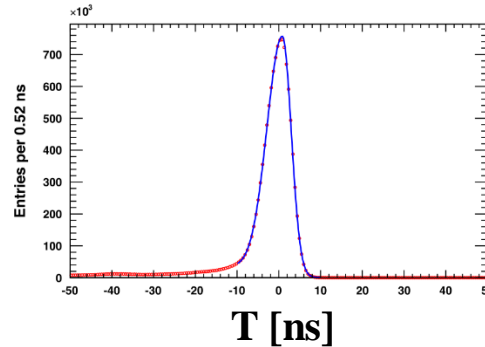
- Intense N₂ LASER, $\lambda=337\text{nm}$, repetition time 3ns, converted to $\lambda=384\text{nm}$, near the lower edge of sensitive region \rightarrow TiO₂ diffuser and further diffused by LUDOX



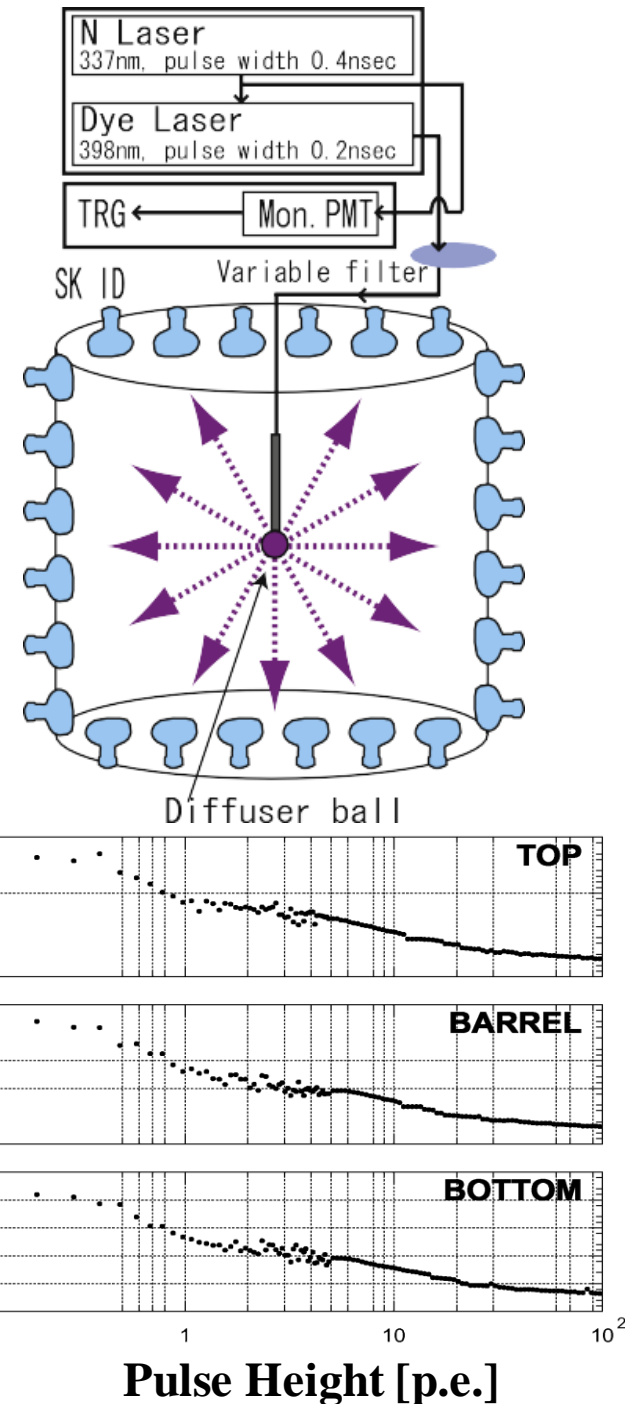
$$f(t; t > T_{peak}) \equiv A_1 \cdot \exp\left(-\frac{(t - T_{peak})^2}{\sigma_t^2}\right) + B_1$$

$$f(t; t < T_{peak}) \equiv A_2 \cdot \exp\left(-\frac{(t - T_{peak})^2}{\sigma_t'^2}\right) + B_2$$

$$A_1 + B_1 = A_2 + B_2$$

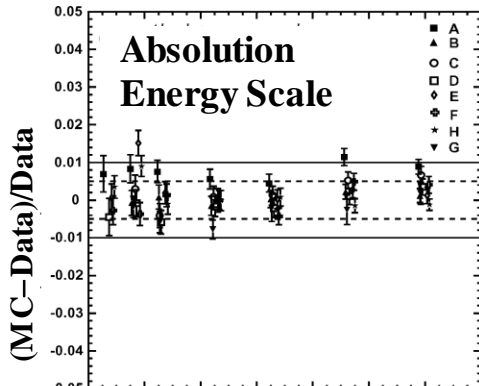
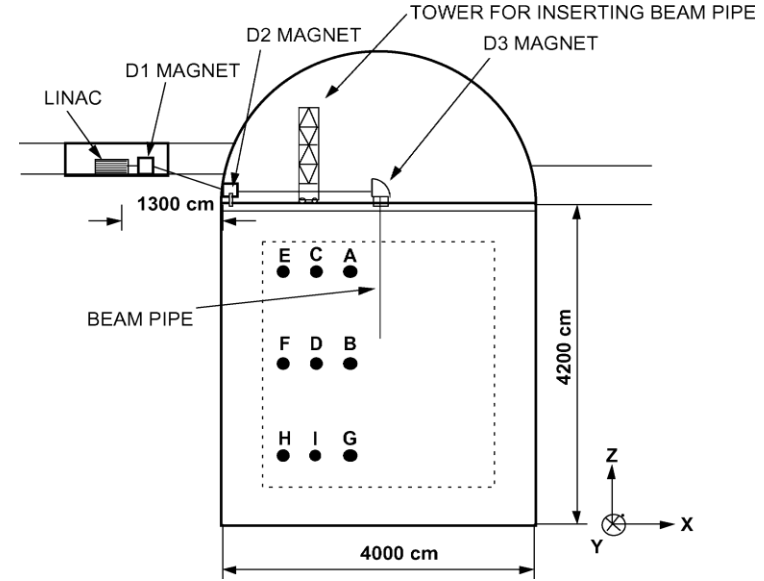


Q corrected timing

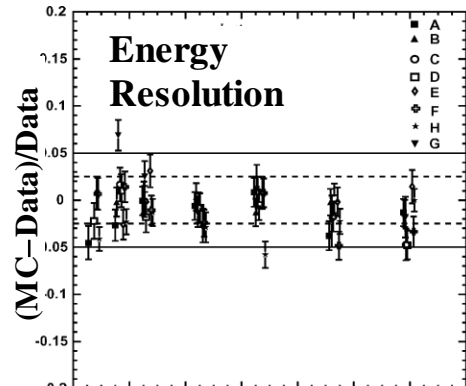


LINAC as a source of electrons of known energy

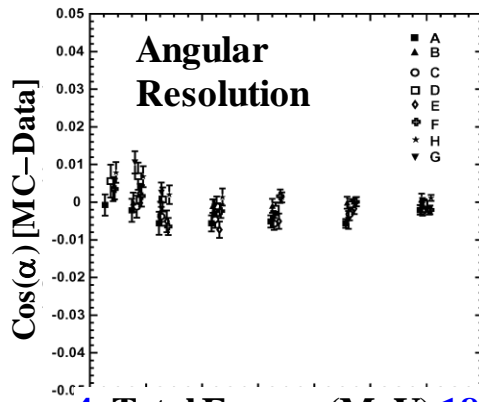
- The accuracy of the absolute energy scale is better than 1% in the energy range from 5 to 16.3 MeV.
- The LINAC calibration data were taken once or twice per year



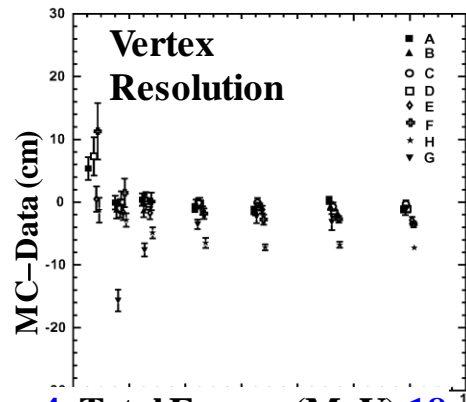
(a) 4 Total Energy (MeV) 18



4 Total Energy (MeV) 18



(c) 4 Total Energy (MeV) 18



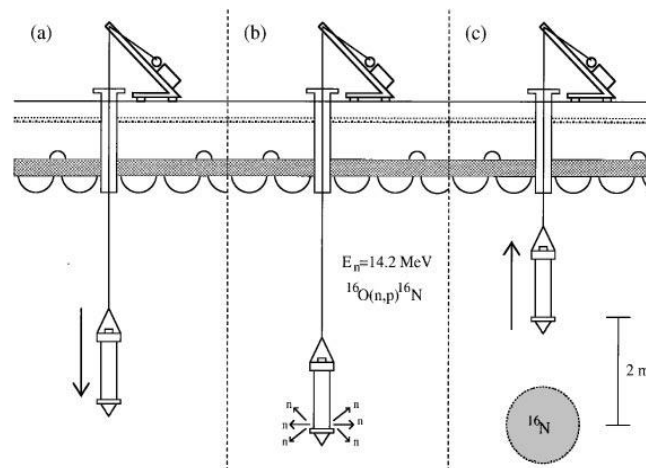
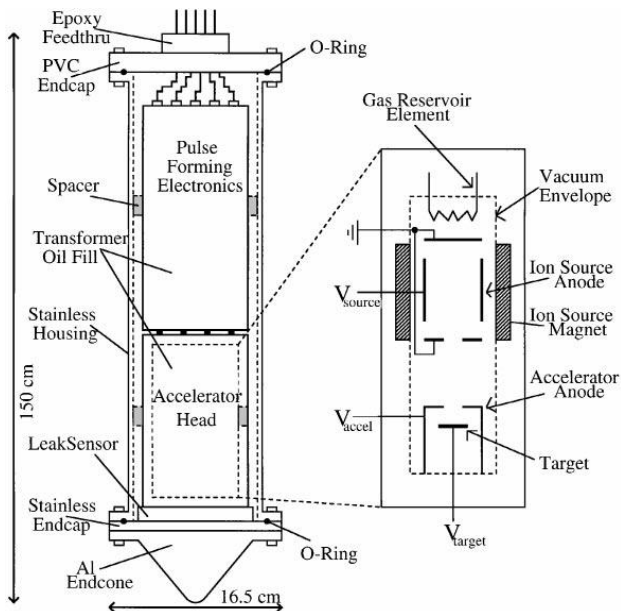
4 Total Energy (MeV) 18

| Energy (MeV) | Energy resol(%) | Ang resol (degree) | Vertex resol(cm) |
|--------------|-----------------|--------------------|------------------|
| 4.89 | 20.9±0.6 | 36.7±0.2 | 182±21 |
| 5.84 | 19.2±0.5 | 34.6±0.2 | 133±8 |
| 6.79 | 18.0±0.3 | 32.9±0.1 | 108±5 |
| 8.67 | 16.2±0.2 | 28.4±0.2 | 85±2 |
| 19.78 | 14.7±0.3 | 25.3±0.1 | 73±2 |
| 13.44 | 13.5±0.3 | 22.5±0.1 | 65±2 |
| 16.09 | 12.6±0.3 | 20.6±0.1 | 50±2 |

^{16}N Calibration : deuterium-tritium neutron generator (DTG)

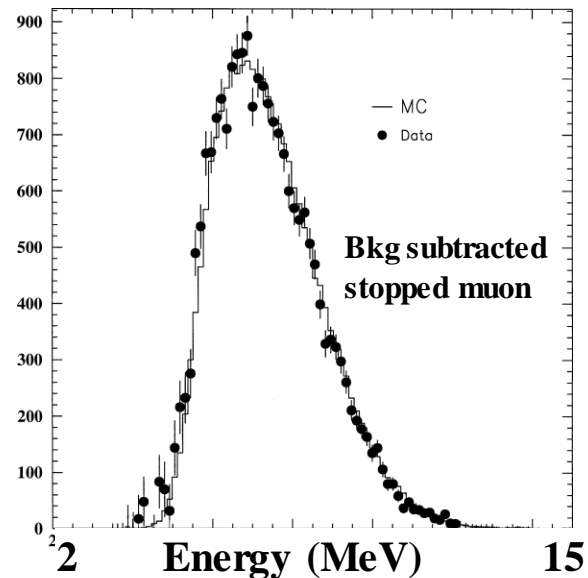
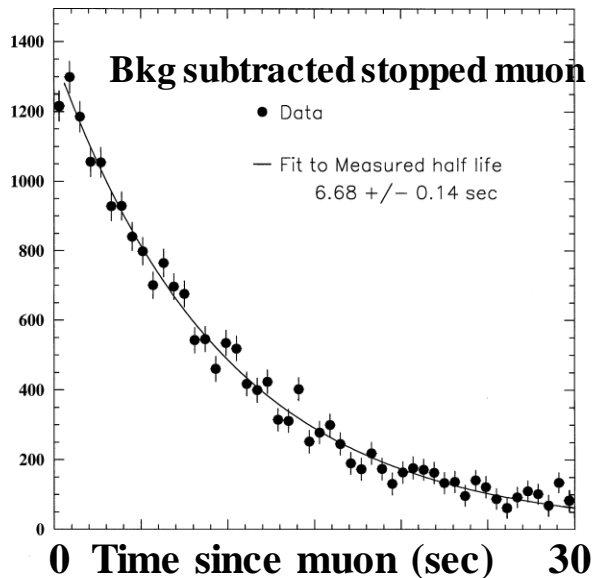
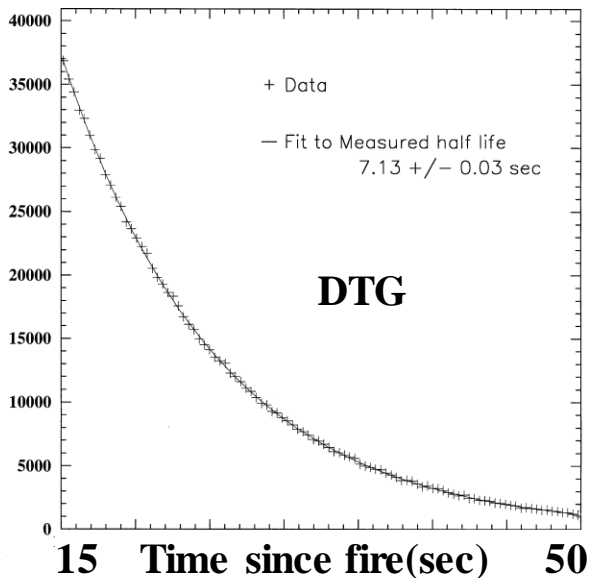
- A DTG is employed to create ^{16}N via the (n,p) reaction on ^{16}O ($E_{\text{th}} \sim 11 \text{ MeV}$) in the water of the detector. Efficiency $\sim 1\%$
- Isotropic and different systematic than LINAC : An independent measurement
- The decay of ^{16}N ($\rightarrow ^{16}\text{O} + \beta^- + \bar{\nu}_e$), with a Q value of 10.4 MeV, $E_\beta = 4.3 \text{ MeV}$ (Maximum), $E_\gamma = 6.1 \text{ MeV}$, $\tau_{1/2} = 7.13 \text{ s}$
- Production of ^{16}N
 - $^3\text{H} + ^2\text{H} \rightarrow ^4\text{He} + \text{n}$: reaction yield isotropic distribution 14.2 MeV neutron
 - 80-180 kV accelerating voltage for this reaction
 - Maximum rate 100 Hz and $\sim 10^6$ n/pulse

- $^{16}\text{O} + \mu^- \rightarrow ^{16}\text{N} + \nu_\mu$
- Naturally occurring background
- Found by collecting events that occur in the area surrounding the stopping point
- $N_{ev} = N_{stop} \mu \left(\frac{\mu^-}{\mu^+ + \mu^-} \right) f_{capture} f_{gs} \epsilon$
- $\sim 1 \text{ evt/kTon fiducial vol/day}$

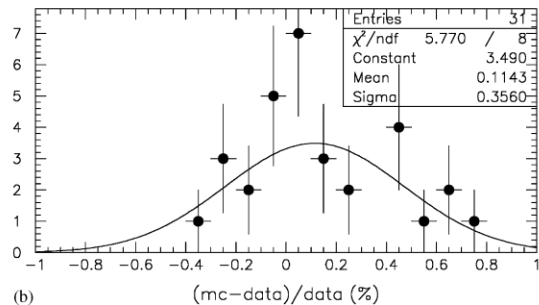
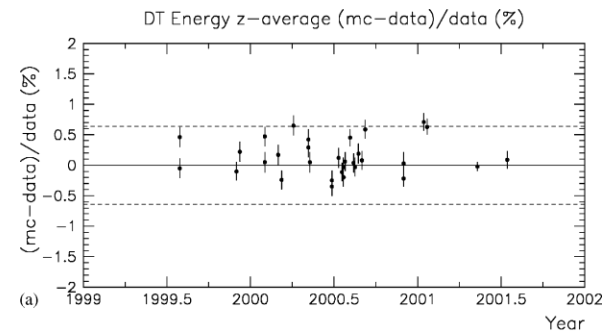
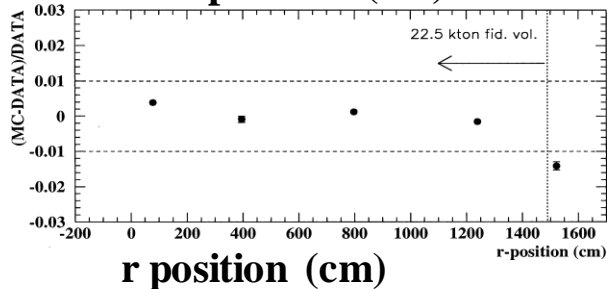
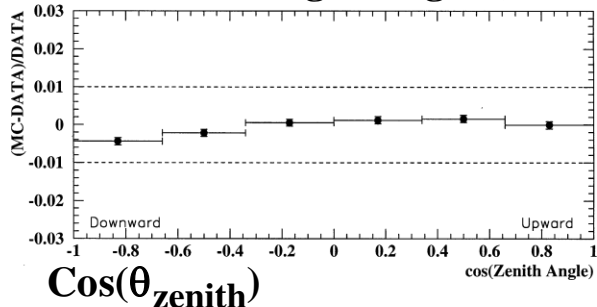
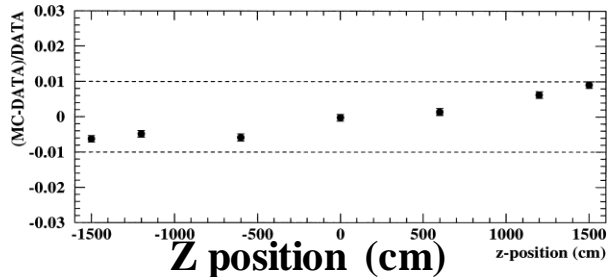
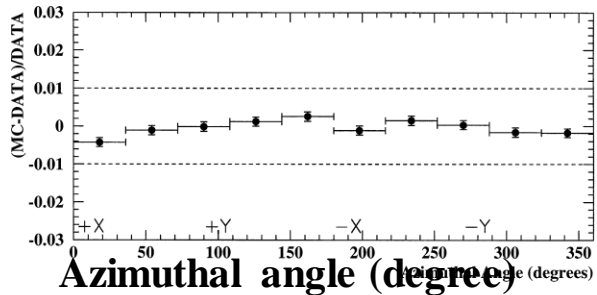


NIMA 458 (2001) 636

^{16}N Calibration : DTPG

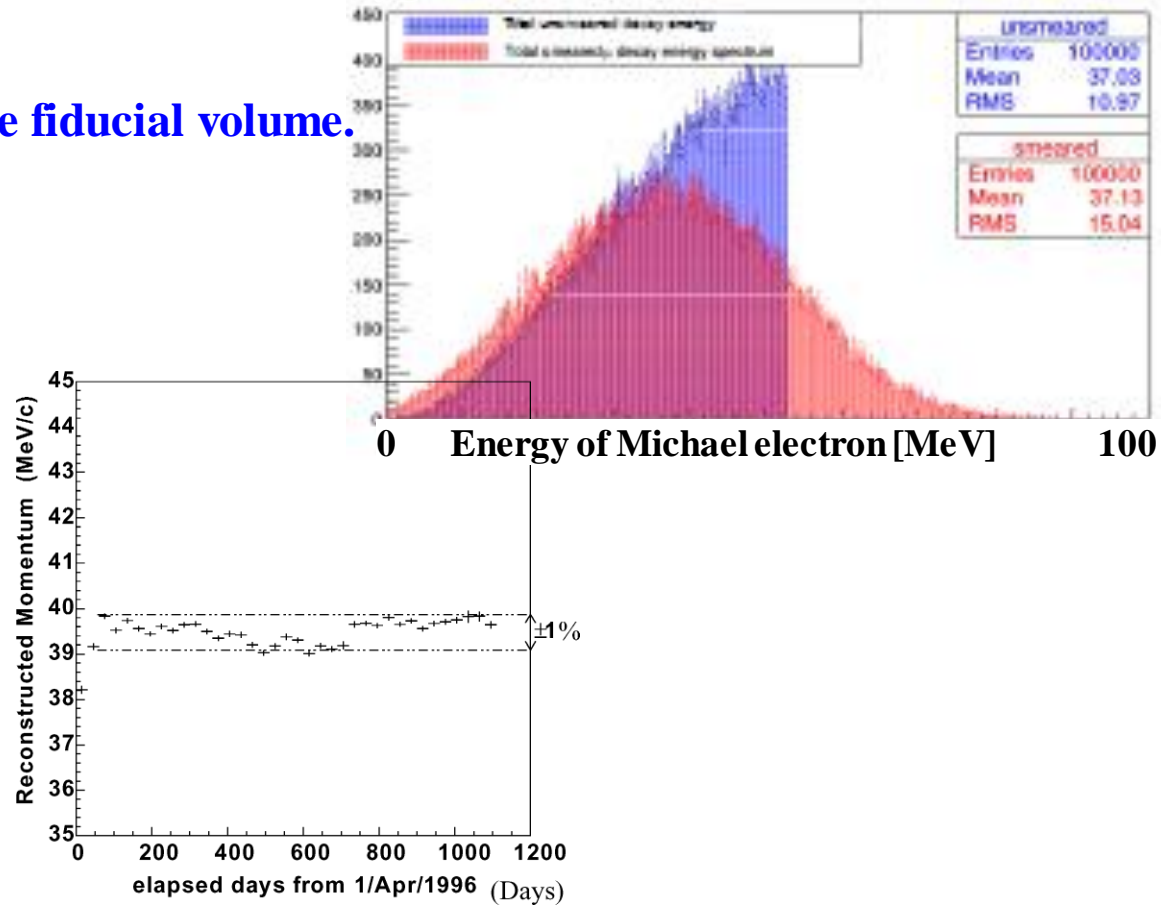
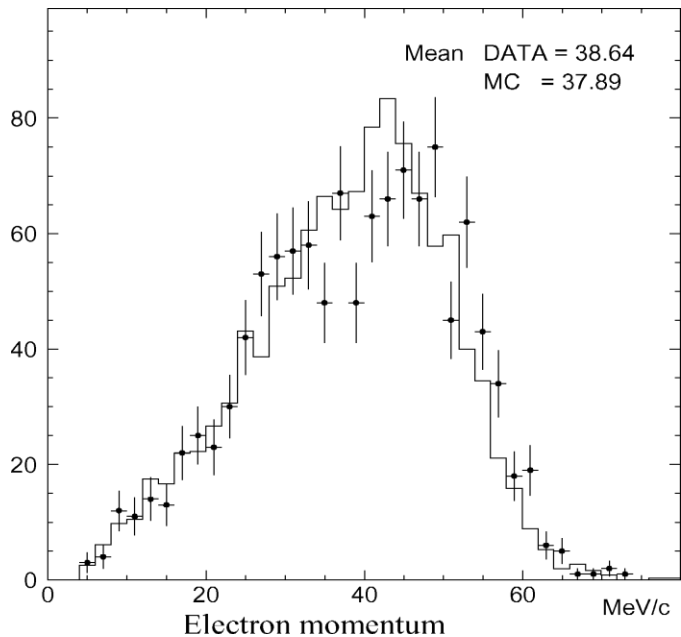
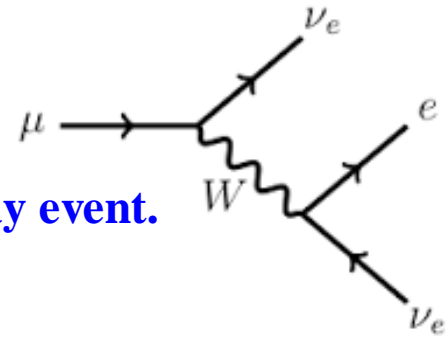


• Comparison of Data/MC with ^{16}N source



Calibration with decayed electron

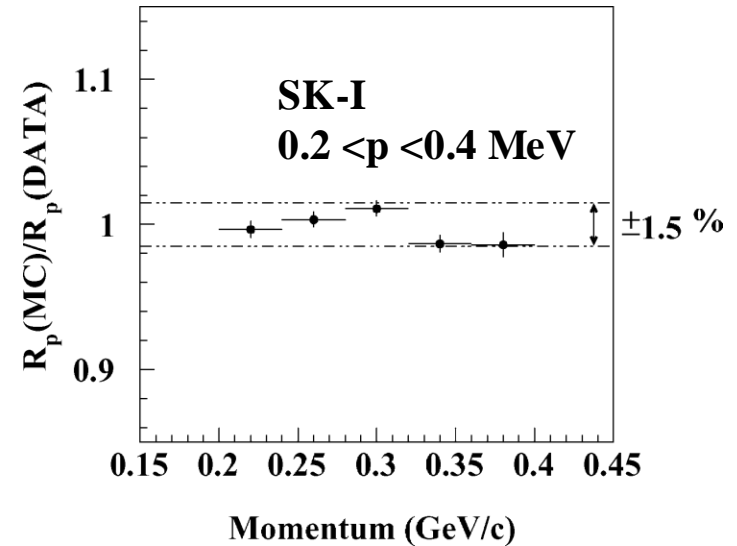
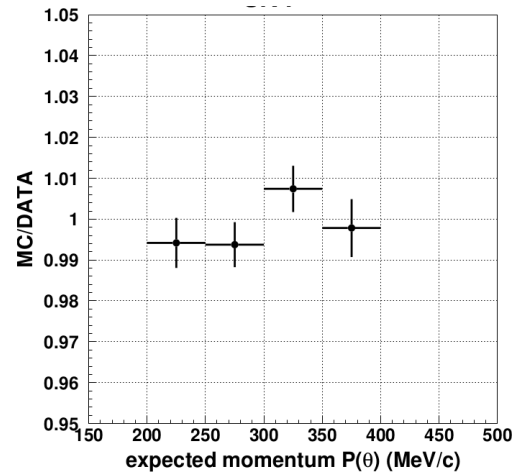
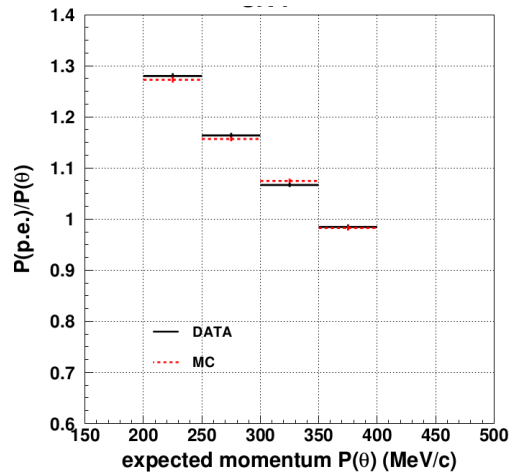
- Commonly known as Michael electron
- Must occur between $2 \mu\text{s}$ and $8 \mu\text{s}$ following a stopping cosmic ray event.
- Vertex fit goodness > 0.5
- Vertex reconstructed inside the fiducial volume.



Pre-calibration discrepancy for SK-I to IV is 0.6%, 1.6%, 0.8% and 1.6% respectively.

Calibration with stopping muon : θ_C

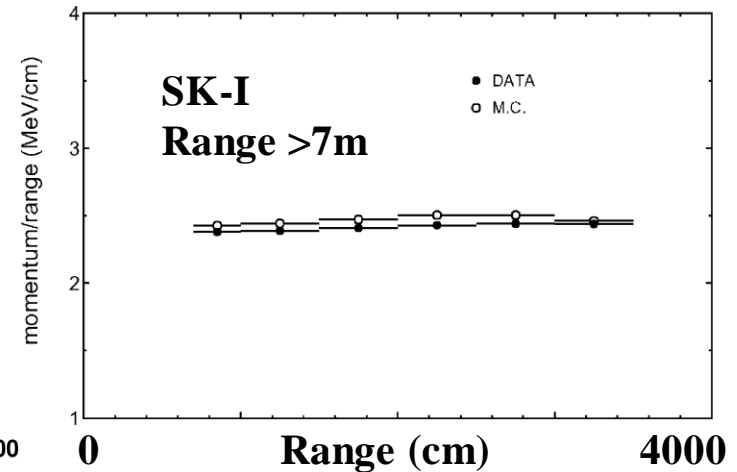
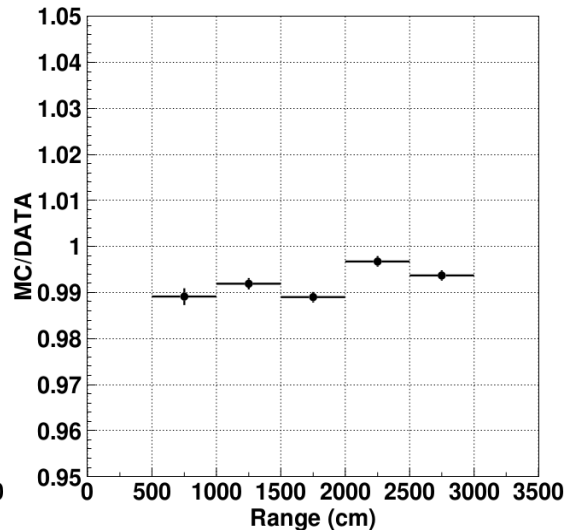
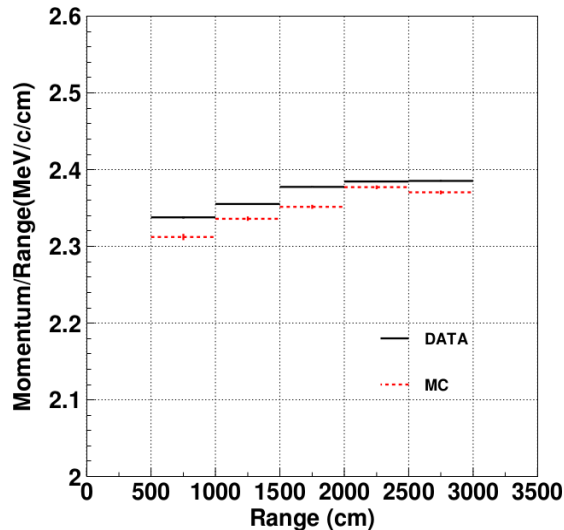
- Cherenkov angle < 400 MeV/c, $\cos\theta_C = (1/n\beta) = \sqrt{p^2 + m^2}/np$
- Total ID photo-electrons < 1500 (750 for SK-II)



- Disagreement between data and MC pre calibration is **0.7%, 1.3%, 2.1% and 2.1%** for SK-I to IV.

High energy stopping muon : Range ($-dE/dx$)

- Enters through the top wall of the detector.
- Reconstructed direction must be downward ($\cos \theta > 0.94$, where θ is the zenith angle).
- A single decay electron is detected.
- The track length of the muon must be ($7 < L < 30$)m.

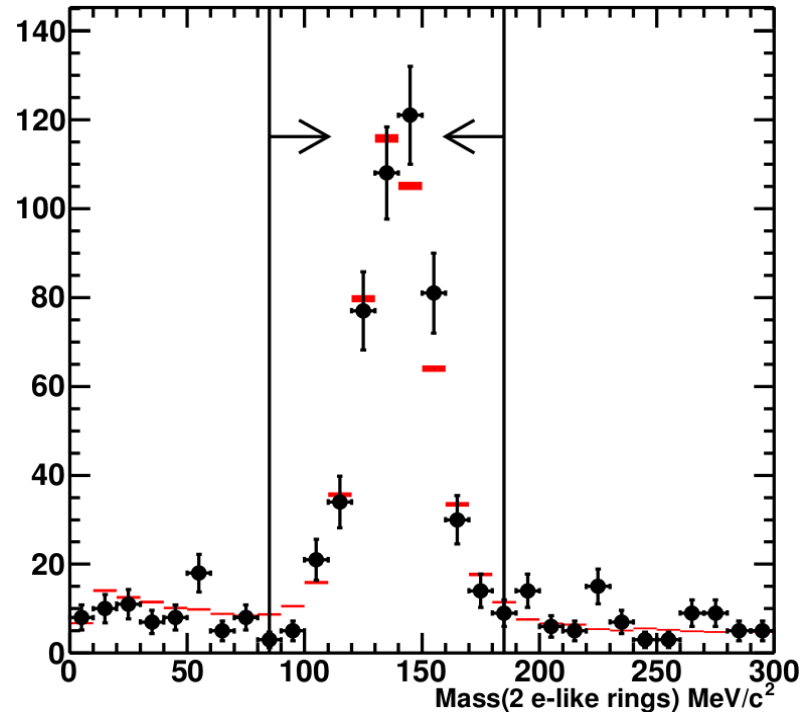


Data/MC discrepancies before calibration are **0.7%, 1.1%, 2.0% and 2.2%** for SK-I to IV respectively, depending on track length .

Calibration with π^0

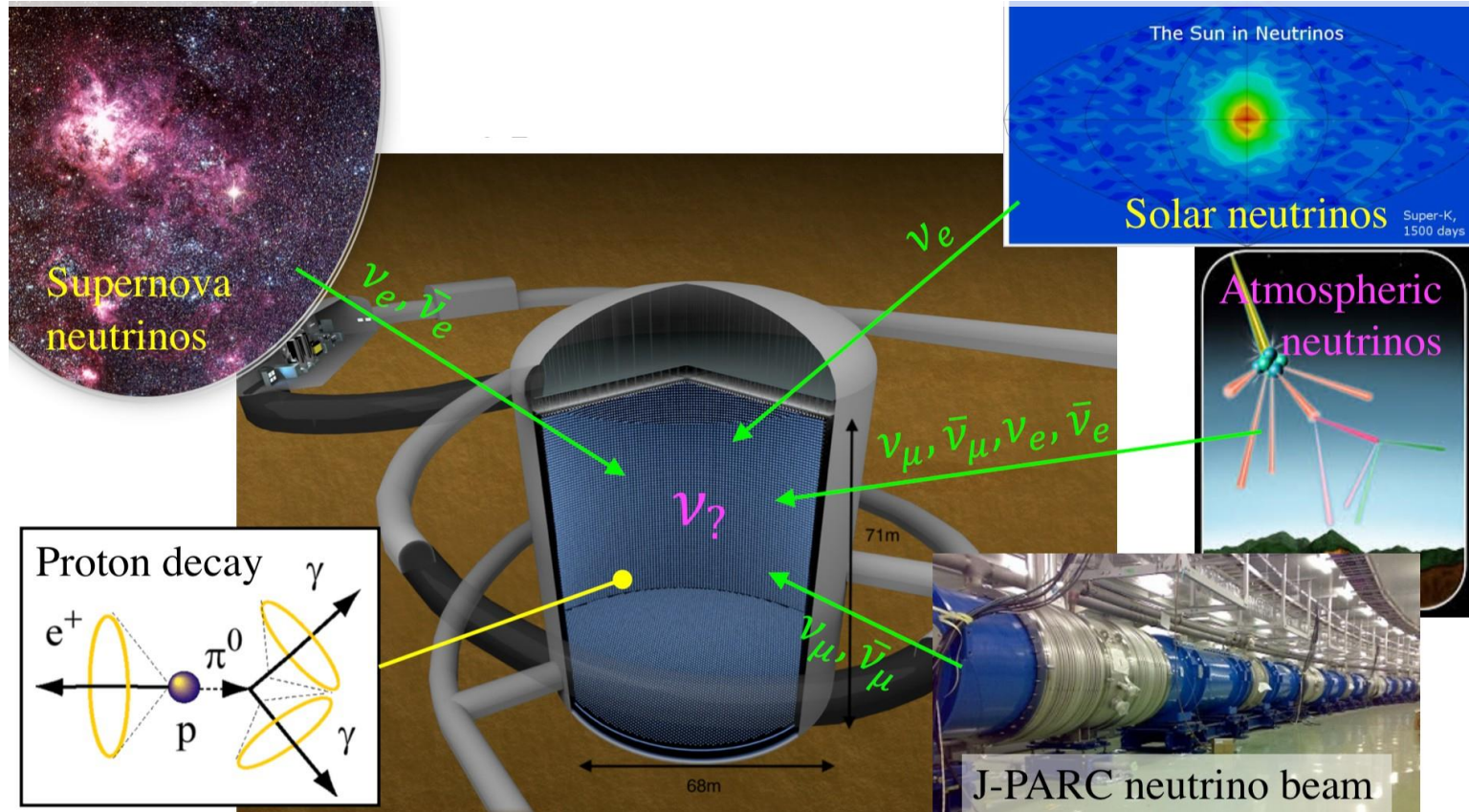
- Weak neutral current interaction of atmospheric muon and SK material frequently produces events with a single π^0
- Event vertex reconstructed within tank fiducial volume (> 2 m from ID wall, no large clusters of hits in OD). This is a standard criteria for selecting any fully-contained neutrino events.
- No decay electron (as this would imply a muon was present in the interaction).

$$M_{\pi^0} = \sqrt{2P_{\gamma 1} P_{\gamma 2}(1 - \cos\theta)}$$



- The shift of mass from 135 to 140 MeV (both in Data&MC) is due to de-excitation γ from the oxygen nucleus and a 20–30 cm vertex reconstruction bias.
- the discrepancies between data and MC are **0.7%**, **1.3%**, **0.3%** and **1.7%** for SK-I to IV.

Hyper-K will address broad science questions with unprecedented sensitivities



For example, Hyper-K(HK) will

- Determine the size of CP violation
- Explore baryon number violation

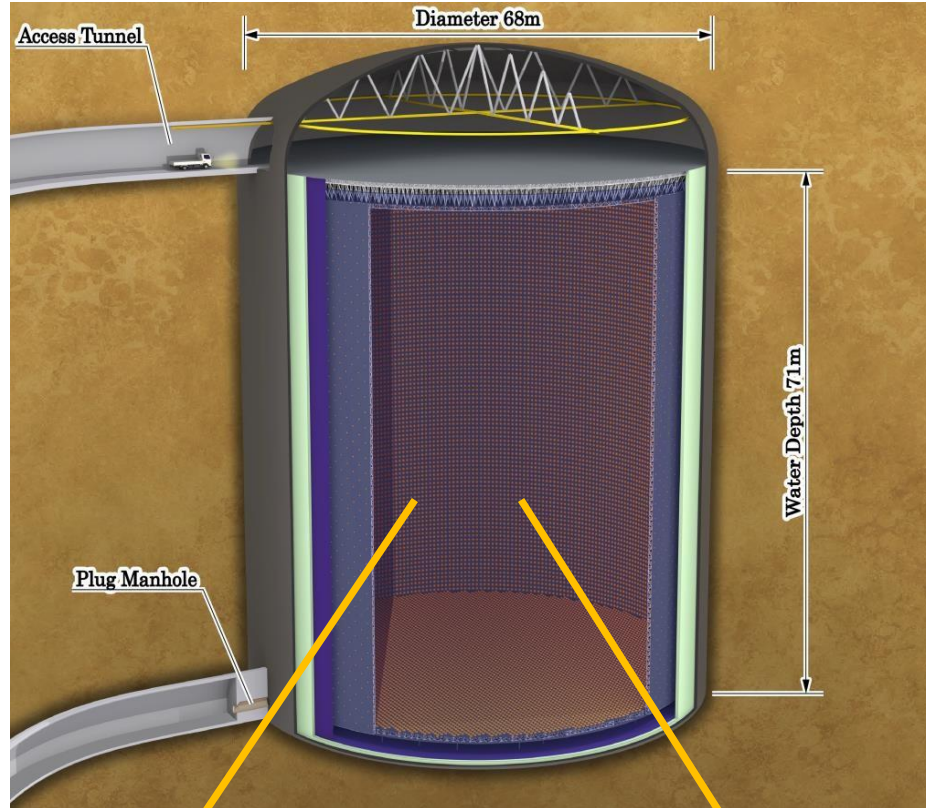
Hyper-Kamokande detector

Hyper-K will adopt the successful strategies used to study neutrino oscillations in Super-Kamiokande, K2K and T2K. Main improvements will be:

- Larger detector for increased statistics;
- Improved photo-sensors for better efficiency;
- Higher intensity beam and updated/new near detectors for the accelerator neutrino part.

The Hyper-K Far Detector (HK-FD) will be characterised by:

- Cylindrical tank: $\Phi = 68 \text{ m}$ and $H = 71 \text{ m}$
- ❖ Cavern: $\Phi = 69 \text{ m}$, $H = 73 \text{ m}$ + dome on top
- Fiducial volume: **0.19 Mtons**; $\times 8 \text{ SK} \rightarrow$ **HK-FD** (Total mass = 0.258 Mtons)
- Baseline design: 20% photo-coverage with
- 20,000 20'' B&L PMTs combined with few thousands of multi-PMT modules.



Photosensors: mPMTs vs 20" PMTs

complementary measurements of Cherenkov light systematic error reductions

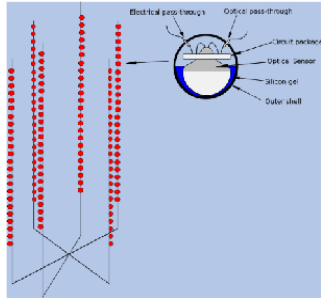


| | mPMT: 19 × 3" PMTs | 20" 'B&L' PMT |
|-----------------------|--|---|
| photo-cathode area | 870 cm² | 2000 cm ² |
| effective light yield | ~ 1 hit/MeV/5,000 mPMTs | ~6 hits/MeV/20,000 PMTs |
| dark noise | 19 × 200-300 Hz | ~4kHz (typical) |
| transit time spread | 1.3ns | 2.7ns |
| comments | <ul style="list-style-type: none"> • granularity • directionality • better time resolution | <ul style="list-style-type: none"> • performance confirmed • high photon detection efficiency |

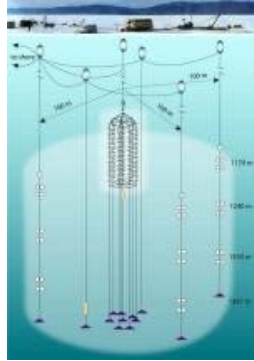
It will take 8 months to fill the complete HK with purified water

Water Cherenkov Detectors : Embedded” (TeV-PeV)

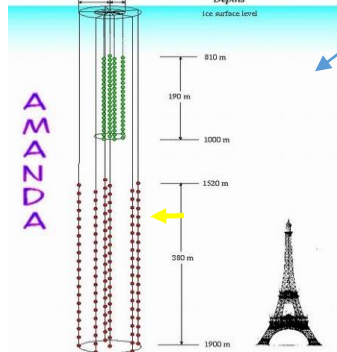
DUMUND Sea Water (Hawaii)



Lake Baikal Water under ice



Amanda Antarctic ice



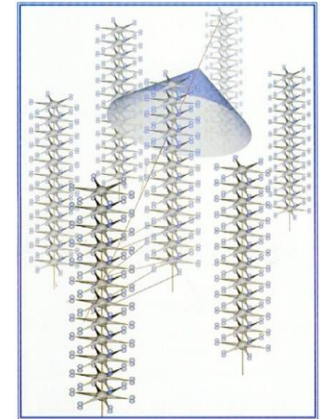
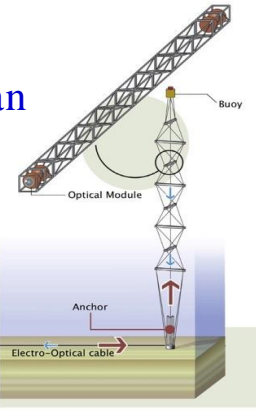
Pioneering

Current/recent

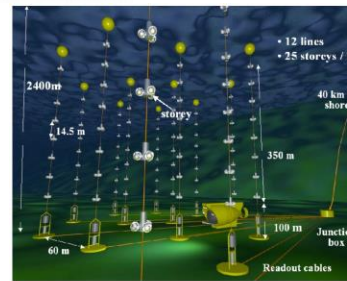
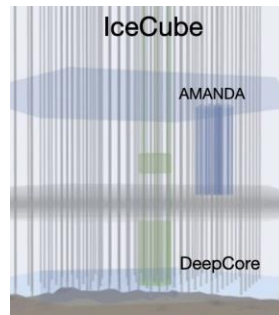
NEMO mediterranean

NESTOR mediterranean

Antares Mediterranean

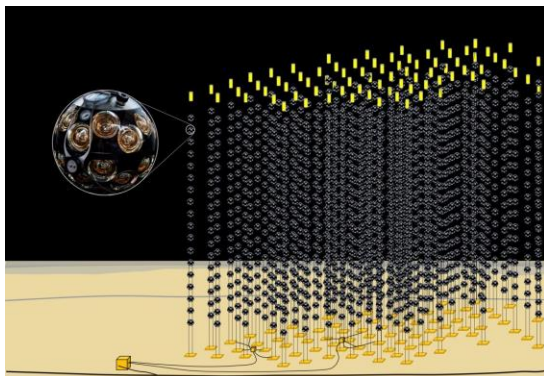


ICECUBE/Deep Core Antarctic Ice

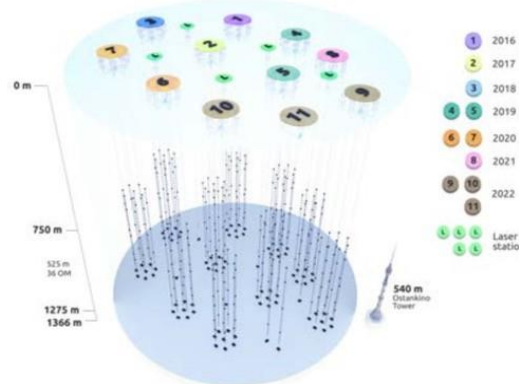


Operating/Expanding

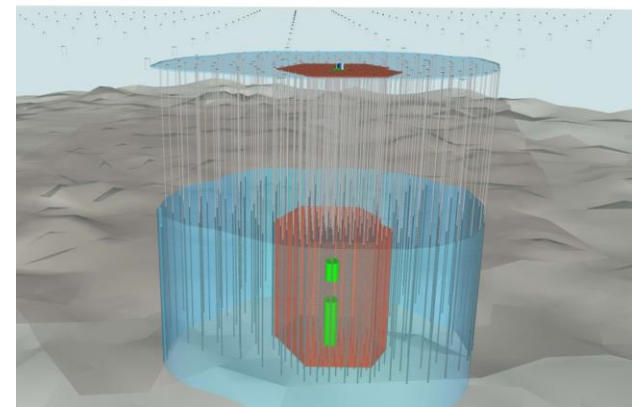
KM3NET:ARCA/ORCA Mediterranean



Baikal-GVD



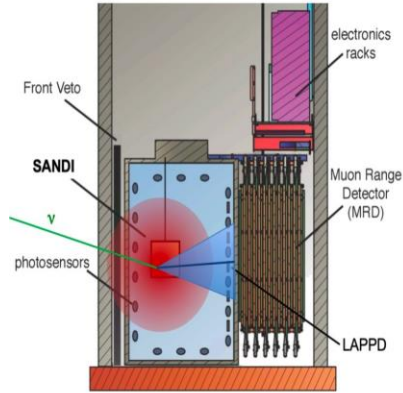
ICECUBE-GEN2 Antarctic Ice



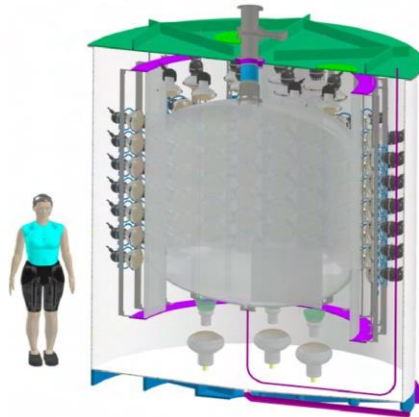
Water Cherenkov Detectors : Scale/Demonstrators

ANNIE (FNAL)
Water/Water-based LS

Operat
ing

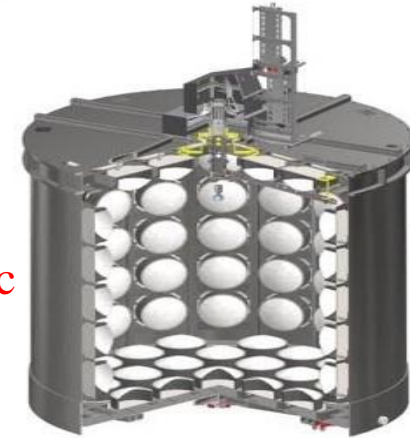


Eos (LBNL)
Water/Water-based LS



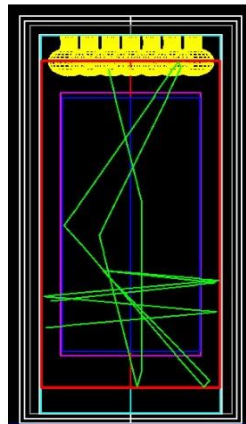
Construc
tion

WCTE
(CERN)



COHERENT HWD
(SNS) D₂O

Plann
ing

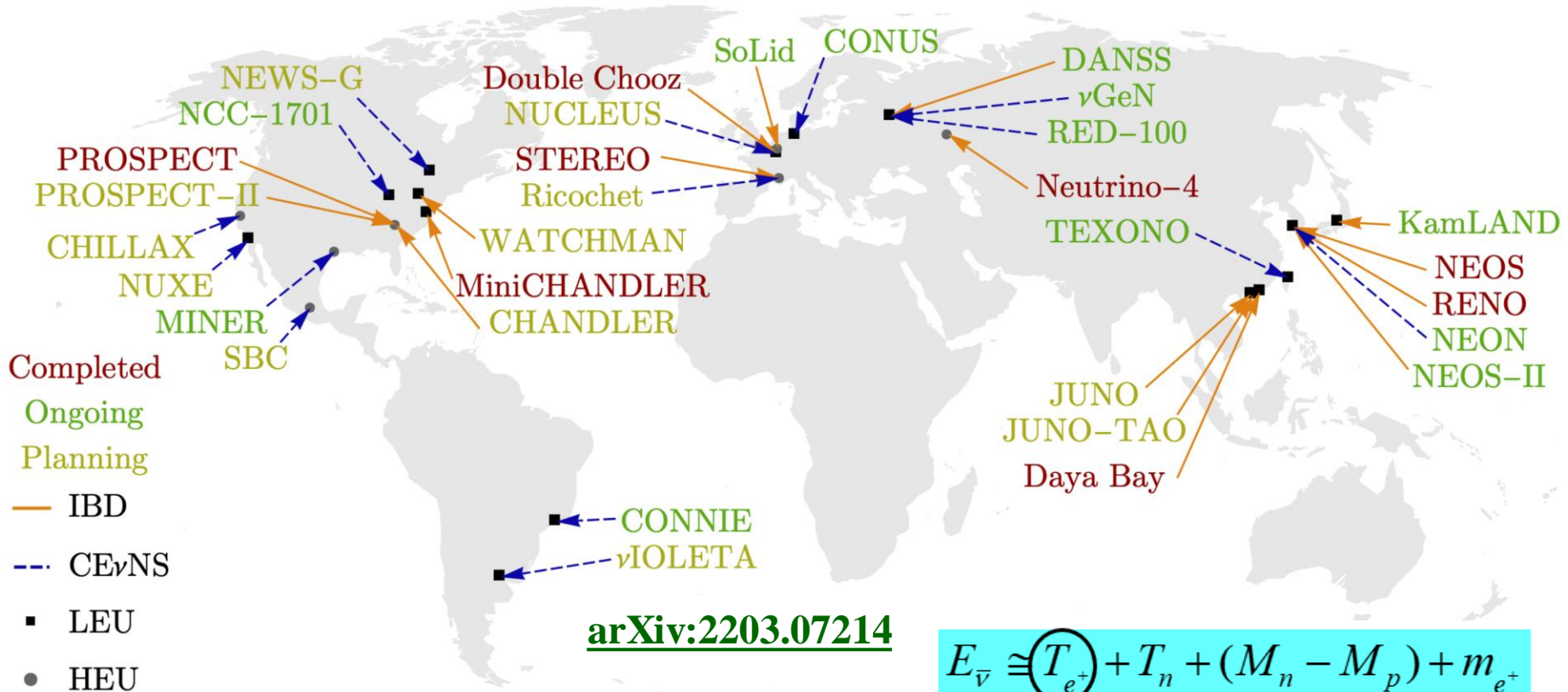


“30 ton” WbLS
demonstrator (BNL)



Construction

LS-based Reactor Neutrino Experiments

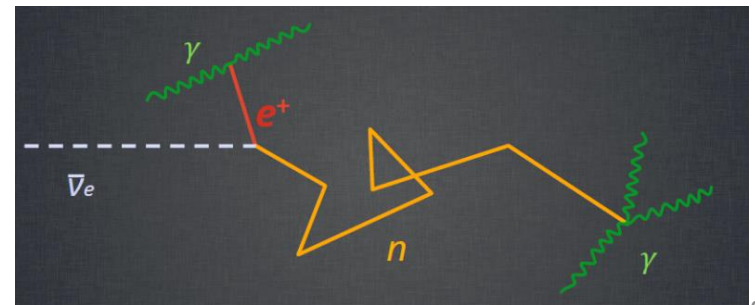


$$E_{\bar{\nu}} \cong \underbrace{(T_{e^+})}_{10-40 \text{ keV}} + \underbrace{T_n + (M_n - M_p)}_{1.8 \text{ MeV: Threshold}} + m_{e^+}$$

❖ Measure neutrino oscillations with different baselines

- LBL (>100 km): KamLAND
- MBL (<100 km): Daya Bay, D-Chooz, RENO, JUNO, etc
- SBL (~10 m): Prospect, Stereo, NEOS, TAO, etc

❖ LS is a common use to detect neutrinos via IBD



Mass hierarchy through reactor neutrino

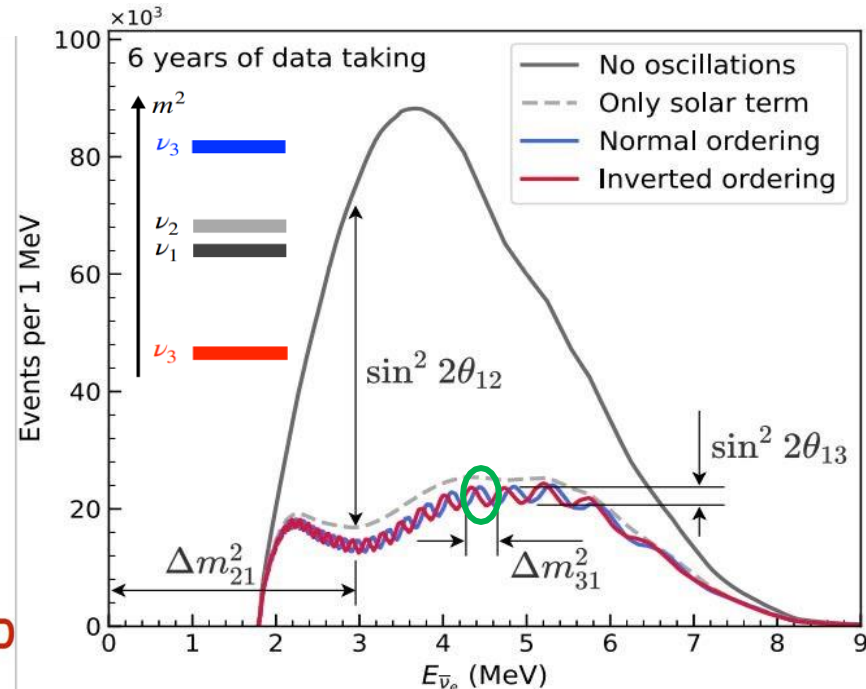
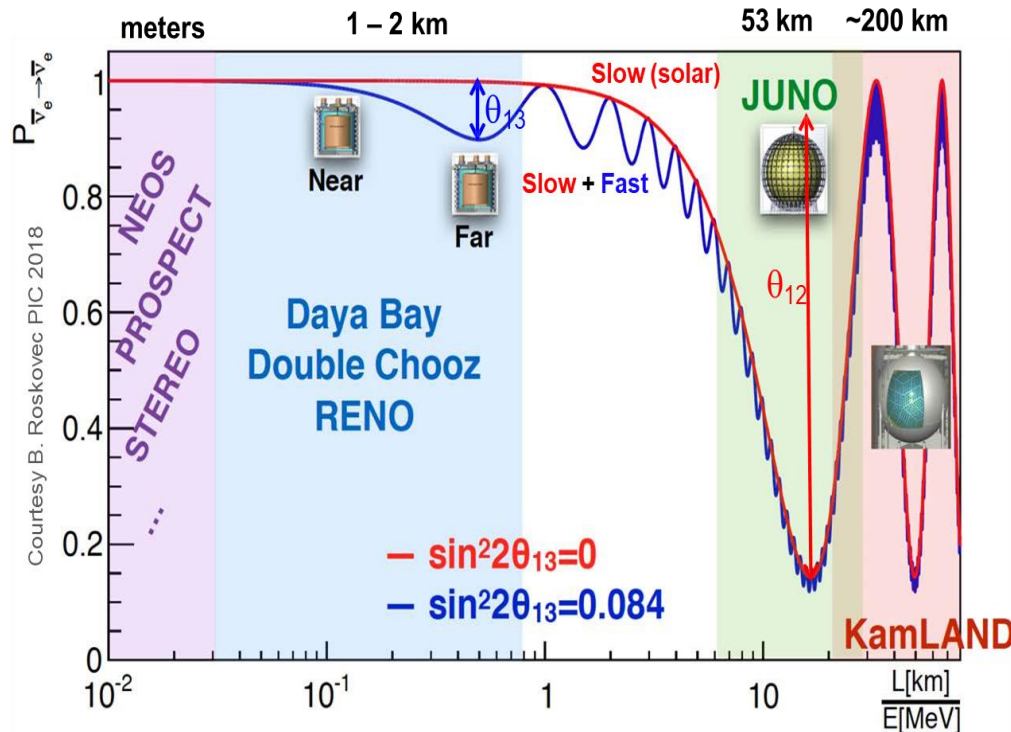
Interference in vacuum

$$\begin{aligned}
 P(\bar{\nu}_e \rightarrow \bar{\nu}_e) &= 1 - \sin^2 2\theta_{13} (\cos^2 \theta_{12} \sin^2 \Delta_{31} + \sin^2 \theta_{12} \sin^2 \Delta_{32}) - \cos^4 \theta_{13} \sin^2 2\theta_{12} \sin^2 \Delta_{21} \\
 &= 1 - \frac{1}{2} \sin^2 2\theta_{13} \left[1 - \sqrt{1 - \sin^2 2\theta_{12} \sin^2 \Delta_{21}} \cos(2|\Delta_{ee}| \pm \phi) \right] - \cos^4 \theta_{13} \sin^2 2\theta_{12} \sin^2 \Delta_{21}
 \end{aligned}$$

Where $\Delta_{ij} \equiv \Delta_{ij}^2/4E$, $\Delta m_{ee}^2 = \cos^2 \theta_{12} \Delta m_{31}^2 + \sin^2 \theta_{12} \Delta m_{32}^2$

$$\sin \phi = \frac{c_{12}^2 \sin(2s_{12}^2 \Delta_{21}) - s_{12}^2 \sin(2c_{12}^2 \Delta_{21})}{\sqrt{1 - \sin^2 2\theta_{12} \sin^2 \Delta_{21}}}, \quad \cos \phi = \frac{c_{12}^2 \cos(2s_{12}^2 \Delta_{21}) + s_{12}^2 \cos(2c_{12}^2 \Delta_{21})}{\sqrt{1 - \sin^2 2\theta_{12} \sin^2 \Delta_{21}}}$$

- The \pm sign is decided by the MH (+ for NH and - for IH)

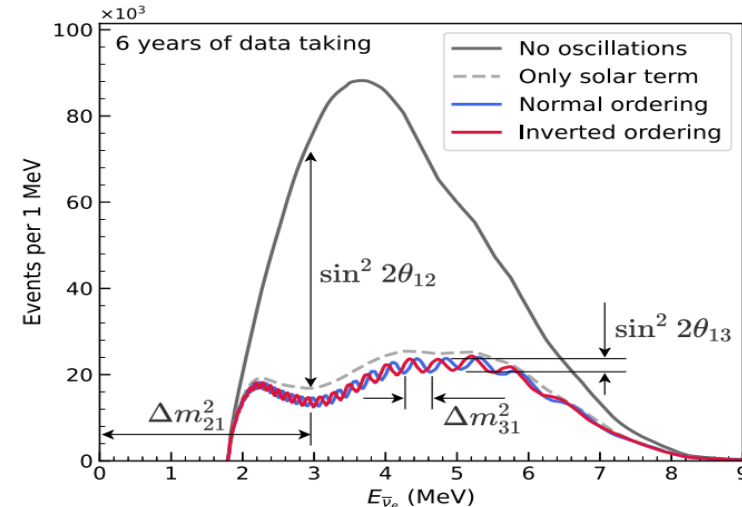


Jiangmen Underground Neutrino Observatory (JUNO)

- Proposed to determine **Neutrino Mass Ordering (NMO)** via detecting reactor neutrinos
 - Independent of the CP phase, and the large θ_{13} makes it easier
- Critical requirements to make it to be realized
 - Site selection → optimum baseline (oscillation maximum of θ_{12})
 - Sufficient statistics → large LS detector and powerful reactors
 - Good E resolution → highly transparent LS and high LY, highly efficient PMTs and high coverage
 - Shape uncertainty → satellite detector (TAO) provides reference spectrum, comprehensive calibration system
 - Low BKG → good overburden, highly efficient veto and shielding, material screening, clean installation

$$P(\bar{\nu}_e \rightarrow \bar{\nu}_e) = 1 - \sin^2 2\theta_{12} \cos^4 \theta_{13} \sin^2 \frac{\Delta m_{21}^2 L}{4E} - \frac{1}{2} \sin^2 2\theta_{13} \left[\sin^2 \frac{\Delta m_{31}^2 L}{4E} + \sin^2 \frac{\Delta m_{32}^2 L}{4E} \right] - \frac{1}{2} \cos 2\theta_{12} \sin^2 2\theta_{13} \sin \frac{\Delta m_{21}^2 L}{4E} \sin \frac{(\Delta m_{31}^2 + \Delta m_{32}^2) L}{4E}$$

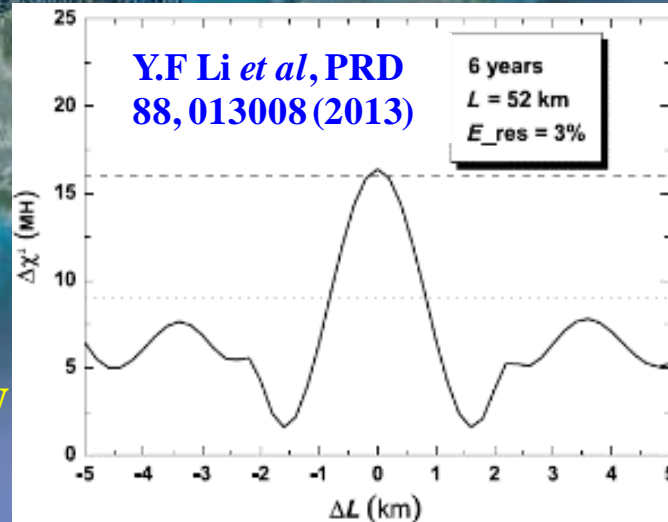
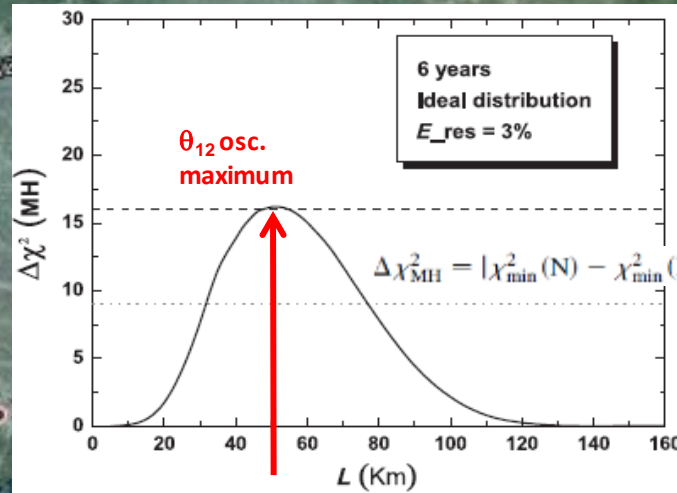
Sensitive to mass ordering



Optimum Baseline and Site Selection

- Optimum sensitivity at the oscillation maximum of θ_{12}
- Multiple baseline reactors may wash out the oscillation structure
 - Baseline difference should be < 500 m

site candidate



The Jiangmen underground laboratory

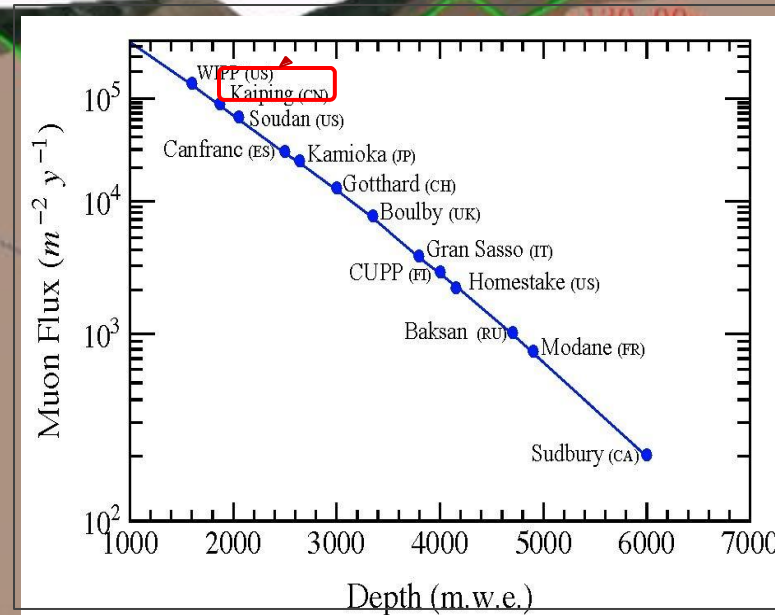
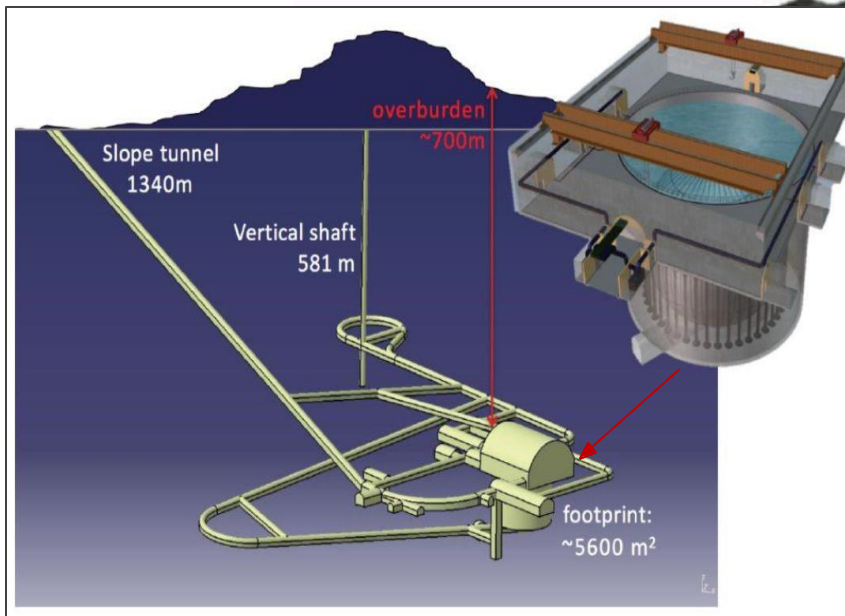
JUNO site

Overburden ~650 m (1800 m.w.e.)

700 meter



$$\Phi(\mu) \sim 0.004 \mu/m^2/s \rightarrow 10^5 \mu/m^2/y$$



729m

16000m

Underground Facility Layout

控制点坐标表

| 坐标点 | X | Y |
|-----|-------------|------------|
| KP | 2447649.232 | 347030.623 |
| K4' | 2447666.377 | 347004.496 |
| KV' | 2447680.093 | 346983.595 |
| X5 | 2447616.713 | 346879.258 |
| X6 | 2447599.594 | 346905.486 |
| X7 | 2447388.070 | 346922.910 |
| X8 | 2447602.442 | 346992.145 |
| X9 | 2447608.548 | 346996.020 |
| X10 | 2447629.874 | 346950.341 |
| S1 | 2447753.981 | 347015.689 |
| S2 | 2447717.944 | 347011.124 |
| S3 | 2447699.342 | 346998.917 |
| F1 | 2447669.893 | 346950.289 |
| F2 | 2447642.199 | 346956.038 |
| F3 | 2447659.664 | 347063.494 |
| F4 | 2447687.338 | 347057.735 |

Transportation tunnel

LS room

Pure water room

LS filling room

Water pump

Restroom

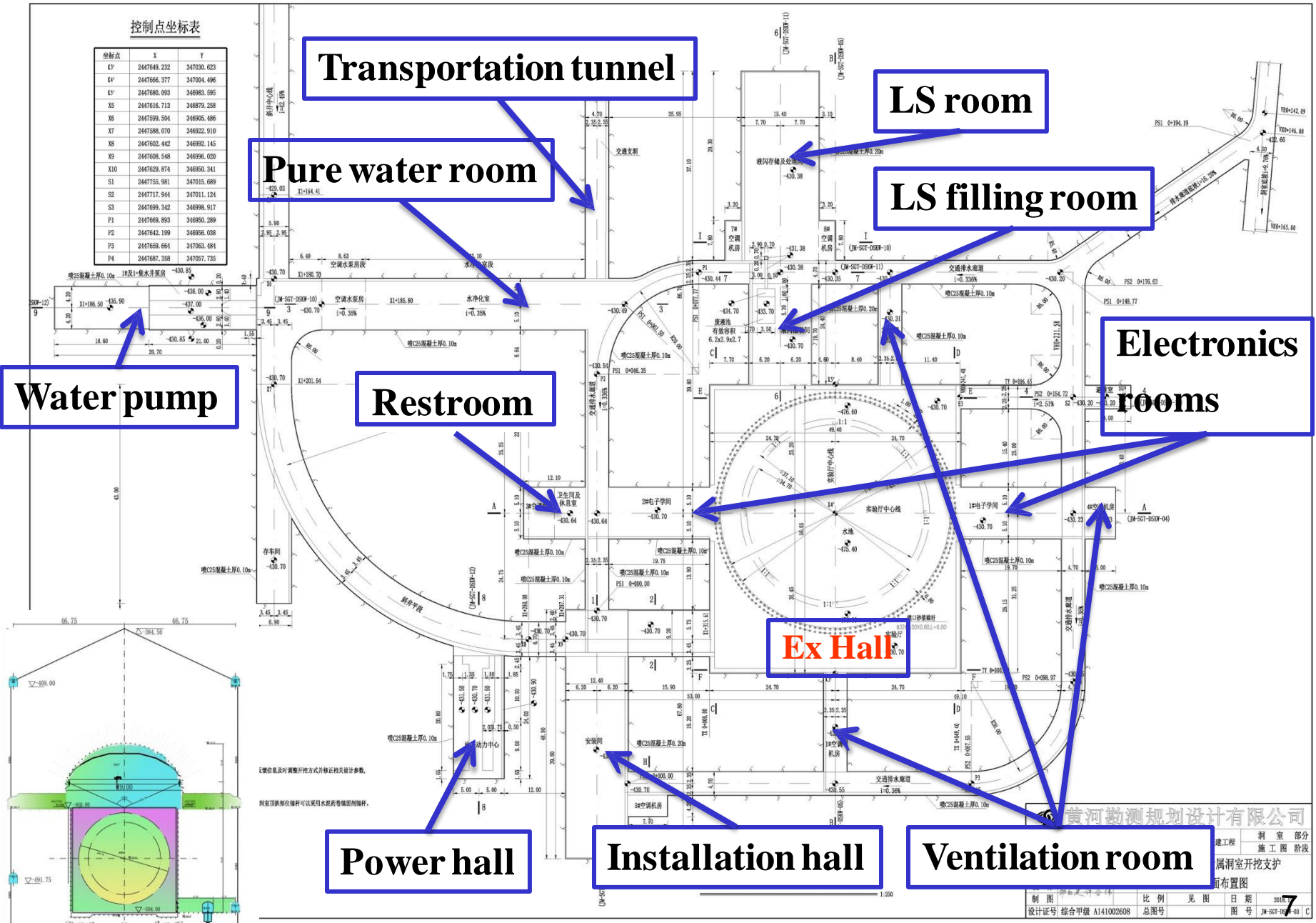
Electronics rooms

Ex Hall

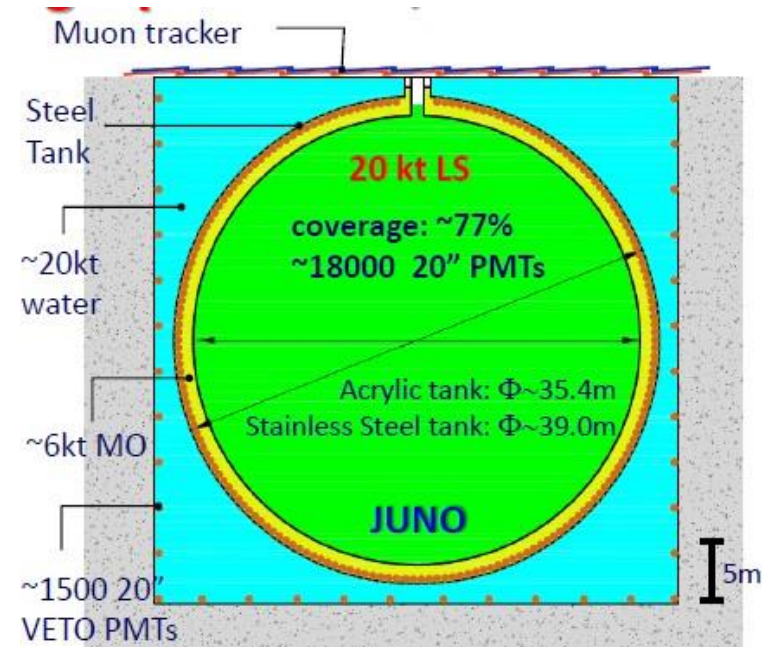
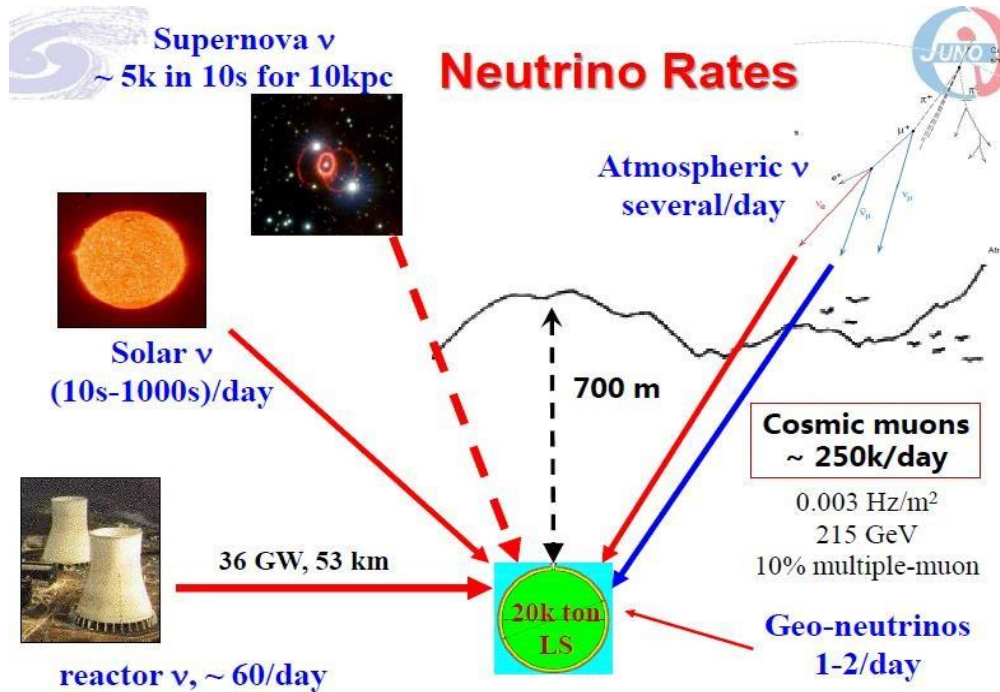
Power hall

Installation hall

Ventilation room



Jiangmen Underground Neutrino Observatory - The JUNO experiment



Estimated numbers of neutrino events in JUNO (Supernova)

| Channel | Type | Events for different $\langle E_\nu \rangle$ values | | |
|---|------|---|-------------------|-------------------|
| | | 12 MeV | 14 MeV | 16 MeV |
| $\bar{\nu}_e + p \rightarrow e^+ + n$ | CC | 4.3×10^3 | 5.0×10^3 | 5.7×10^3 |
| $\nu + p \rightarrow \nu + p$ | NC | 6.0×10^2 | 1.2×10^3 | 2.0×10^3 |
| $\nu + e \rightarrow \nu + e$ | NC | 3.6×10^2 | 3.6×10^2 | 3.6×10^2 |
| $\nu + {}^{12}\text{C} \rightarrow \nu + {}^{12}\text{C}^*$ | NC | 1.7×10^2 | 3.2×10^2 | 5.2×10^2 |
| $\nu_e + {}^{12}\text{C} \rightarrow e^- + {}^{12}\text{N}$ | CC | 4.7×10^1 | 9.4×10^1 | 1.6×10^2 |
| $\bar{\nu}_e + {}^{12}\text{C} \rightarrow e^+ + {}^{12}\text{B}$ | CC | 6.0×10^1 | 1.1×10^2 | 1.6×10^2 |



JUNO Detector

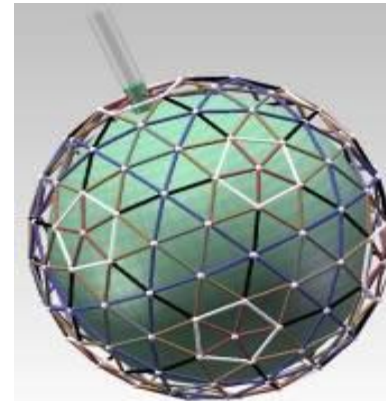
- Target mass of 20 kt liquid scintillator
- Energy resolution $< 3\%$ @ 1MeV

Technology R&D since 2009:

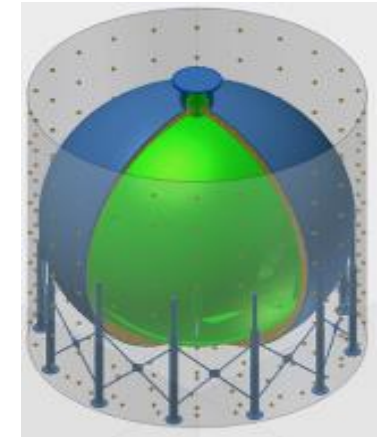
- Transparent & high light yield liquid scintillator
- High detection efficiency 20" PMTs
- Radiopurity U/Th/K $< 10^{-17}$ g/g for 20 kt LS

Detector Design(tens of options) :

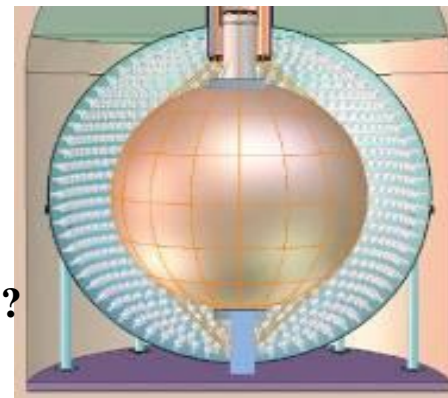
- Central target container: acrylic or Nylon balloon ?
 - Nylon, acrylic & Teflon : Only three materials, compatible with LS for long time operation, but Teflon is not transparent
- Mechanical structure: steel frame or steel tank ?
- Buffer layer: Water or Mineral oil ?



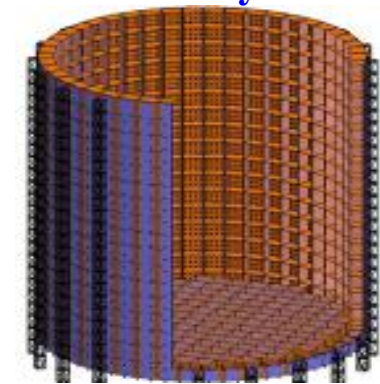
Steel frame+ Acrylic tank



Steel tank+ Acrylic tank



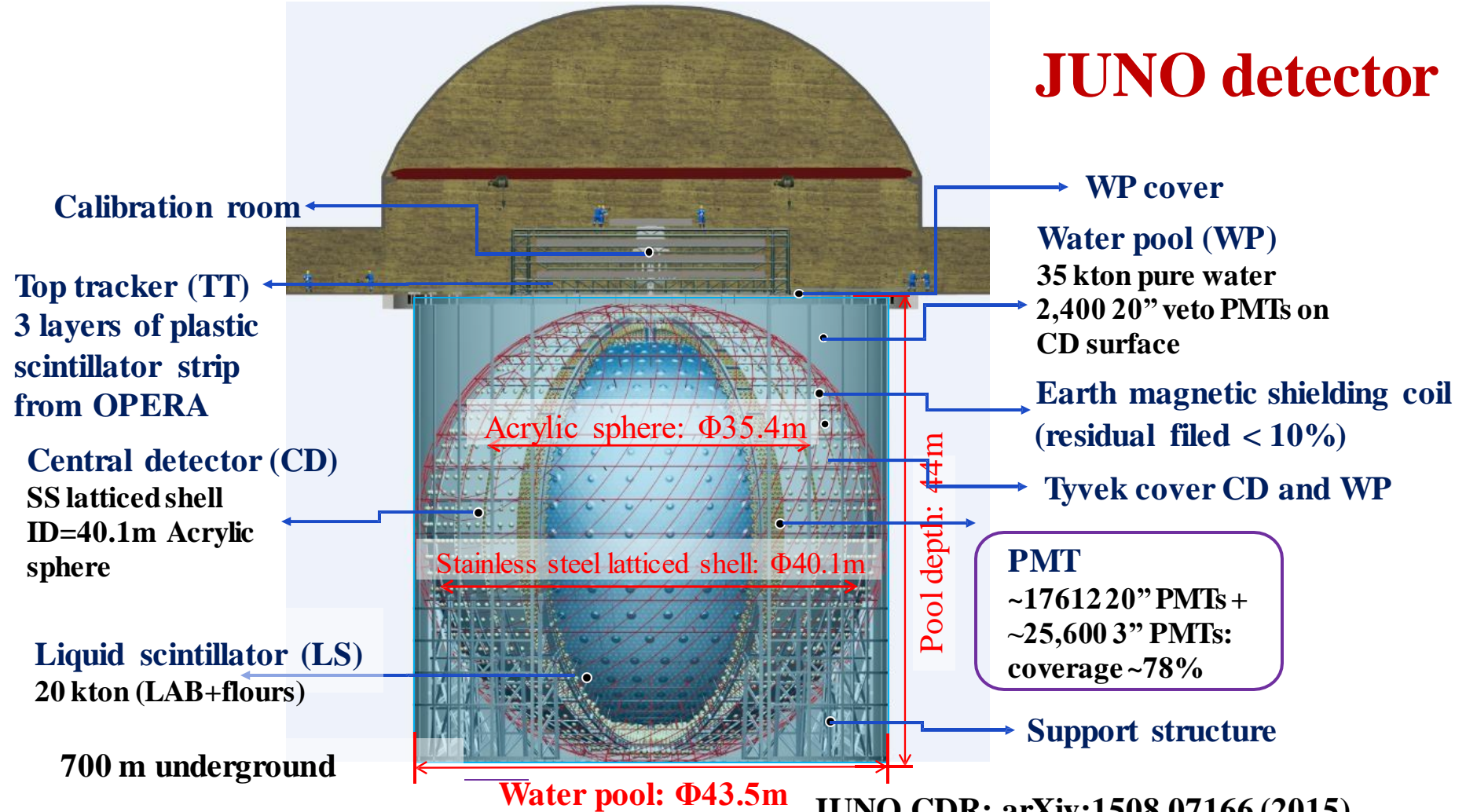
Steel Tank + Balloon



Steel Tank + Acrylic blocks

| Experiment | Daya Bay | Borexino | Kamland | JUNO |
|--------------|---------------|---------------|---------------|----------------|
| LS mass | 8×20 ton | ~300 ton | ~1 kton | 20 kton |
| PMT coverage | ~12% | ~34% | ~34% | ~78% |
| σ_E/E | ~8.5%/√E(MeV) | ~5%/√E(MeV) | ~6%/√E(MeV) | ~3%/√E(MeV) |
| Yield | ~160 p.e./MeV | ~500 p.e./MeV | ~250 p.e./MeV | >1345 p.e./MeV |

JUNO detector



Neutrino mass ordering

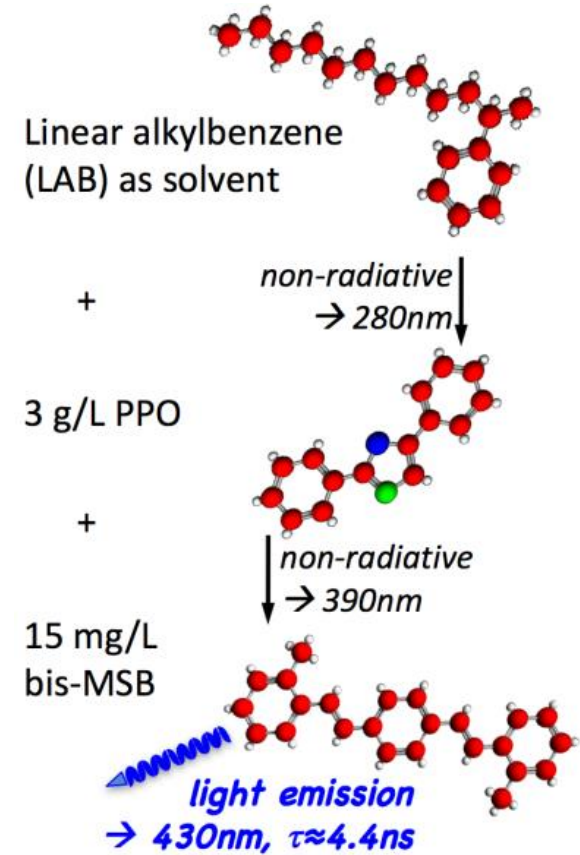
JUNO CDR: arXiv:1508.07166 (2015)

Update in arXiv:2104.02565

- 3σ neutrino mass ordering sensitivity within 6 years (78% photo-cathode coverage).
- 4σ with Δm^2_{32} input from accelerator experiments.
- $> 5\sigma$ combined analysis with IceCube within 3–7 years or PINGU in 2 years (arXiv: 1911.06745)

JUNO Scintillator

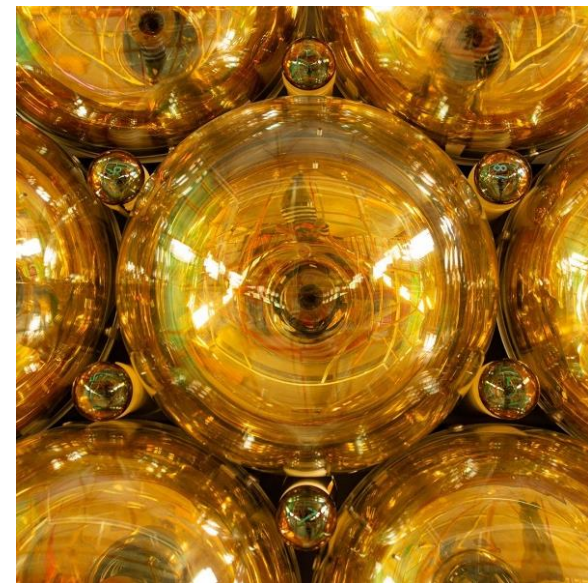
- **Liquid scintillator (LS) recipe:**
 - 2.5 g/L PPO + 3 mg/L bis-MSB
- **Low radioactive backgrounds:**
 - 10^{-15} g/g for neutrino mass ordering determination
 - 10^{-17} g/g for solar neutrino detection
- **Attenuation Length: > 20 m @430 nm**
- **Improve raw materials and production process**
- **Purification systems (Al₂O₃ Filtration column, water extraction, gas stripping)**
- **Radiopurity requirements:**
 - **Reactor neutrinos**
 - $^{238}\text{U}/^{232}\text{Th} < 10^{-15}$ g/g
 - $^{40}\text{K} < 10^{-16}$ g/g,
 - ^{210}Pb (^{222}Rn) $< 10^{-22}$ g/g
 - **Solar Neutrinos**
 - $^{238}\text{U}/^{232}\text{Th} < 10^{-17}$ g/g
 - $^{40}\text{K} < 10^{-18}$ g/g
 - ^{210}Pb (^{222}Rn) $< 10^{-24}$ g/g
 - $^{226}\text{Ra} < 5 \times 10^{-24}$ g/g
 - $^{85}\text{Kr}/^{39}\text{Ar} < 1 \mu\text{Bq}/\text{m}^3$



- **High Light yield: >1345 p.e./MeV**
- **Technological Challenges**
 - constant delivery of purified LS
 - underground laboratory
 - Reduce the risk of contaminating the purified LS

JUNO PMTs

- **17612 20-inch PMTs** (75% coverage) in CD, 2400 20-inch PMTs in the veto detector
- **15012 20-inch MCP-PMTs**, produced by NNVT, with higher PDE
- **5000 20-inch dynode PMTs** from Hamamatsu, with better TTS
- **25,600 3-inch PMTs** (3% coverage) in CD to ensure energy resolution and charge linearity
- **All PMTs have been produced, tested, and instrumented with waterproof potting**



Acrylic cover



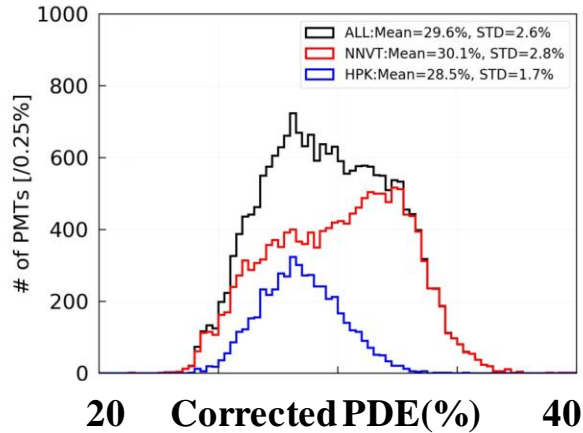
Stainless Steel cover



Clearance between PMTs: 3 mm
→ Assembly precision: < 1 mm

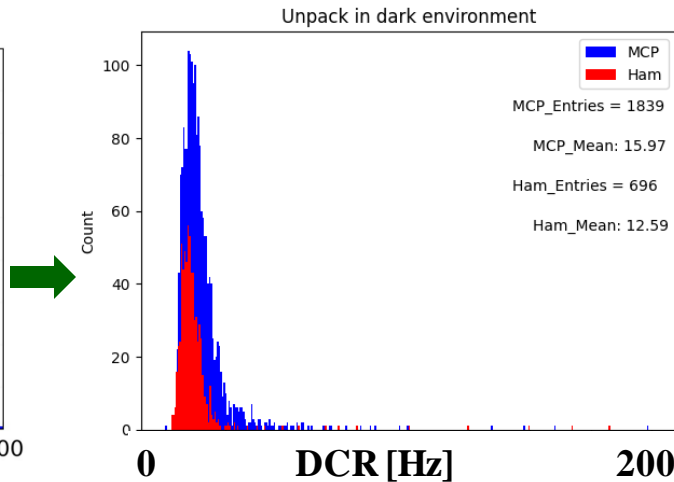
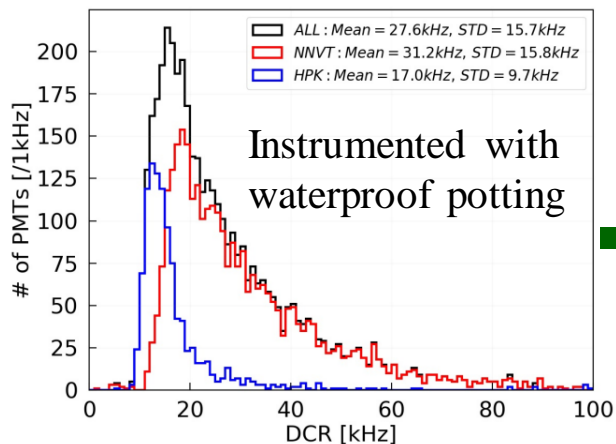
PMT Performance

Photon Detection Efficiency, PDE



| | | LPMT (20-inch) | | SPMT (3") |
|---------------------------------------|---------------|---------------------|--------------|-------------------|
| | | Hamamat | NNVT | HZC |
| Quantity | | 5000 | 15012 | 25600 |
| Charge Collection | | Dynode | MCP | Dynode |
| Photon Detection Efficiency | | 28.5% | 30.1% | 25% |
| Dark Count Rate [kHz] | Bare | 15.3 | 49.3 | 0.5 |
| | Potted | 17.0 | 31.2 | |
| TTS (σ) [ns] | | 1.3 | 7.0 | 1.6 |
| Dynamic range [0-10] MeV | | [0, 100] PEs | | [0, 2] PEs |
| Coverage | | 75% | | 3% |

Dark Counting Rate, DCR



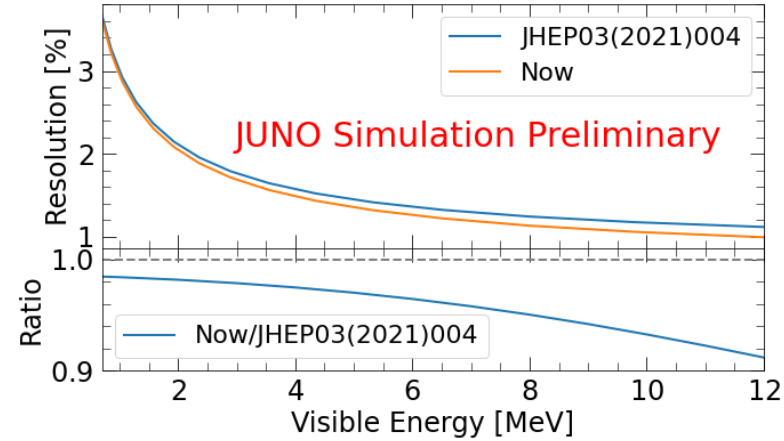
- Mass testing was done with the commercial electronics
- With JUNO's electronics, MCP-PMTs present the similar DCR with HPK's

Predicted Energy Resolution in JUNO

Positron energy resolution is understood:

$$\frac{\sigma}{E_{\text{vis}}} = \sqrt{\left(\frac{a}{\sqrt{E_{\text{vis}}}}\right)^2 + b^2 + \left(\frac{c}{E_{\text{vis}}}\right)^2}$$

- **Photon statistics**
- **Scintillation quenching effect**
 - LS Birks constant from table-top measurements
- **Cherenkov radiation**
 - Cherenkov yield factor (refractive index & re-emission probability) is re-constrained with Daya Bay LS non-linearity
- **Detector uniformity and reconstruction**
- **Annihilation-induced γ s**
- **Dark noise**

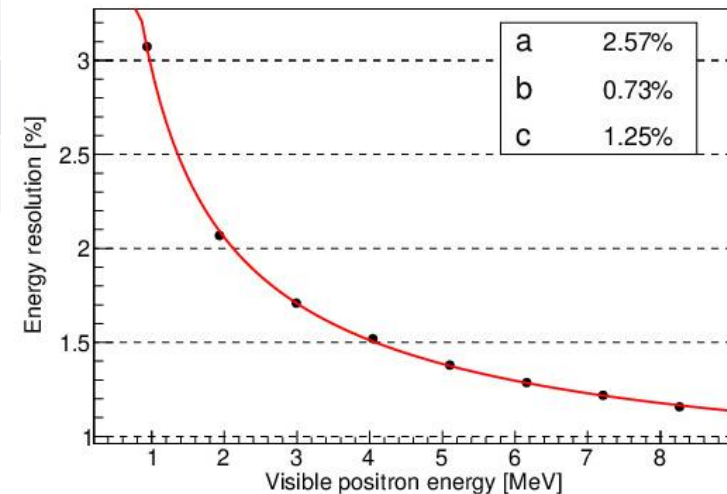
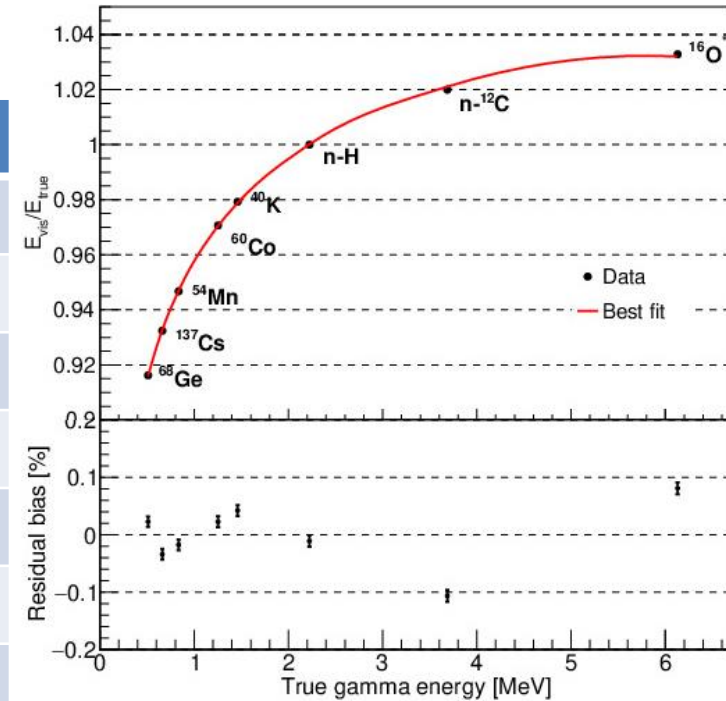


Calibration Strategy of the JUNO expt : 2011.06405

JUNO physics requirement : **better than 1% energy linearity and a 3% effective energy resolution**

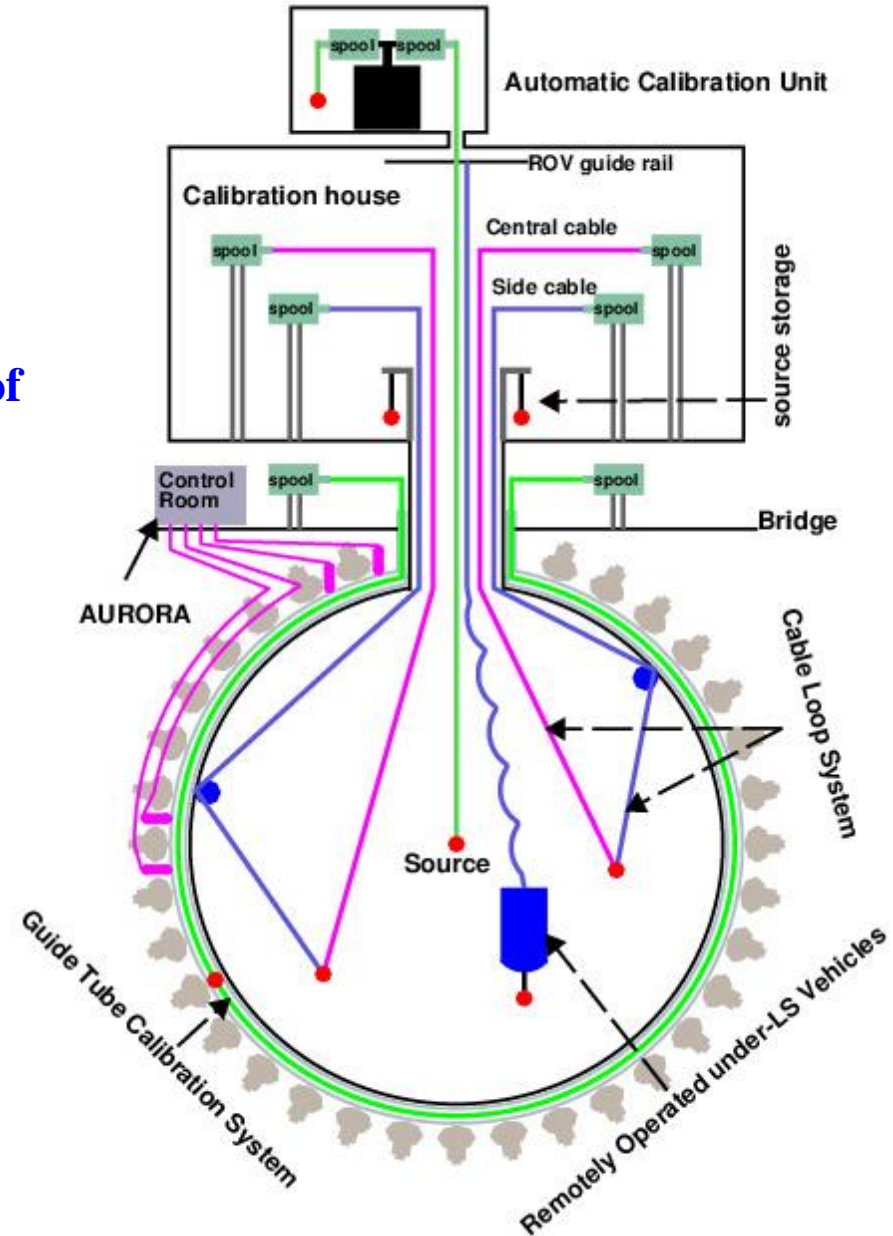
| Source/Process | Type | Radiation |
|---------------------------------|-------------|--|
| ^{137}Cs | γ | 0.662 MeV |
| ^{54}Mn | γ | 0.835 MeV |
| ^{60}Co | γ | 1.173+1.333 MeV |
| ^{40}K | γ | 1.461 MeV |
| ^{68}Ge | e^+ | Annihilation 2×0.511 MeV |
| $^{241}\text{Am-Be}$ | n, γ | Neutron + 4.4 MeV ($^{12}\text{C}^*$) |
| $^{241}\text{Am-}^{13}\text{C}$ | n, γ | Neutron + 6.13 MeV ($^{16}\text{O}^*$) |
| $(n, \gamma)p$ | γ | 2.22 MeV |
| $(n, \gamma)^{12}\text{C}$ | γ | 4.94 MeV or 3.68+1.26 MeV |
| Cosmogenic ^{12}B | β | 0 – 13.4 MeV |

- $E_{vis}^{\gamma} = \int_0^{E^{\gamma}} P(E^e) \times f_{nonlin}(E^e) E^e dE^e \times I$
- $I = \frac{1}{\int_0^{E^{\gamma}} P(E^e) \times E^e dE^e}$
- $\frac{\sigma_E}{E} = \frac{a}{\sqrt{E}} \oplus b \oplus \frac{c}{E}$

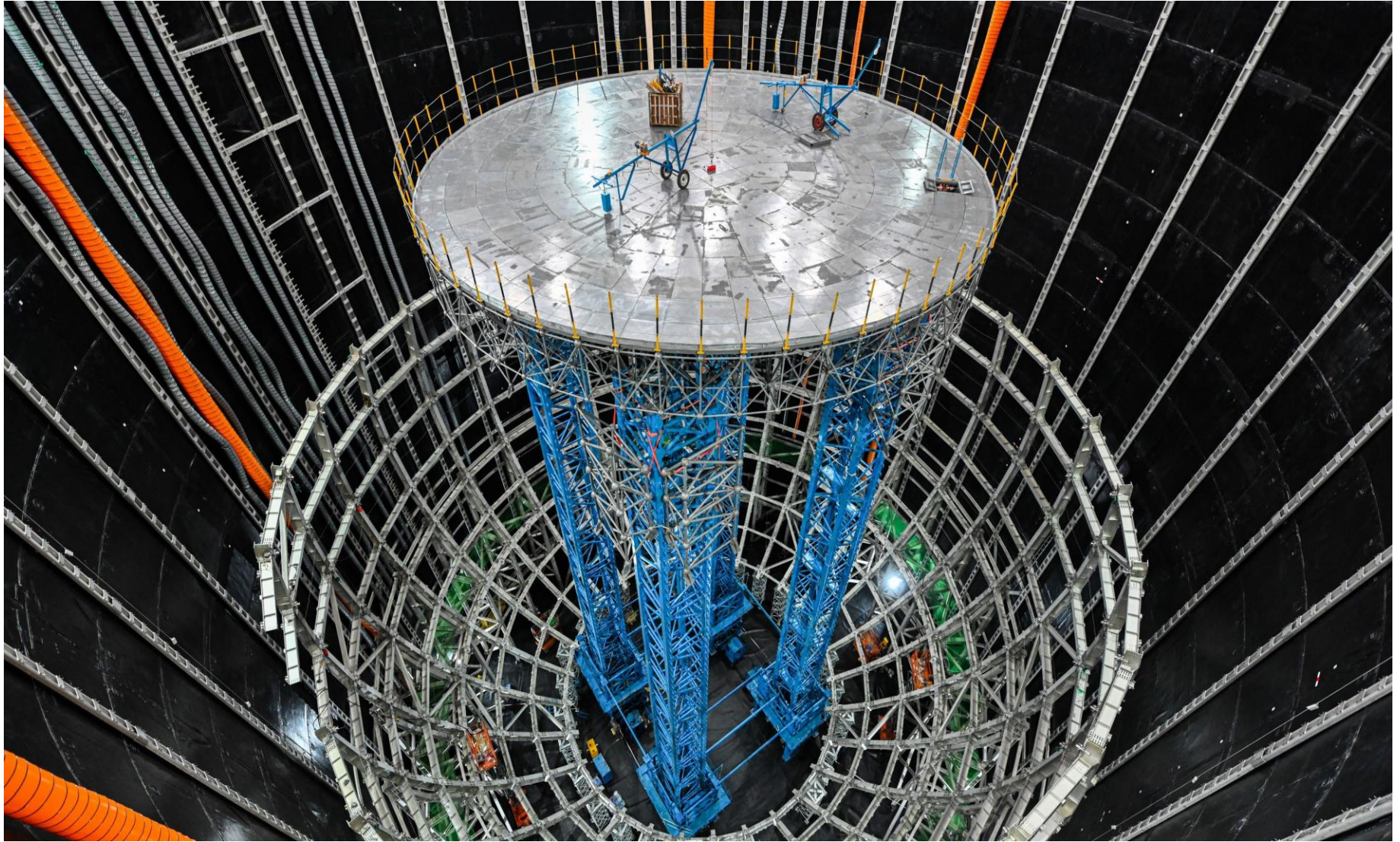


Calibration Strategy of the JUNO expt : 2011.06405

- Dual calorimetry, utilising a comparison between LPMT and SPMT for the calibration of LPMT
- Positron annihilation produce 2/3 gamma
- Light yield, $Y_0 = 1345/\text{MeV}$, α is about 2.7%
- PE depends on the angle, due to mismatch of r.i. between acrylic and water.
- Spallation neutron background, $\sim 1.8\text{evt/s}$
- A 4% reduction of absorption length (default 77m) can also produce 1% reduction of Y_0 .



Central Detector Lifting Structure



Central Detector SS structure



Central Detector : Acrylic Annealing



